

# HABILITATION THESIS

## ASSESSMENT OF STRUCTURAL RETROFITTING AND ENERGY EFFICIENCY THROUGH TESTING, MODELLING AND MONITORING

Assoc. Prof. NAGY-GYÖRGY Tamás, PhD  
Civil Engineering Faculty  
Politehnica University Timisoara

## ACKNOWLEDGEMENTS

I would like to thank my friends and colleagues, Demeter István, Dăescu Cosmin, Floruț Codruț, Sas Gabriel and Boros Iosif, for many interesting discussions, for their valuable contributions, for scientific and professional collaboration in our joint projects. In the same time I am also thankful to all the co-authors of the papers which stay at the origin of the present habilitation thesis.

I owe my gratitude for Prof. Stoian Valeriu, Prof. Iosip-Moț Ștefan and Prof. Dan Daniel for the useful advices and commitment to the highest standards, inspiring and motivating me.

Finally, my very special thanks go to my family. For everything!

## A. ABSTRACT

The research activity of the candidate started in December 1999, when he was recruited as PhD student at the Politehnica University of Timisoara under the coordination of Professor Valeriu Stoian. His PhD thesis entitled Using the FRP Composite Materials for Strengthening Brick Masonry and Reinforced Concrete Elements was defended at the Politehnica University of Timisoara in July 2004, with the distinction of Magna Cum Laude. The present thesis summarizes a part of the research activity of the candidate after this date.

The selected post-doctoral activity considered to be relevant and original was developed within the main thematic direction of Structural Strengthening using FRP Composites, presented in Chapter 2. A second direction was also considered, entitled Structural Health Monitoring of Energy Efficient Buildings, presented in Chapter 3.

Through the years the candidate was member in 11 national and 5 international research grant or program, in 4 as coordinator. The main researches was in the field of Structural Strengthening using FRP Composites (13 grants), while in the last 3 years interest was shifted towards to the Structural Health Monitoring and Energy Efficiency of structures.

Continuing the main theme of the PhD thesis the candidate won by competition a research grant offered by the Romanian Ministry of Education (title : Advanced systems for strengthening reinforced concrete structural elements as beams, columns, walls and slabs using fiber reinforced polymer composites - CEEX program). In the frame of the project new and innovative anchorage systems and strengthening technologies for reinforced concrete beams were developed, the confining effect of carbon and glass fiber reinforced polymers (FRP) and their superposition with the application of innovative near surface mounted (NSM) steel and FRP bars were studied. Another focus of the project was represented by the study of the influence of various sized cut out openings created in structural walls and slabs retrofitted using externally bonded and NSM FRP composites.

In parallel, the subject of advanced techniques used for structural strengthening of masonry elements was also studied in a CNCSIS as well as in a frame of a European FP6 project called ProHiTech - Earthquake PROtection of HIstorical buildings by reversible mixed TECHnologies. As main results, the stiffening effect of different retrofitting systems was evaluated, the efficiency of solutions was categorized in terms of resistance, ductility and costs, and a new strengthening solution was proposed and investigated, based on a new concept of steel wire mesh applied with epoxy resins.

The accumulated knowledge in the field of retrofitting, permitted to use and apply the FRP strengthening methods even in the field of steel-concrete composite walls, which was investigated in the frame of the project entitled Innovative structural systems of composite steel-concrete materials and polymer composites, project type PN II. One of the most promising results of the experimental program was a further development of an anchorage system used for FRP lamellas subjected to bending superposed with a confinement FRP fabric.

Later on, the investigation of full scale precast prestressed concrete element support zone was studied and the strengthening possibilities were analysed. Based on the initial nonlinear modelling, the strengthening strategy was determined and an experimental test was designed. The experimental part was followed by a numerical calibration and by an extension of the strengthening matrix.

The second subject of research covered by the candidate is related to the Structural Health Monitoring of Energy Efficient Buildings, in order to validate design principles, to evaluate real energy demands and to optimize and reduce energy consumptions. This field is time dependent, because it is based on recorded parameters throughout several years. The research in this field started in 2012 through PASSHOUSE (Performance ASSESSment of energy efficient HOUSEs Through Monitoring) program, financed by the European Regional Development Fund, and continued with a PN II program, entitled Nearly Zero Energy Building and Passive House - sustainable solutions for residential buildings. In these projects, the objectives were to conceive, realize and put in function a complex monitoring system, to collect data from internal and external parameters and finally to provide a practice guide based on the results.

It must be mentioned, that all the above cited research was performed in cooperation with the PhD students within the Department of Civil Engineering and Building Services from Politehnica University of Timisoara.

The candidate is member of important scientific associations in the field of structural engineering, such as American Concrete Institute (ACI) and International Federation for Structural Concrete (*fib*). The candidate published a series of books in the fields of structural use FRP composites in constructions for practical use of designers and researchers, as well as several design guides addressed especially to students in many subjects.

The involvement of the candidate in several national and international grants as director or team member developed abilities and competences on management of such projects. It has to be mentioned that the candidate already guided four doctoral students for obtaining their Ph.D. degree at the Politehnica University of Timisoara. He is an active member on two ongoing project, one in the field of energy efficiency and monitoring (the above mentioned PN II project) and the second in the field of FRP in construction, in the frame of COST Action TU1207, entitled Next Generation Design Guidelines for Composites in Construction.

The relevance of the scientific activity and the recognition of the national and international activity in the field of the Structural strengthening using FRP is emphasised by the publications of the candidate, several of them in cooperation with recognized European and US researchers. The fact that all the problems were investigated through a theoretical approach, with numerical simulations, as well as in an experimental part, through several real, large or reduced scale elements, raises the real value of the performed studies and research projects.

## A. REZUMAT

Candidatul a început activitatea de cercetare a în decembrie 1999, când a fost angajat ca doctorand la Universitatea Politehnica Timișoara sub coordonarea Domnului Profesor Stoian Valeriu. Teza de doctorat a candidatului intitulată Utilizarea materialelor compozite polimerice la consolidarea elementelor din zidărie de cărămidă și beton armat a fost susținută la Universitatea Politehnica Timișoara în iulie 2004, cu distincția Magna Cum Laude. Teza de abilitare sintetizează o parte din activitatea de cercetare a candidatului după această dată.

Activitatea post-doctorală selectată, considerată a fi relevantă și originală a fost dezvoltată în cadrul direcției principale tematice și prezentată în Capitolul 2, intitulat Consolidare structurală utilizând compozite polimerice armate cu fibre (FRP). O a doua direcție a fost, de asemenea, luată în considerare prezentată în Capitolul 3, cu titlul Urmărirea în timp a structurilor eficiente energetic.

Pe parcursul anilor, candidatul a fost membru în 11 granturi de cercetare naționale și 5 internaționale, dintre care 4 au fost gestionate în calitate de coordonator. Principalele direcții de cercetare cuprinse au fost în domeniul consolidărilor structurale folosind materiale compozite FRP (13 granturi), în timp ce în ultimii 3 ani accentul s-a pus pe monitorizare și urmărirea comportării structurilor și a clădirilor eficiente energetic.

Imediat după finalizarea tezei de doctorat, candidatul a câștigat prin competiție un grant de cercetare oferit de Ministerul Educației și Cercetării, cu titlul ”Sisteme avansate pentru consolidarea elementelor structurale din beton armat de tip grinzi, stâlpi, pereți și planșee folosind materiale compozite polimerice armate cu fibre” - Program CEEEX. În cadrul proiectului s-au dezvoltat sisteme de ancoraje noi și inovatoare și tehnologii de consolidare pentru grinzi de beton armat, s-au studiat efectele de confinare al compozitelor polimerice armate cu fibre de carbon și de sticlă și suprapunerea acestor efecte cu aplicarea în șlițuri (NSM) a unor bare de oțel și de compozite. Totodată s-a studiat și influența dimensiunii diferitelor goluri create prin tăiere în pereți structurali și în plăci consolidați apoi cu materiale compozite aplicate prin lipire pe exterior sau în șlițuri.

În paralel, candidatul a studiat tema unor tehnici avansate utilizate pentru consolidarea structurală ale elementelor de zidărie în cadrul unui program CNCISIS, precum și în cadrul unui proiect European tip FP6, cu acronimul ProHiTech (Earthquake PROtection of HHistorical buildings by reversible mixed TECHnologies - Protecția clădirilor istorice la cutremur prin tehnologii mixte reversibile). Ca și rezultate principale, s-a evaluat efectul de rigidizare ale diferitelor sisteme de consolidare, eficiența soluțiilor de intervenție a fost clasificată în termeni de rezistență, ductilitate și costuri. Suplimentar, s-a propus și s-a investigat o nouă soluție de consolidare bazată pe un nou concept, folosind plase de sârmă din oțel aplicate cu rășini epoxidice.

Cunoștințele acumulate în domeniul consolidărilor a permis utilizarea metodelor de reabilitare structurală chiar și în domeniul pereților compuși oțel-beton, problematică studiată în cadrul proiectului intitulat ”Sisteme structurale inovative din materiale compuse oțel-beton și compozite polimerice”, proiect de tip PN II. Unul dintre cele mai promițătoare rezultate ale programului experimental a fost dezvoltarea unui sistem de ancorare pentru lamele FRP din zona de încovoiere suprapuse cu țesături FRP de confinare.

Tot în cadrul unui program de cercetare finanțat de CNCSIS s-a studiat zona de rezemare pentru o grindă de beton prefabricat precomprimat la scară reală și s-au analizat posibilitățile de consolidare folosind compozite FRP, iar după testele experimentale au urmat calibrări numerice și în final s-a realizat extinderea matricei de consolidare.

Cea de a doua temă de cercetare acoperită de candidat se leagă de urmărirea în timp (monitorizarea) a structurilor eficiente energetic, în scopul de a valida principiile de proiectare, pentru a evalua cerințele reale de energie și pentru a optimiza și a reduce consumurile de energie. Acest subiect este o temă de durată, pentru că se bazează pe parametri înregistrați pe mai mulți ani. Cercetarea în acest domeniu a început în 2012 cu programul PASSHOUSE (Performance ASSESSment of energy efficient HOUSEs Through Monitoring - Evaluarea performanțelor caselor eficiente energetic prin monitorizarea), program finanțat de Fondul European de Dezvoltare Regională, și a continuat cu programul PN II, cu titlul "Casa aproape zero energie și casa pasivă soluții sustenabile pentru clădiri rezidențiale". În aceste proiecte, obiectivele au fost de a concepe, crea și pune în funcțiune un sistem de monitorizare complexă, pentru a colecta date privind parametrii interni și externi, iar în final de a oferi un ghid practic pe baza rezultatelor.

Trebuie menționat, că toate cercetările de mai sus s-au realizat în colaborare cu doctoranzii din cadrul Departamentului de Construcții Civile și Instalații (CCI) din Universitatea Politehnica Timișoara.

Candidatul este membru în unele dintre cele mai importante asociații științifice în domeniul ingineriei structurale, cum sunt Institutul American de Beton (ACI) și Federația Internațională pentru Beton Structural (*fib*). Candidatul a publicat pentru proiectanți și cercetători o serie de cărți în domeniul utilizării structurale în construcții a materialelor compozite FRP, precum și mai multe ghiduri de proiectare adresate în special studenților în mai multe subiecte.

Participarea candidatului în mai multe granturi naționale și internaționale în calitate de director sau membru de echipă, a dezvoltat abilitățile și competențele sale privind managementul unor astfel de proiecte. Trebuie menționat că patru doctoranzi ai Universității Politehnica din Timișoara au fost ghidați, de-a lungul anilor, de către candidat în vederea realizării cercetărilor din cadrul tezelor de doctorat. El este membru activ în două proiecte în curs de desfășurare, unul în domeniul eficienței energetice și monitorizare (proiectul PN II de mai sus), iar al doilea în domeniul utilizării compozitelor FRP în construcții, în cadrul acțiunii COST TU1207, intitulat "Ghiduri de calcul de generația următoare pentru compozite în construcții" (Next Generation Design Guidelines for Composites in Construction).

Relevanța activității științifice și recunoașterea activității naționale și internaționale în domeniul consolidărilor structurale folosind compozite FRP este subliniat de publicațiile candidatului, mai multe dintre ele în colaborare cu cercetători recunoscuți din Europa sau Statele Unite. Valoarea reală a studiilor efectuate și a proiectelor de cercetare iese în evidență prin faptul că toate problemele au fost investigate atât printr-o abordare teoretică cu simulări numerice, precum și cu parte experimentală prin încercarea a mai multor elemente la scară reală, mare sau redusă.

## TABLE OF CONTENTS

<b>ACKNOWLEDGEMENTS</b> .....	1
<b>A. ABSTRACT</b> .....	2
<b>REZUMAT</b> .....	4
<b>B. SCIENTIFIC, PROFESSIONAL AND ACADEMIC ACHIEVEMENTS</b> .....	8
<b>1. INTRODUCTION</b> .....	8
<b>2. STRUCTURAL STRENGTHENING USING FRP COMPOSITES</b> .....	12
<b>2.1 Introduction</b> .....	12
<b>2.2 Experimental assessment on shear strengthening of clay brick masonry walls using different techniques</b> .....	13
2.2.1 Numerical analysis .....	14
2.2.2 Experimental test set-up .....	14
2.2.3 Experimental tests on masonry walls retrofitted with FRPs .....	15
2.2.4 Experimental tests on masonry walls retrofitted with RMJ .....	18
2.2.5 Experimental tests on masonry walls retrofitted with SWM .....	18
2.2.6 Economic assessment of different strengthening methods .....	20
2.2.7 Conclusions .....	21
<b>2.3 Theoretical and experimental study of reinforced concrete shear walls with cut-out openings retrofitted using FRP composites</b> .....	23
2.3.1 Introduction .....	23
2.3.2 Building inventory .....	24
2.3.3 Database of RC structural wall seismic test programs .....	26
2.3.4 Experimental program .....	31
2.3.5 Strengthening procedure .....	36
2.3.6 Experimental results .....	40
2.3.7 Conclusions .....	47
<b>2.4 Theoretical and experimental study of precast reinforced concrete slabs with cut-out openings retrofitted using FRP composites</b> .....	50
2.4.1 Introduction .....	50
2.4.2 Experimental program .....	51
2.4.3 Results of tests on bare elements .....	53
2.4.4 Design of strengthening solution .....	56
2.4.5 Behavior of strengthened elements .....	58
2.4.6 Conclusions .....	58

<b>2.5 Theoretical and experimental study of precast reinforced concrete dapped-end RC beams' retrofitted using FRP composites</b> .....	61
2.5.1 Introduction .....	61
2.5.2 The context of the study .....	63
2.5.3 Research program .....	64
2.5.4 Numerical investigation .....	67
2.5.5 Results of the experimental program .....	69
2.5.6 Numerical optimization of the strengthening using NSM and EBR CFRP .....	77
2.5.7 Assessment of the strengthening systems based on the numerical modeling .....	79
2.5.8 Discussion and conclusions .....	82
<b>3. Structural health monitoring of energy efficient structures</b> .....	85
<b>3.1 Introduction</b> .....	85
<b>3.2 Performance assessment of energy efficient houses through monitoring</b> .....	86
3.2.1 Background and description of the research program .....	86
3.2.2 Impact of the program .....	87
3.2.3 Materials and methods .....	88
3.2.4 Monitoring activities .....	90
3.2.5 Objective and output indicators .....	93
<b>3.3 Concept, specific details and monitoring strategy for energy efficient building</b> .....	94
3.3.1 Introduction .....	94
3.3.2 Functionalities and the adopted solutions .....	94
3.3.3 Monitoring system .....	100
3.3.4 Experience of the planning and implementation process .....	101
3.3.5 Preliminary results .....	102
<b>C. SCIENTIFIC, PROFESSIONAL AND ACADEMIC FUTURE DEVELOPMENT PLANS</b> .....	103
<b>C1. SCIENTIFIC DEVELOPMENT PLANS</b> .....	103
<b>C2. PROFESSIONAL DEVELOPMENT PLANS</b> .....	106
<b>C3. ACADEMIC DEVELOPMENT PLANS</b> .....	106
<b>REFERENCES</b> .....	107

## **B. SCIENTIFIC, PROFESSIONAL AND ACADEMIC ACHIEVEMENTS**

### **1. INTRODUCTION**

The research activity of the candidate started in December 1999, when he was recruited as PhD student at the Politehnica University of Timisoara under the coordination of Professor Valeriu Stoian. His PhD thesis entitled Using the FRP Composite Materials for Strengthening Brick Masonry and Reinforced Concrete Elements was defended at the Politehnica University of Timisoara in July 2004, with the distinction of Magna Cum Laude. The present thesis summarizes a part of the research activity of the candidate after this date.

The selected post-doctoral activity considered to be relevant and original was developed within the main thematic direction of Structural Strengthening using FRP Composites, presented in Chapter 2. A second direction was also considered, entitled Structural Health Monitoring of Energy Efficient Buildings, presented in Chapter 3.

Through the years the candidate was member in 11 national and 5 international research grant or program, in 4 as coordinator. The main researches was in the field of Structural Strengthening using FRP Composites (13 grants), while in the last 3 years interest was shifted towards to the Structural Health Monitoring and Energy Efficiency of structures.

Continuing the main theme of the PhD thesis the candidate won by competition a research grant offered by the Romanian Ministry of Education (title : Advanced systems for strengthening reinforced concrete structural elements as beams, columns, walls and slabs using fiber reinforced polymer composites - CEEX program). In the frame of the project new and innovative anchorage systems and strengthening technologies for reinforced concrete beams were developed, the confining effect of carbon and glass fiber reinforced polymers (FRP) and their superposition with the application of innovative near surface mounted (NSM) steel and FRP bars were studied. Another focus of the project was represented by the study of the influence of various sized cut out openings created in structural walls and slabs retrofitted using externally bonded and NSM FRP composites.

In parallel, the subject of advanced techniques used for structural strengthening of masonry elements was also studied in a CNCSIS as well as in a frame of a European FP6 project called ProHiTech - Earthquake PROtection of HIstorical buildings by reversible mixed TECHnologies. As main results, the stiffening effect of different retrofitting systems was evaluated, the efficiency of solutions was categorized in terms of resistance, ductility and costs, and a new strengthening solution was proposed and investigated, based on a new concept of steel wire mesh applied with epoxy resins.

The accumulated knowledge in the field of retrofitting, permitted to use and apply the FRP strengthening methods even in the field of steel-concrete composite walls, which was investigated in the frame of the project entitled Innovative structural systems of composite steel-concrete materials and polymer composites, project type PN II. One of the most promising results of the experimental program was a further development of an anchorage system used for FRP lamellas subjected to bending superposed with a confinement FRP fabric.

Later on, the investigation of full scale precast prestressed concrete element support zone was studied and the strengthening possibilities were analysed. Based on the initial nonlinear modelling, the strengthening strategy was determined and an experimental test was designed.

The experimental part was followed by a numerical calibration and by an extension of the strengthening matrix.

The second subject of research covered by the candidate is related to the Structural Health Monitoring of Energy Efficient Buildings, in order to validate design principles, to evaluate real energy demands and to optimize and reduce energy consumptions. This field is time dependent, because it is based on recorded parameters throughout several years. The research in this field started in 2012 through PASSHOUSE (Performance ASSESSment of energy efficient HOUSEs Through Monitoring) program, financed by the European Regional Development Fund, and continued with a PN II program, entitled Nearly Zero Energy Building and Passive House - sustainable solutions for residential buildings. In these projects, the objectives were to conceive, realize and put in function a complex monitoring system, to collect data from internal and external parameters and finally to provide a practice guide based on the results.

The immediate results of the researches in this field of SHM and energy efficiency was the publication of 2 journal papers indexed in international database and several conference papers which are not indexed, yet.

Most of the above mentioned research was done in cooperation with the PhD students within the Department of Civil Engineering and Building Services from Politehnica University of Timisoara. Throughout his grants, the candidate partially supported a part of the doctoral studies, thus he was involved in guiding a number of PhD students in the subject of the main of research activities, as follows:

- Dăescu Cosmin, PhD – research related to evaluate the effect of glass and carbon FRP confinement on elements retrofitted with EBR and NSM rebars and plates.
- Demeter István, PhD – research on the RC shear walls with different sizes of cut-out opening strengthened with EB FRP composites
- Floruț Codruț, PhD – research on RC slabs with cut-out opening retrofitted with mixed EB-NSM FRP composites
- Diaconu Dan, PhD – research on anchorage systems for FRP retrofitted RC beams
- Toduț Carla, PhD – research on the RC shear walls with cut-out opening strengthened by applying NSM FRP and Textile Reinforced Mortars.

The candidate is member of the most important scientific associations in the field of structural engineering as American Concrete Institute (ACI) and International Federation for Structural Concrete (*fib*), in the same time also member of the Association of Structural Designer Civil Engineers (AICPS), as well as Member of public body of Hungarian Academy of Sciences (2008). The candidate published a series of books in the fields of structural use FRP composites in constructions for practicing designers and researchers as author / author of chapters:

- Nagy-György Tamás, Materiale compozite polimerice pentru consolidarea elementelor din zidărie și beton, Ed. Politehnica, 2007, pp 295, ISBN 978-973-625-445-1
- Stoian V., Nagy-György Tamás, Dan D., Gergely J., Dăescu C., Materiale compozite pentru construcții, Ed. Politehnica, 2004, pp 316, ISBN 973-625-148-9
- Stoian V., Nagy-György Tamás, Dan D., Gergely J., Dăescu C., Materiale compozite pentru construcții – II revised edition , Ed. Politehnica, 2009, pp 316, ISBN 973-625-948-7
- Earthquake Protection of Historical Buildings by Reversible Mixed Technologies - FP6 PROHITECH project: Volume 5: Seismic protection of historical buildings: calculation models, Ed. Polimetrica, 2012, pp 282, ISBN 978-88-7699-177-6

- Earthquake Protection of Historical Buildings by Reversible Mixed Technologies - FP6 PROHITECH project: Volume 3: Seismic Protection of historical buildings: experimental activity, Ed. Polimetrica, 2012, pp 754, ISBN 978-88-7699-173-8

As the teaching activity of the candidate there were elaborated several courses, as well as several project and laboratory guides addressed especially for students, as follows:

- Course on Reinforced Concrete (in Romanian) for bachelor students;
- Course on Experimental techniques (in Romanian and English) for undergraduate and Master students;
- Composite for Constructions (in Romanian) for undergraduate and Master students;
- Guides for Design Reinforced Concrete members, Prestressed Concrete elements and Reinforced Concrete Structures (in Romanian and English) for undergraduate students;
- Durability of RC structures (in Romanian) for Master students.

The involvement of the candidate in several national and international grants as director or team member developed abilities and competences on management of such projects. It has to be mentioned that the candidate already guided four doctoral students for obtaining their Ph.D. degree at the Politehnica University of Timisoara. He is an active member on two ongoing project, one in the field of energy efficiency and monitoring (the above mentioned PN II project) and the second in the field of FRP in construction, in the frame of COST Action TU1207, entitled Next Generation Design Guidelines for Composites in Construction.

The relevance of the scientific activity and the recognition of the national and international activity in the field of the Structural strengthening using FRP is emphasised by the publications of the candidate, several of them in cooperation with recognized European and US researchers. The fact that all the problems were investigated through a theoretical approach, with numerical simulations, as well as in an experimental part, through several real, large or reduced scale elements, raises the real value of the performed studies and research projects.

During 2004 - 2013 the candidate obtained the following professional certifications, attested by State Inspectorate for Constructions:

- Laboratory Chief for research and testing activities (from 2008)
- Energy Auditor of Romanian Ministry for Public Works and Buildings (from 2010)
- Responsible for Structural Health Monitor of Buildings (from 2008).
- Responsible for Quality in construction for Buildings and Monuments.

## Relevant Publications:

The list of 10 publications selected by the candidate, considered to be relevant for the professional achievements obtained by the candidate for the postdoctoral period, sustaining his activity presented in the Habilitation Thesis are listed below:

1. **Nagy-György T.**, Moșoarcă M., Stoian V., Gergely J., Dan D., Retrofit of reinforced concrete shear walls with CFRP composites, fib Symposium - Keep Concrete Attractive, Budapest, Hungary, 2005, ISBN 963 420 838 X (BDI)
2. **Nagy-György T.**, Stoian V., Dan D., Dăescu C., Demeter I., Diaconu D., Dogariu A., Experimental assessment on shear strengthening of clay brick masonry walls using different techniques, PROHITECH, Rome, 2009, ISBN 978-0-415-55804-4, pp 1653-1658 (ISI)
3. Demeter I., **Nagy-György T.**, Stoian V., Dăescu C., Dan D., FRP Composites for Seismic Retrofitting of RC Wall Panels with Cut-Out Openings, First International Conference on Structures and Architecture (ICSA2010), Guimaraes, Portugal, 2010, ISBN 978-0-415-49249-2, pp 1902-1908 (ISI)
4. **Nagy-György T.**, Sas G., Dăescu C., Barros J.A.O., Stoian V., Experimental and numerical assessment of the effectiveness of FRP-based strengthening configurations for dapped-end RC beams, Engineering Structures 44 (2012) 291–303, ISSN: 0141-0296 (IF: 1.838/2014)
5. Dan D., **Nagy-György T.**, Stoian V., Fabian A., Demeter I., FRP Composites for Seismic Retrofitting of Steel-Concrete Shear Walls with Steel Encased Profiles, STESSA 2012, Santiago, Chile, 2012, ISBN 978-0-415-62105-2, pp1071-1076 (ISI)
6. **Nagy-György T.**, Demeter I., Floruț C., Dan D., Causes and required interventions on the rehabilitation process of large panel buildings in Romania, 2nd International Conference on Civil Engineering and Building Materials (CEBM 2012), November, Hong-Kong, 2012, ISBN 978-0-415-64342-9, pp 853-858 (BDI)
7. Floruț C., Stoian V., **Nagy-György T.**, Dan D., Diaconu D, Performance assessment of mixed CFRP retrofitting solution for RC slabs, 2nd International Conference on Structures and Architecture (ICSA2013), July 24-26, 2013, Guimaraes, Portugal, ISBN 978-041566195-9, pp. 727-732 (ISI)
8. Sabău C., Stoian D., Dan D., **Nagy-György T.**, Floruț C., Stoian V., Partial results of monitoring in a passive house, Journal of Applied Engineering Sciences, V1(16), Issue 1, 2013, ISSN 2247-3769, pp 107-111 (BDI)
9. Sas G., Dăescu C., Popescu C., **Nagy-György T.**, Numerical optimization of strengthening disturbed regions of dapped-end beams using NSM and EBR CFRP, Composites Part B: Engineering 67 (2014), 381-390, ISSN: 1359-8368 (IF: 2.983/2014)
10. Toduț C., Stoian V., Demeter I., **Nagy-György T.**, Dan D., Ungureanu V., Seismic Strengthening of a Precast Reinforced Concrete Wall Panel Using Combined NSM and CFRP-EBR Method, FRPRCS-11, June 26-28, 2013, Guimaraes, Portugal, ISBN 978-972-8692-84-1, pp 269-270

## 2. STRUCTURAL STRENGTHENING USING FRP COMPOSITES

### 2.1 Introduction

The fibers used in construction industry can be carbon (graphite), glass, aramide, basalt and hybrids (i.e. combination of these), the diameter varying between 5-20  $\mu\text{m}$ . The fiber behaviour is linear and brittle. The modulus of elasticity, tensile strength and strain at failure are function of the material type and structure. The embedding material, named matrix has the principal role to bond the fiber and to ensure load transfer to the fibers, respectively to protect against mechanical and environmental effects. It is composed from thermosetting and thermoplastic resins, the most important are the epoxys, polyesters and vinyl esters. In present, the principal domain of utilizing in the construction industry is the structural retrofitting. The strengthened elements can be concrete, brick, timber, steel or stone, and from the structural point of view beams, walls, columns, slabs and floors. In the following the type of these strengthening and their principal characteristics are presented.

These strengthening systems use strips manufactured by pultrusion process, having a fiber content of 60-70%, oriented in one direction. The strips are bonded manually with an adhesive to the prepared surface of the element, in this way increasing the load bearing capacity for shear and bending moment. Because of reduced flexibility, these systems are used more frequently in the case of plane surfaces, such as the floors, walls and beams. The strips can have different width, thickness and quality, being available in any desired length.

The strengthening process is very simple, quick and easy, however qualified work is needed.

In the case of strengthening the elements for bending moment the strips can be bonded simply, existing the possibility of prestressing. At the shear strengthening of the reinforced concrete beams can be used L shaped strips, which work as the stirrups after the bonding.

The strengthening systems with fabrics (called wet lay-up systems) generally are applied manually, using fiber sheets bonded to the prepared element surface with resins, in this way increasing the flexural and shear strength, respectively the impact and explosion resistance of the element. Because of the flexibility it is easy to apply to the circular and rectangular elements, or with curvatures. The available fabrics are from carbon, glass, aramide or hybrid fibers, usually oriented in one ( $0^\circ$ ) or two ( $0^\circ/90^\circ$  or  $45^\circ$ ) directions.

At the application of this system is very important the direction of lay-up. In the case of more layers, when the lay-up direction is different, or when the fabric has more direction, the value of the strength is decreasing. The fiber content has also an important influence, the strength increasing with the increasing of this.

Completely wrapping around the section on all four sides is the most efficient scheme and is commonly used in column applications, where access to all four sides of the column is usually available. In beam application, where the slab makes it impractical to completely wrap the element, the shear strength can be improved by wrapping the fabric around three sides of the member (U-wrap) or bonding to the two sides of the member.

In construction the composite rebars are usually used in concrete reinforcement, but in the last time also as externally strengthening. The main advantages of the composites are the increased corrosion resistance and the high tensile strength, respectively reduced weight, with 25% less than the steel.

Strengthening with prefabricated bars are very advantageous, because are easy to apply, quick and efficient. At the installation a groove is cut in the desired direction into the surface of the element and then filled half way with resin. The rebar is placed in the groove and lightly pressed. This forces the resin to flow around the rebar and fill completely between the rebar and the sides of the groove. Finally, the groove is filled with more resin and the surface is levelled. The method can be used very well in combination with fabrics.

To use the composite materials correctly and with maximum efficiency it is necessary to know the advantages and disadvantages of these. The principal advantages of the retrofitting with composites are the high ultimate tensile strength, low weight, versatile of the systems and solutions, durability, reduced construction period, ability of prestress, not require maintenance.

The potential disadvantages of the composites are the followings: relatively high cost of the systems, susceptibility for mechanical damage, sensibility for ultraviolet (UV) radiation and for increased humidity, reduced fire resistance, modulus of elasticity and ultimate tensile strain lower in some cases.

The use of strengthening with composites is recommended in the following structural modification:

- structural deterioration caused by the environmental action (ex. reinforcement corrosion)
- inadequate exploitation or rigidity of the structure or the element
- overstresses appeared after the structural or functional changes
- change of the conditions and (renewed) the design codes
- increase of the safety requirements
- modifying the live loads
- tension losses in the reinforcement due to corrosion in the prestressed concrete
- inadequate deformation capacity

Strengthening with composites also can be used successfully when is reducing the installation period is needed, respectively in places with limited access and when is not permitted to add significant loads to the structure.

## **2.2 Experimental assessment on shear strengthening of clay brick masonry walls using different techniques**

The seismic vulnerability of the masonry buildings was obvious during the major seismic events across the world. One of the latest examples was the case of the residential buildings from the town Moldova Noua, Romania, which were damaged after the earthquake in 2002. A significant number of masonry elements suffered serious damages, and the use of an effective retrofit technique was needed to increase the in-plane and out-of-plane strength and stiffness of the masonry walls.

The investigated retrofitting systems were the fibre reinforced polymer (FRP) composites, the reinforced mortar jacketing (RMJ) and the steel wire meshes (SWM). All these strengthening methods were studied in the Department of Civil Engineering of the Politehnica University of Timisoara, Romania, the SWM being a part of the international project PROHITECH. The objective was to investigate the behaviour of the unreinforced clay brick masonry walls subjected to in-plane shear loads strengthened with different techniques.

Although initially the cost of the materials of FRP and SWM solutions is higher than the traditional retrofit methods for the masonry walls investigated, such as the RMJ, the efficiency and the ease of application can lead to an economic result.

### 2.2.1 Numerical analysis

In the first stage, it was performed an analytical study with a simplified (theoretical) model of the wall. The goal was to conceive a device in which the load system creates a pure in-plane shear of the wall, without much influence from the bending moment. This system is auto-equilibrant and, theoretically, the crack should form in the diagonal direction. The loads applied to the specimen were a constant vertical (V) force and an increasing horizontal (H) force. With this set-up a large number of finite element analyses (FEA) were performed, by modifying the width to height ratio ( $d/h$ ) of the elements ( $d/h=1$ ,  $d/h=1.5$  and  $d/h=2$ ), the quality of the brick and of the mortar, through the strength and the modulus of elasticity of the element, the horizontal load-steps, and finally by applying a constant vertical force of different magnitudes.

The first analyses were performed with the program BIOGRAF, developed in the Department of Civil Engineering from Timisoara, which allows a step by step modification in principal stresses and the formation of the cracks, their angles and widths. After every step, the program recalculates the stiffness and the modulus of the element. For complementary analyses AXIS VM software was used. Taking into account the dimensions of the bricks, the studied wall specimen had height to width ratio equal to unit, thus the final width of the wall was chosen 150 cm. This aspect ratio also represents the masonry wall pier dimensions widely encountered in older brick structures. From the analytical models were obtained the distribution of the principal stresses, the crack propagation in the wall, the probable failure load and the collapse mechanism.

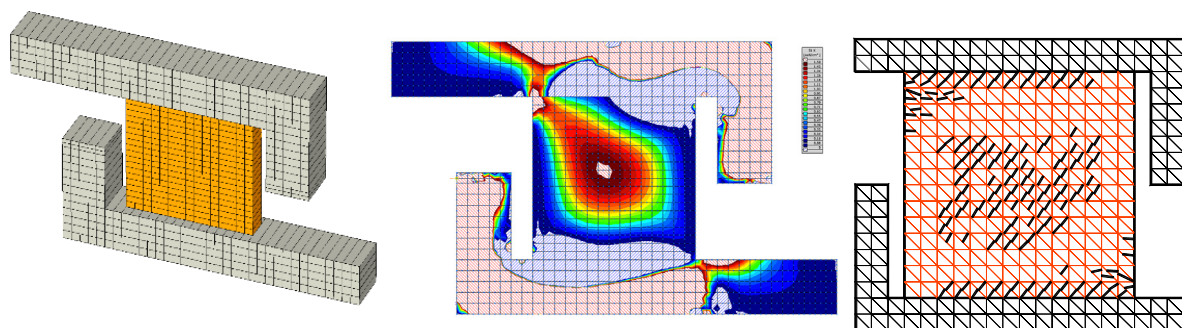


Figure 1. *Finite element analysis of the masonry specimens*

Theoretically, the application of the vertical force is not necessary in the case of homogenous materials, but the brick wall is composed of clay brick units and mortars, which have different characteristics. Therefore, to prevent a sliding failure mode, a vertical force was applied.

### 2.2.2 Experimental test set-up

The experimental specimens were 150 cm wide and 150 cm high, built of from solid clay bricks with dimensions  $6.3 \times 24.0 \times 11.5$  cm and unit strength  $9.0 \div 10.0$  N/mm<sup>2</sup> and cement based mortar with strength  $10 \div 16$  N/mm<sup>2</sup>. At the top and at the bottom of the wall it was placed a reinforced concrete beam with dimensions  $50 \times 150 \times 25$  cm.

The walls were tested in a special device, composed of a pair of L-shaped solid steel elements attached to the massive reinforced concrete block, which was part of the wall at the top and the bottom. The forces have been applied in monotonic way using hydraulic jacks. The vertical force was applied on the top of the specimen, acting through the reinforced concrete bond beam. The horizontal (shear) force was applied through a series of steel bolts embedded in the reinforced concrete block and mounted on the L-shaped steel elements at the top as well as at the bottom. In the frame of the project were performed also cyclic load tests in the CEMSIG Laboratory of the Department of Steel Structure (Dogariu et al. 2007).

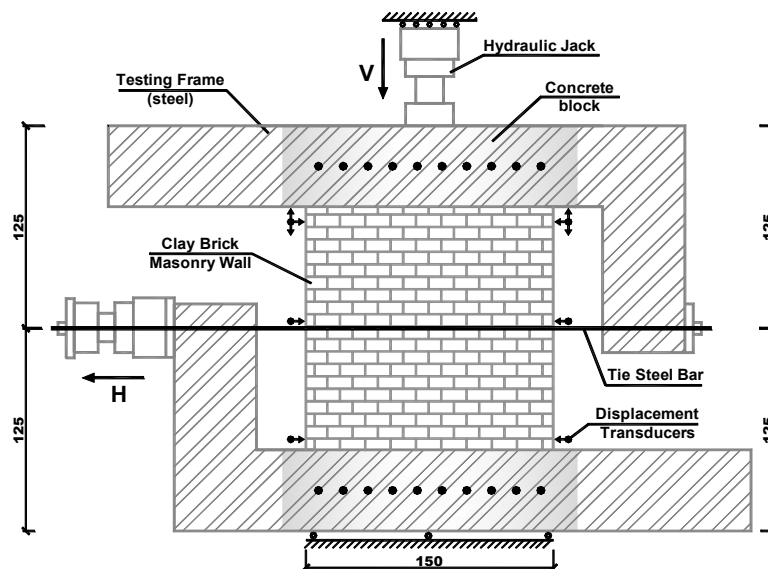


Figure 2. The specimen test set-up

The horizontal deformations of the wall were measured with displacement transducers, which were placed along the height of the wall, on the left and the right side. Other transducers measured the vertical displacements on each side of the specimen at the first and the last mortar bed joints, respectively.

A part of the masonry specimens were tested in as-built condition up to failure and then retrofitted and retested afterwards, another part were strengthened before testing. The walls were subjected to a constant vertical force ( $V$ ) and the monotonic increasing horizontal force ( $H$ ), applied by an increment of 5 kN up to failure, which generated the required in-plane shear forces in the specimen. The recorded data were the horizontal load, the horizontal and vertical displacement, the strain in the composite and the specimens' failure modes.

### 2.2.3 Experimental tests on masonry walls retrofitted with FRPs

The FRP composites are one of the most fastest and efficient strengthening systems used for retrofit structural masonry elements. In this test series the contribution of these materials was studied. First, Unreinforced Masonry (UM) walls were initially tested in the as-built condition. The failure of the walls was brittle through a diagonal crack from the top-right to bottom-left corner, as was expected. The load-displacement diagrams were typical for unreinforced masonry, the behaviour of the specimens being close to linear.

In the second step all the pre-tested UM specimens were retrofitted with FRPs. The composites were applied only on one side because in many situations, the modification of the facades is

not permitted or it is very expensive to execute. Therefore, in these cases only the inside surfaces of the walls are accessible.

The strengthening procedure was performed in several steps. Primary the cleaning of the wall surface with a grinder was done, followed by the blowing off the surface with compressed air. Afterwards the cracks were filled with resin or cement mortar and the unevenness of the surface were corrected, providing a smooth contact surface for the composite. The composite systems were applied with dry or wet fibre application process. Using plastic tools all the air-bubbles were dissipated and the excess resin was removed from the wall. After the retrofit was completed, the composite system was allowed to cure for seven days before testing.

The test set-up for Retrofitted Masonry (RM) wall specimens was identical as was used for the baseline specimen (UM). In addition, strain gages were attached to the composite in the maximum stress zones, which were aligned in the direction of the carbon fibres.

In the first set the UM1 wall was subjected to a constant vertical force which was  $V = 200$  kN, the failure produced through a diagonal crack from the top-right to bottom-left corner. The behaviour of specimen was close to linear, typical for unreinforced masonry. The appeared crack was filled with epoxy mortar. The failure mode of the retrofitted RM1 wall was extensive cracking, followed by composite debonding at the cracks. The strain in the composite reached 0.5 %, demonstrating that this retrofit solution works really well with clay brick masonry.

In all the following sets the constant vertical force was increased with 100 kN, correlating with the previous case, because the quality of the walls was superior to the first element and it was necessary to avoid the sliding in the horizontal bed joint.

The failure of the UM2 wall was brittle through a diagonal crack, which was filled with epoxy mortar before strengthening. The RM3 wall failure was produced through the development of a new crack and through its extensive opening. The composite debonded just in the crack zone, but it was not broken. The strain in the composite reached 0.15 %, demonstrating that the system had high reserves in the moment of the specimen failure.

The failure of the UM4 specimen was also brittle through a diagonal crack, which opened approximately 1.0 cm. Afterwards the crack was filled with cement mortar. The RM5 wall failure was produced through the extensive opening of the existing crack, simultaneously with the composite debonding in the crack zone, but without its rupture. The strain in the composite at failure reached 1.78 %.

The UM5 failed through a diagonal crack with the maximum horizontal displacement just 4 mm. The failure of the RM6 specimen was produced by forming of many new cracks (especially in the upper half) and through the extensive opening of the existing one. The composite debonded on large areas, near the crack zone, but it was not broken. The strain in the composite reached 0.18 %.

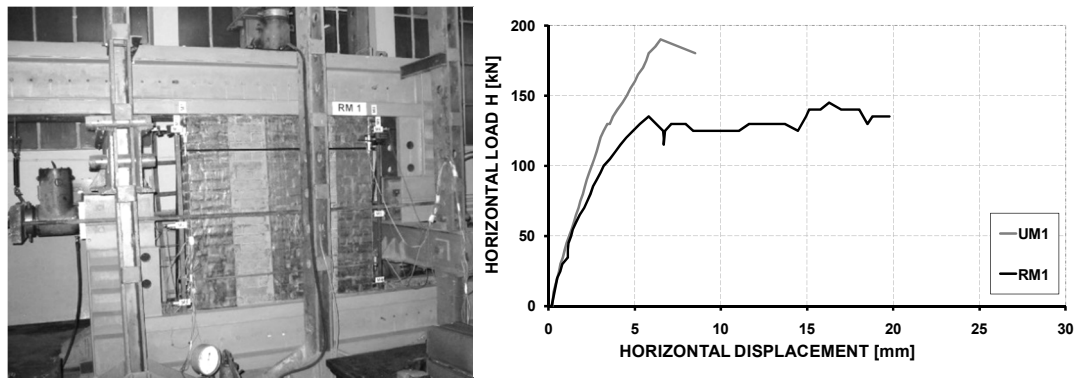


Figure 3. RM1 retrofitted wall and the load-displacement diagram of UM1 and RM1

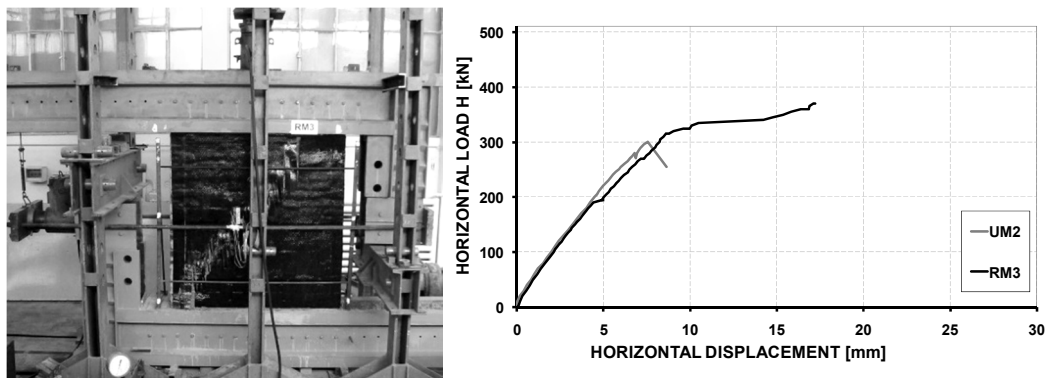


Figure 4. RM3 retrofitted wall and the load-displacement diagram of UM2 and RM3

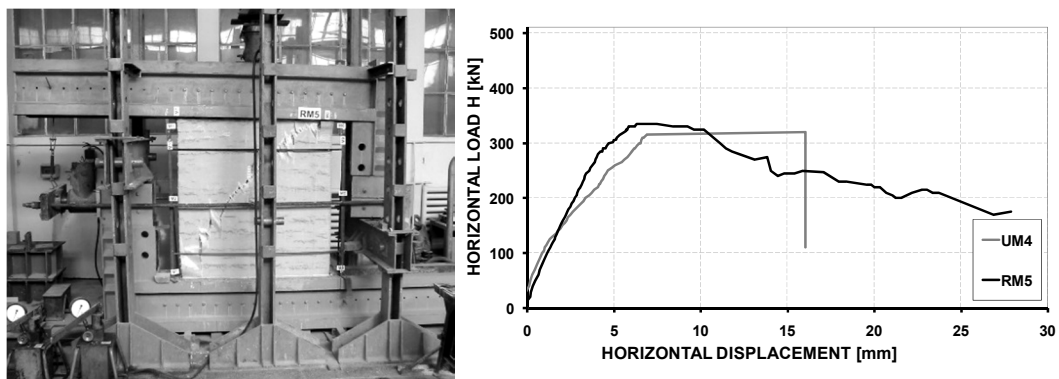


Figure 5. RM5 retrofitted wall and the load-displacement diagram of UM4 and RM5

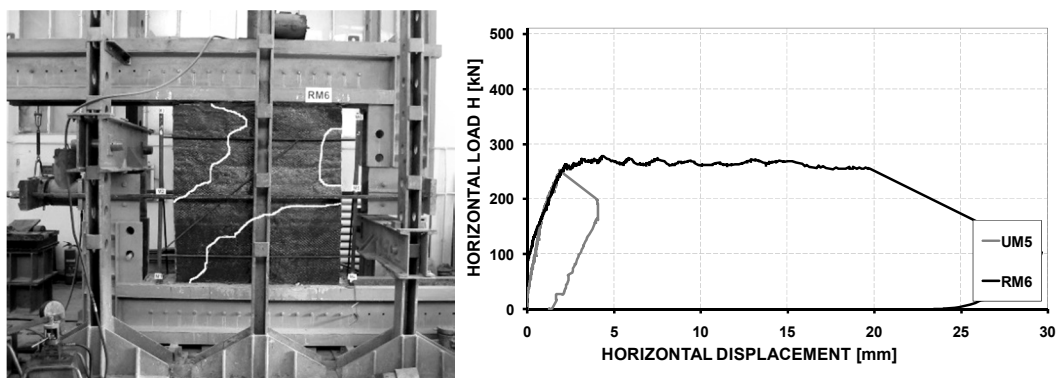


Figure 6. RM6 retrofitted wall and the load-displacement diagram of UM5 and RM6

## 2.2.4 Experimental tests on masonry walls retrofitted with RMJ

The classical solution for retrofitting a masonry wall is assumed to be the Reinforced Mortar Jacketing (RMJ). In the first step of this set an unreinforced masonry wall (UM2) was tested in the as-built condition up to failure, serving as reference wall. Learned from the first series of experiments the testing frame was slightly modified, blocking the vertical displacement of the top beam at the left end of the concrete block. The behaviour of the wall was similar to the previous ones, the crack developing from the top-right to bottom-left corner, but slightly curved, not in linear way. The load-displacement behaviour of specimen suffered some modification, the plastic deformations increased significantly, becoming more ductile than the specimens tested before (UM1 to UM5).

The strengthening was done using steel welded mesh with 4 mm diameter and 100 mm spacing, applied on both sides. For fixing and connecting the meshes, a number of 14 pieces of 6 mm steel bar was mounted and then covered with cement based mortar.

The test set-up for Retrofitted (R) wall specimens was identical as was used for the baseline test set-up (M). In addition, strain gages were attached to steel in the maximum stress zones, in horizontal and vertical direction also. The failure was produced by cracking of the wall in the same location as was before, followed by debonding of the jacketing in the compressed zones (top-right and bottom-left) and finally by tensional failure of several horizontal reinforcement.

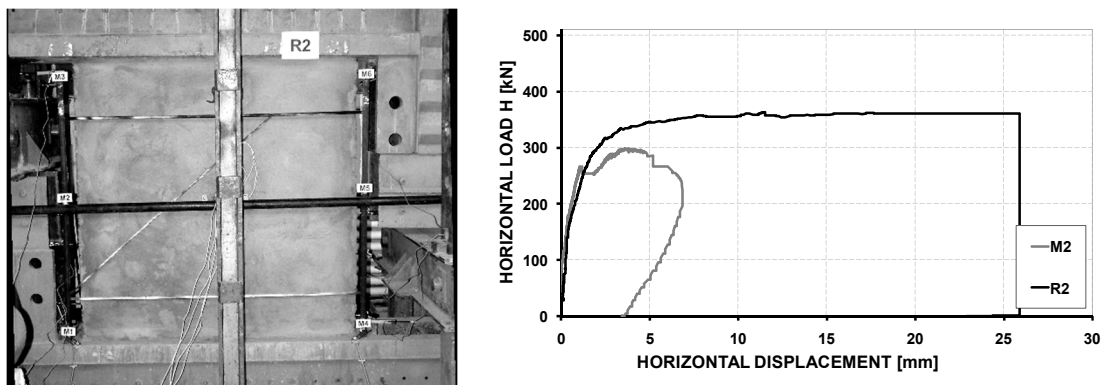


Figure 7. The R2 retrofitted wall and the load-displacement diagram of M2 and R2

## 2.2.5 Experimental tests on masonry walls retrofitted with SWM

Masonry walls strengthened with SWM system seems to be a promising solution in the increasing of the load bearing capacity. In this case the masonry wall specimens were strengthened before the testing and then were compared with the reference wall M2, tested at the RMJ system.

The SWM strengthening system used in this series was composed by stainless steel bidirectional fabric (wire mesh) applied with an epoxy based mortar. The spacing of the mesh was 1.0 mm, while the wire diameter was 0.4 mm.

The strengthening procedure was similar as the used for FRP systems. Primary the wall surface was cleaned and blown with compressed air. The unevenness of the surface was corrected, providing a smooth contact face. The wire mesh was cut to the prescribed dimensions and then fixed with short nails to the specimen. In the next step the application of the resin was done, in this case using metallic tools, up to the complete saturation of the mesh. Finally the excess resin

was removed and the system was allowed to cure for seven days before testing. Prior testing, strain gages were attached to the SWM in the maximum stress zones, aligned in horizontal and vertical direction, along the fibres. Additionally, for surface strain monitoring an optical measurement technique was used.

The test set-up for SWM strengthened wall specimens was identical as was used for the baseline test set-up (M2).

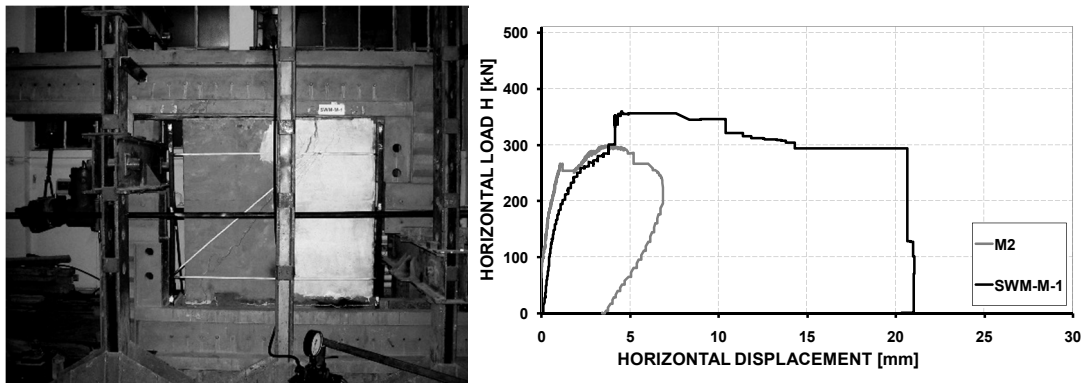


Figure 8. SWM-M-1 retrofitted wall and the load-displacement diagram of M2 and SWM-M-1

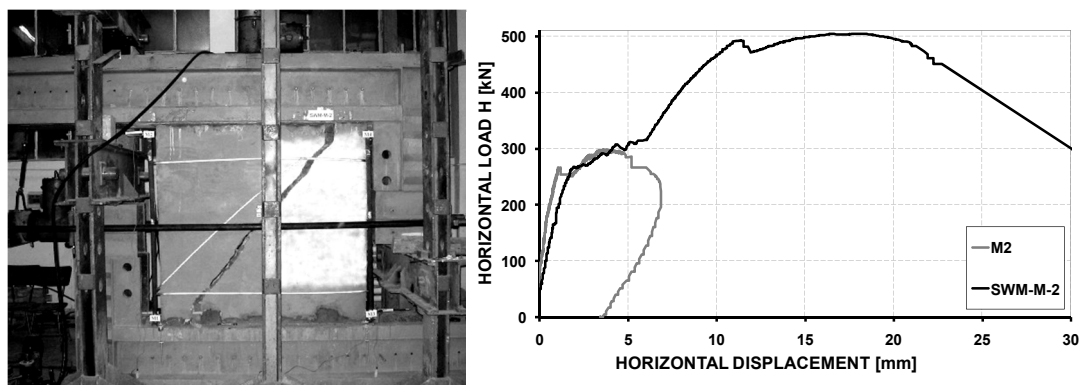


Figure 9. SWM-M-2 retrofitted wall and the load-displacement diagram of M2 and SWM-M-2

The SWM-M-1 failure was produced by gradually opening of a diagonal crack, yielding and finally tensile broken of the wires. Debonding of the strengthening system was observed just in the close vicinity of the crack. The strain at failure in the SWM system reached 0.317 %.

The failure of the SWM-M-2 was similar with the previous one, by gradually opening of a diagonal crack, debonding of the SWM in the compressed zone, yielding and then tensile broken of the steel wires. The failure was more sudden at a higher load. The strengthening system behaved well, other debondings were not observed, just in the close vicinity of the crack. The strain at failure in the SWM system reached 0.072 %.

Table 1. *Tested elements and the used strengthening*

Specimens Sets	Retrofit System	Application process	Retrofit Direction	Covering [%]
UM1/RM1	1	dry fabric	90	60 / 1 side
UM2/RM3	2	wet fabric	90	100 / 1 side
UM4/RM5	3	wet fabric	90	100 / 1 side
UM5/RM6	2	wet fabric	0	100 / 1 side
M2/R2	4	jacketing	0/90	100 / 2 sides
M2/SWM-M-1	5	dry swm	0/90	100 / 1 side
M2/SWM-M-2	5	dry swm	0/90	100 / 2 sides

Table 2. *Characteristics of the strengthening systems*

System	Components	Tensile Strength [N/mm <sup>2</sup> ]	Tensile Modulus [N/mm <sup>2</sup> ]	Thickness [mm]	Strain at Failure
1	Carbon Fabric	4000	231000	0.12	0.017
	Resin	30	4500	≈1.5	0.09
2	Carbon Fabric	3500	231000	0.34	0.015
	Resin	45	3500	≈1.5	-
3	Glass Fabric	2600	72400	0.36	0.037
	Resin	45	3500	≈1.5	-
4	Steel fabric	510	210000	4.0	6
	Cement mortar	3	-	20.0	-
5	SWM	650	-	0.4	0.40
	Resin	45	3500	≈4.0	0.09

### 2.2.6 Economic assessment of different strengthening methods

In the economical assessment of retrofitting systems five cases were investigated, consisted of: reinforced mortar jacketing (RMJ), steel shear plates (SSP), aluminium shear plates (ASP), steel wire mesh (SWM) and fibre reinforced polymer (FRP) composites. The impact of materials, manual labour and equipments (tools) on the final retrofitting cost was analyzed. Also, the execution time and conditions were taken into consideration. The purpose of these economic studies is to determine which of the proposed solutions proves to be more economically efficient. The economical assessment was conducted taking into account the structural performance of the masonry element for in plane shear stresses and the technological requirements.

After analyzing these data, several conclusions can be drawn regarding the solutions' economic efficiency, the amount of needed execution time and ease of application, data corroborated with the solutions' structural performances. This information can be observed in the chart presented in Figure 10, where for each of the methods the total costs and the execution time were highlighted, all of the values being calculated for one square meter. The value of the horizontal failure force is also presented.

The solutions that involved strengthening both faces of the wall were marked with an ellipse. Referring only to these methods, it can be observed that the most economically efficient is the jacketing (RMJ). This is quite normal since the largest influence into the final cost is the cost of the materials, and this method requires the most used materials in the construction industry (sand, steel reinforcement and cement), materials that have a relatively low price.

On the other hand, the most expensive method is the one that uses aluminium shear plates, with a cost 4 to 6 times higher than the cost of RMJ method. This method costs so much mainly because the use of the aluminium. As it was observed, the cost of the materials for the solution with aluminium is 8 to 12 times than for that of the RMJ solution.

The major advantages of using aluminium are the high increase in capacity and ductility, the ultimate horizontal displacement reaching values of 27 to 30 mm, in contrast with the solutions SWM-M-2 and SSP-CA-2 that reached the lowest values recorded in these test, around 15 mm. By analyzing the results obtained for the methods that involved strengthening of only one face of the wall, the most economically efficient prove to be methods SSP-PT-1 and SWM-M-1. These two methods require quite similar costs and execution time but the gain in ultimate capacity and maximum horizontal displacement is larger for the method SSP-PT-1.

Similar to the strengthening methods applied on both faces, for those that involve strengthening of only one face, the final cost is most influenced by the cost of the materials, the solutions that involves use of aluminium plates being the most economically inefficient. Basically, the methods that consist in using uncommon materials such as FRP and aluminium, prove to be more expensive.

The advantages conferred by the modern solutions in opposition with the traditional one are: the ease of application, shorter execution time, effortless handling due to the low weight of the materials, low supplementary loads induced by the strengthening materials, insignificant increase of the cross-sections' dimensions.

The manual labour cost is more or less the same for all of the methods, slightly higher for the methods that involve FRP. However, the cost of the equipment is the lowest for the ones that use FRP.

Each method has its advantages and disadvantages, and none of them is universally adequate. Choosing of one method or the other is the decision of the consultant, taking into account the purpose, location of the strengthened element, access, degradation, specific damages, ease of application. Demands imposed by the investor regarding architecture, cost or execution time are also decisive.

### **2.2.7 Conclusions**

The research program has been carried out in order to study the capacity increase of the pre-cracked (damaged) masonry walls retrofitted with different techniques, which are subjected to pure shear forces.

The theoretical calculus for the un-retrofitted elements was made with two design programs using the finite element analysis. The results obtained were the stress distribution, the crack pattern and the probable failure load. The strengthening was designed to restore the initial capacity of the elements without the modification of the stiffness. In the experimental part of the program more than twenty clay brick masonry walls were tested. Here were presented some

of the results considered by the authors more interesting and characteristic. Based on the test results, in following are presented the most important conclusions and observations.

1) The correction and the injection mortars had an important role in restoring the load bearing capacity. The width of the initial crack is decisive in the evolution of the final capacity of the strengthened wall: when tight, the capacity increased significantly over the reference value; when wide, the ultimate load capacity was approximately equal or lower compared to the baseline values.

2) A considerable capacity increase was observed for the pre-cracked shear walls retrofitted with all systems (practically, the load bearing capacity of the cracked walls was negligible). The failure of the retrofitted walls was different in function of the system used.

In the case of FRP strengthened walls the failure was caused by the extensive opening of the principal crack followed by FRP debonding and not due to tensile or shear failure of the FRP. It is necessary to mention, that the vertically applied composites debonded just in the vicinity of the major crack, while those applied horizontally debonded in large areas, in the middle part and even on entire wall width. In this case the use of anchorages could increase substantially the final capacity of the retrofitted wall.

In the case of RMJ strengthened walls the failure was caused by cracking of the jacketing in tension, followed by debonding of the mortar jacket in the compressed corners and finally through tensional failure of some horizontal steel bars of the mesh.

In the case of SWM strengthened elements the failure was produced by yielding and then by rupture of the horizontal and the vertical wires along the diagonal principal crack, with small debonding near the crack.

3) The maximum horizontal displacements increased at least twice compared with the displacements of the reference specimens that demonstrated the increase of the ductility and of the energy absorbing capacity of the retrofitted walls.

4) The most advantageous strengthening system with respect to the increasing of load bearing capacity proved to be the SWM system, while the FRP system with the dry fibre application process proved to be the fastest application method. The cheapest system, considering the material and application costs, and at the same time the most efficient system, calculated from the ratio of the execution costs and the reached maximum loads, proved to be the RMJ system.

Unreinforced masonry walls subjected to shear forces behave in a very brittle way and fail with or without warning. By strengthening such a non-ductile structural element with the above mentioned techniques the characteristic behaviour became rather ductile than elastic.

### **Acknowledgement**

The tests were carried out in the Laboratory of the Department Civil Engineering from the Politehnica University of Timisoara. A part of the techniques were developed in the frame of PROHITECH project (Earthquake PROtection of HIs torical buildings by reversible mixed TECHnologies, Grant FP6, 2005 - 2008, coordinated by Prof. Dubina D.). The studies and research work was granted to some extent by the National University Research Council, Romania.

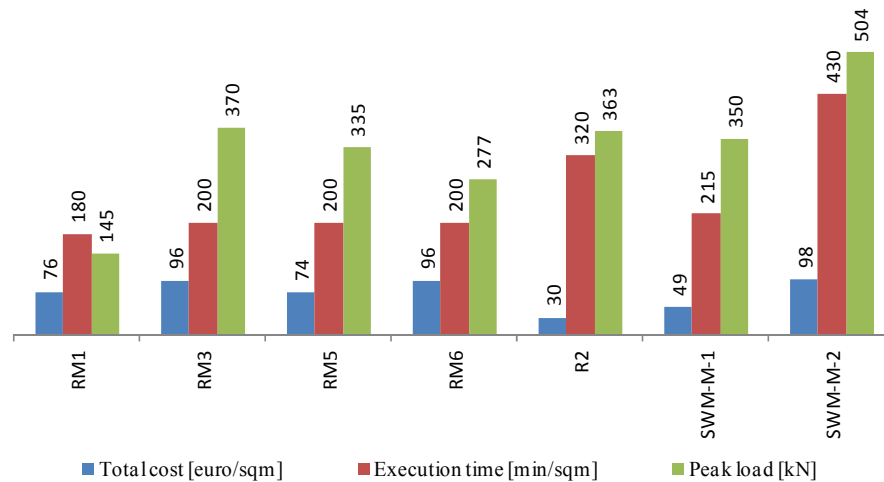


Figure 10. Economical comparison of the strengthening solutions

## 2.3 Theoretical and experimental study of reinforced concrete shear walls with cut-out openings retrofitted using FRP composites

### 2.3.1 Introduction

The load resisting structural systems evolved considerably in the past one hundred years from masonry and timber to reinforced concrete (RC) and structural steel. The analysis and design of materials and structures was one step behind of the technology and consequently the process of learning from faults prevailed. These faults were evidenced most strikingly by earthquakes, when life and economic losses were put in the balance. The structural engineers are required to devise lateral load resisting systems and the lateral load demand must be evaluated. There is a 100 year old debate on this subject involving explanatory theories and design philosophies, thousands of experimental tests and a series of earthquake reports. However, almost each significant earthquake reveals unaccounted issues.

The seismic performance of reinforced concrete wall structural systems was reportedly satisfactory as opposed to the performance of frame systems. This can be attributed to the wide diagonal load path available to transfer the lateral loads from one level to the other with sufficient stiffness to avoid large deformations which would cause eccentric gravity loads and non-structural damage. The degree of engineering of a shear wall improves its lateral load response, but even plain concrete walls were effective in avoiding catastrophic collapses. There is an ongoing scientific debate regarding the shear transfer mechanism in RC walls and whether design assumptions of ductility and the extent of energy dissipation are correctly accounted for with respect to the as-built response.

Despite this excellent seismic performance, the general use of RC wall structural systems is hindered by a series of factors such as functional space requirements and some professional and social antagonism. Instead, structural systems that combine RC frames and walls are preferred more widely. Nevertheless, in some regions of the world like Eastern Europe, Russian Federation and Chile a considerable many residential buildings were constructed of wall structural systems of either monolithic or precast reinforced concrete. Romania is a typical example, with tens of thousands of mid-rise apartment blocks built using the precast large panel system. The seismic performance of these structural systems was tested by several Romanian earthquakes (1977, 1986 and 1990) and responded satisfactorily. On the other hand, the large

panel structural system features very limited space flexibility and this constitutes a drawback from a functional standpoint. For instance, an occupancy change from residential to commercial, which is quiet frequently the case of the ground floor apartments, imply a functional vs. structural controversy. The functional side requires more open space and therefore proposes to remove some wall portions while the structural side protects the integrity or performance of the walls.

Structural alterations by doorway cut-outs impair the seismic performance of a reinforced concrete wall member. According to the common sense of structural engineering the weakening effect should be proportional to the size of the cut-out opening, although this assumption needs further data regarding the shape and position of the opening. Moreover, the weakening should be specified in terms of strength, stiffness, ductility and energy dissipation. Even the assumption of weakening may be subject of investigation with respect to the structure's overall response given that slitted walls were adopted as seismic rehabilitation method.

In order to enhance the seismic performance of the cut-out weakened walls retrofitting should be carried out. The strengthening technique of FRP-EBR (Externally Bonded Fibre Reinforced Polymers) was introduced in the past twenty years and gained widespread application for its advantages with respect to conventional/traditional methods primarily for RC beams and column members and masonry elements. As with many other novel techniques, the structural engineering research and design regarding the FRP-EBR strengthening is one step behind technology and application, consequently a series of unaddressed issues are expected. As externally bonded reinforcement (EBR) this technique can be used similarly (emulating) to conventional steel reinforcement, bearing in mind the differences between them in terms of material and geometric properties. In the case of an RC shear wall the reinforcement, either steel or FRP, should be flexural, shear or confinement and should have corresponding directions at specific locations: vertical concentrated at the extremities, horizontal or diagonal in the web, and transversal, respectively. Furthermore the strengthening should address the behaviour aspects as strength, stiffness, ductility and energy dissipation.

The objectives were to investigate the seismic performance of the precast reinforced concrete walls, assess the weakening effects caused by doorway cut-outs and reveal the effects of the seismic retrofit by externally bonded carbon FRPs.

This part presents a brief and partial overview of a wider experimental program on the application of Fiber Reinforced Polymers (FRP) for strengthening of precast concrete large panels affected by cut-out openings. This program was initiated and coordinated by the candidate and it received financial support from the Romanian National University Research Council (CNCSIS) through a number of research grants acknowledged at the end of this chapter. Most of the information presented hereinafter was published in the PhD thesis "Seismic retrofit of precast RC walls by externally bonded CFRP composites" by Demeter István (2011).

### **2.3.2 Building inventory**

Likewise other Eastern European countries, Romanian urban areas underwent significant transformation during the second half of the 20th century, regarding the housing conditions. A considerable 28% of the total room area of residential buildings, as of 2002 according to National Institute of Statistics (NIS 2002) was represented by flat blocks of reinforced concrete construction realised in the period of 1950-2000, totalizing more than 57000 buildings. Over 40000 of these blocks are low-rise 5-storey Precast Reinforced Concrete Large Panel (PRCLP)

buildings, see Figure 11, more than 3500 are 9-storey (P+8) and more than 4500 are 11-storey (P+10) mid-rises. The Romanian terminology used the large-panel residential building or large-panel block.

The construction period of the large panel started in the early 1960-ies and gained wide application starting from 1970, see Figure 11. A landmark event was the Vrancea earthquake of March 4, 1977. This event marked the decline of 11-storey (P+10) but didn't affect the ascent of 5-storey (P+4) and induced the emerging of 9-storey (P+8). Post-1977 large-panel reinforcement was modified, see later in this. The 1970 to 1990 period can be referred to as the decades of P+4 large-panel low-rises, with more than 36000 buildings constructed. The 1989-1990 marked the end of large-panel in Romania.

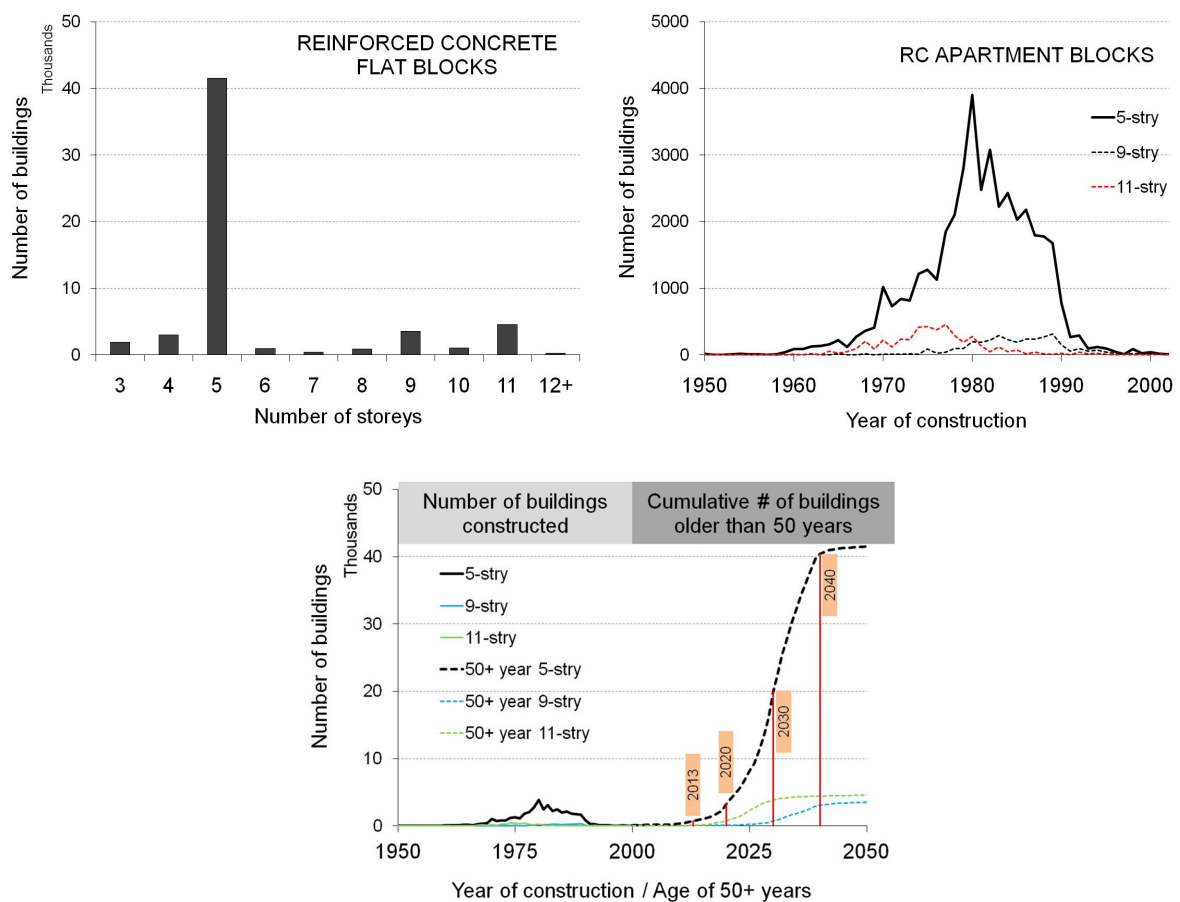


Figure 11. Reinforced concrete blocks of flats - Inventory and construction period of RC flat blocks in Romania

The architectural floor plan of a 5-storey large-panel block consists generally in four flat units and a staircase, without elevator shaft. The ground floor is at about 1 meter above street level and the utility (uninhabitable) basement level is about 2 meters below ground level. Terrace roofs are the prevailing roof types.

The structural system of the 5-storey PRCLP buildings is composed of the cast-in-place RC infrastructure and the entirely precast superstructure. The infrastructure consists in strip foundations and 200 mm thick RC walls. The superstructure was made of room-size (2÷5 m in their plane) precast slab and wall panels, assembled on-site through vertical and horizontal joints along their edges by lap welding of steel reinforcement and casting in-place concrete,

emulating the conventionally formed cast-in-place RC structures. Modular construction was employed using M300 mm as unit.

An analysis regarding the occurrence of the nominal wall lengths is presented in Figure 12. Principal (transverse) direction are only two dimensions, while the orthogonal (longitudinal) walls' length range from 1.8 to 4.5 m. The most frequent dimensions are the 3, 3.3 and 3.6 m. Note that the interior longitudinal walls are mostly solid walls.

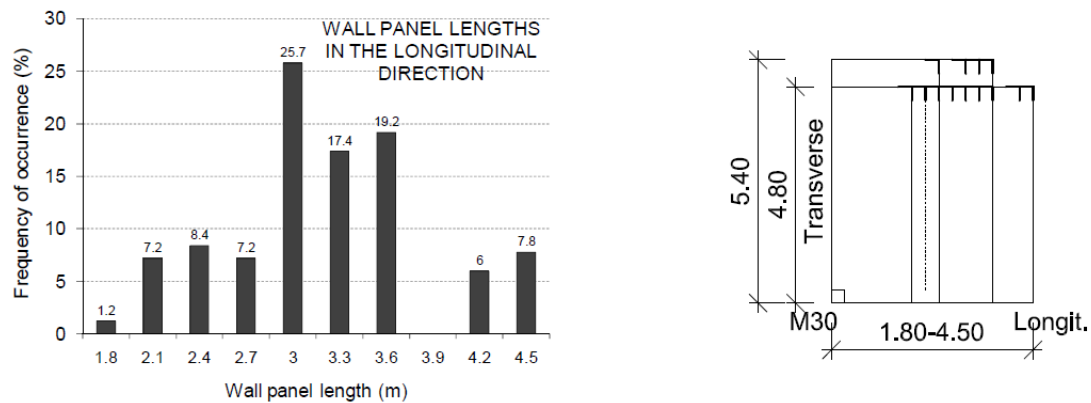


Figure 12. Wall panel lengths (in metres)

### 2.3.3 Database of RC structural wall seismic test programs

Laboratory tests on structural elements are aimed to reproduce the as-built loading and boundary conditions and observe the behaviour mode and measure the response. The experiments are excellent for checking the accuracy of theoretical predictions and/or to assess the behaviour for devising explanatory theories. As the number of experimental investigations increases continuously the need for the data to be ordered emerged also.

Three types of ordered information on lab tests were identified: reference list, catalogue and database. Reference list documents are the most widespread, in fact each experimental investigation report includes a review of the literature regarding other previous works in the field. Extended reference list documents are works dedicated especially to the review of the literature on a specific field. A catalogue type document furnishes more detailed tabulated information on the experiments, mostly on specimen basis. As the number of data lines increases in a catalogue it can be used for statistical evaluations employing specialised computer programs featuring filtering, sorting and searching functions and it can be referred to as database. RC wall cyclic test databases were assembled by Wood, Stanic et al., and Gulec and Whittaker. Online databases are the most easily accessible sources of test information and there is an increasing number of projects in this direction, for example Shear wall database of Palermo, University of Minho's DABASUM on FRP-based shear strengthening of RC beams, and RILEM's MSC Data warehouse on masonry strengthening with composite materials. It is important to note that a significant portion of the test data is not available, for language barrier reasons, proprietary issues or not in mainstream publications. The most important data sources are conference proceedings, journals and research reports.

#### Database characteristics

The database described in the following sections was assembled with the aim of a general overview of the cyclic tests carried out on RC walls. Generally, a database or catalogue has its

unit commonly a specimen. The present database differs from this by having its unit a test program, for reasons of reducing the collection time and bearing in mind the scope of focusing on the boundary conditions, which are in most cases invariables for a program. In general a database has two major clusters of data columns: specimen data and results. In the present phase the database contains information pertaining to the first cluster of program data. In these conditions it can be referred to as a condensed program database.

The data columns were grouped in three sets: program identification, specimen data and boundary conditions. The first set of data columns contains information regarding the laboratory the tests were performed at, year of publication and country name. As a convention, the year of reference was assumed to be corresponding to the earliest publication that contains detailed information on the program. Specimen data columns refers to designation, construction, specimen type, concrete technology, opening condition, strengthening condition, number of specimens, scale and web thickness. The third set of data columns includes information on the test-set-up, loading and boundary conditions.

It is noteworthy that most of the data columns represented a constant parameter for a specific program, therefore suitable for data processing. A few exceptions were represented by the wall thickness and specimen type, par example, which in many cases were variable inside a program, causing an effect of multiplication of the program. This was resolved by dividing the program in smaller units in order to have unique values for the data columns. This explains why other, more detailed information was excluded from the database. As of March 2011, the database contains 151 data lines and 222 reference lines. The discrepancy is owing to the fact that a certain test program commonly is published more than once at different stages of data processing.

### **General overview**

Early laboratory investigations on RC walls subjected to in-plane lateral loads were conducted starting from the 1950s in USA, Japan, Canada and New-Zealand. This early period can be considered until the end of the 1970s (Figure 13). A significant increase in the number of tested specimens in the 1980s and onward can be observed. It is important to mention that the actual content of the database is limited to the available literature in English language and consequently is not exhaustive. It would be of great importance to obtain country-level reports on this topic by resident researchers who have more in-depth view of the situation in their own country. The geographic distribution of the actual content indicates an approximately one-quarter share of the experimental work between USA, Japan, Europe and other countries. The tested walls were representative of prototypes pertaining to civil constructions and to Nuclear Power Plants (NPP), the first case being more common. In the following discussions the NPP-walls were not considered. According to the present content of the database the Romanian contribution to the RC wall experimental investigations is represented by 7 programs conducted at 4 laboratories, the earliest being dated from 1992. This should be also reviewed by researchers from each university centre in order obtain a more accurate view of the situation.

### **Specimen data**

The experimental specimens modelling prototype walls of civil structures were classified in component, element and building system types (Figure 13). Components are web-isolated panels or joint of precast elements. Wall elements are 1-storey, 1-plane and 1-bay structural members not framed by columns and beams. Wall building systems are multi-storey, multi-plane or multi-bay or frame-wall assemblages. A generic loading type data column was also

introduced at this stage in order to separate quasi-static tests from dynamic ones. Complex programs featuring both loading types were divided in two uniform groups so as to comply with this criterion. Subsequent discussions are restricted to wall elements and building systems (components excluded) tested in quasi-static manner (dynamic tests excluded). The distribution of storey numbers amongst the wall building system specimens is also indicated.

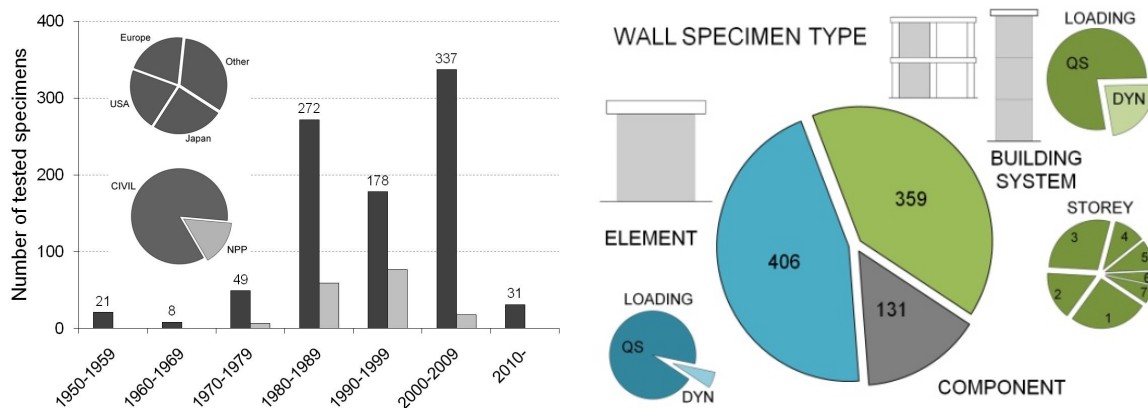


Figure 13. Review of the laboratory tests – timeline and types

Two further data columns referring to model-to-prototype scale and web thickness of the specimens were considered. These parameters exhibited different distribution according to the type of the specimens. The scale of the wall elements was chose to belong to the 0.25÷0.4 or 0.8÷1 ranges, while for the wall building systems the 0.2÷0.33 scale factor range was preferred. As for the web thickness, the 50, 80 and 100 mm values were representative of wall elements and wall building systems too.

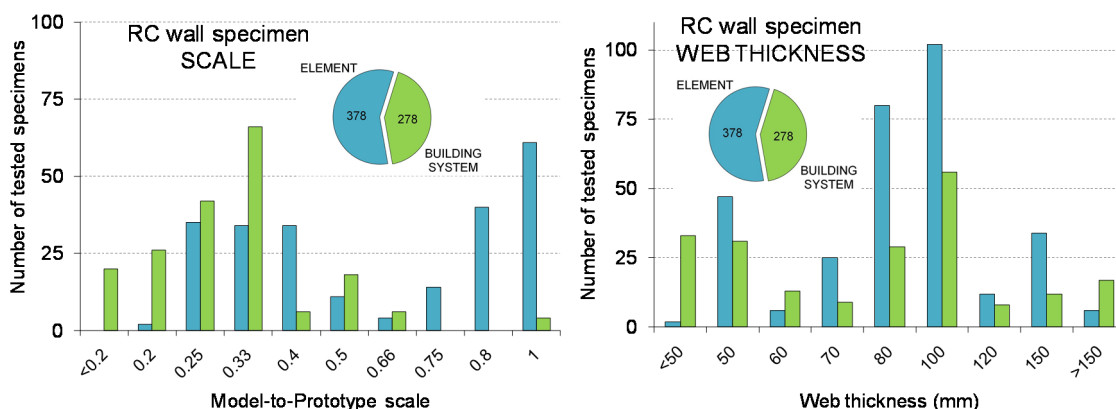


Figure 14. RC walls scale and wall thickness

A series of three data columns were taken referring to concrete technology, opening condition and strengthening condition. As it can be seen in Figure 15 the monolithic, solid and non-strengthened specimens prevailed over test programs including precast, solid with opening or slitted and strengthened specimens, respectively. Amongst the latter category three groups were according to the employed strengthening technique: conventional, FRP-EBR and other. Conventional techniques mean repair of the damaged walls by replacing of the crushed concrete and fractured reinforcements, FRP-EBR (Fiber Reinforced Polymers Externally Bonded on concrete surface), while other techniques included Steel Plates bonded, selective weakening, frame infill or wing walls. The restricted database contains 16 programs that included precast

walls, 14 programs that included walls with openings and 16 programs that included walls strengthened by FRP-EBR technique.

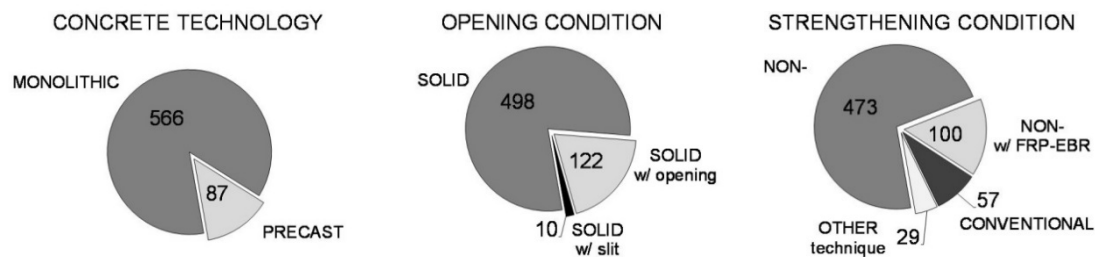


Figure 15. Distribution by concrete technology, opening and strengthening

### Data on test set-up, loading and boundary conditions

As presented in Figure 16, there are three types of boundary conditions, namely cantilever, restrained rotation and additional moment. These are the concerted effect of the test set-up, the loading procedure and the elements adjacent to the wall ends. The present experimental program is featuring a restrained rotation type boundary condition for the wall specimens, with a series of special traits inside this category. The restrained rotation boundary condition is promoting the shear behaviour as opposed to the flexural one, through reducing the shear span, that is, the base moment corresponding to the base shear. The test set-up adopted in the experimental program is featuring a zero overall base moment trait by the hinged end connections, although in the case of the specimens with openings there are interior moments possible to develop through the wall to base beam interface. The development of the moments is limited in both cases by the increasing axial loads, which acts against the vertical tensile forces. Therefore it can be stated that the shear span and the shear span ratio is negligible in the case of the solid wall, while it is slightly greater for the wall piers. The exact value is quiet difficult to evaluate, due to the variable axial loads, differences in the anchored vertical reinforcement in the two loading directions and the coupling effect of the spandrel beam. Consequently, shear behaviour is extensively stimulated.

Table 3. Tests on FRP strengthened walls

PROGRAM ID	SPECIMEN						
Laboratory-Year	Country	Designation	Type	Concrete techn	Opening	Strengthening	No. of spec.
CARLT-2000	Canada	wall	wall element	monolithic	solid	non; FRP-EBR	7
TOKYU-2000	Japan	T; U; RC; CF; CFR;	column wing-wal	monolithic	n/a	non; FRP-EBR	15
TUSJ-2000	Japan	Specimen	wall-frame syster	monolithic	solid; door; wind	non; FRP-EBR	10
AUTH-2003	Greece	MSW; LSW; FRPM	wall element	monolithic	solid	non; FRP-EBR	11
MGILL-2003	Canada	W	wall system	monolithic	solid	non; FRP-EBR; RC;	4
UUTAH-2003	USA	Specimen; wall as	wall system	precast	solid	FRP-EBR connecti	9
HOKU-2004	Japan	WA	wall-frame syster	monolithic	door; window	non; FRP-EBR	3
MMCAN-2004	Canada	CW; RW	wall element	monolithic	solid	non; FRP-EBR	3
NCREE-2004b	Taiwan	PF; WF	wall-frame syster	monolithic	solid; frame	non; FRP-EBR	6
UFUK-2005	Japan	W; specimen	wall-frame syster	monolithic	solid	non; FRP-EBR	6
UPT-2005	Romania	SW; RW	wall system	monolithic	solid; door	non; FRP-EBR	5
NTUSG-2010	Singapore		wall element	monolithic		FRP-EBR	4
UPT-2010	Romania	PRCWP	wall element	precast	solid; door cut-oun	non; FRP-EBR	5
UPT-2011	Romania	CSRCW	wall system	monolithic	solid	non; FRP-EBR	6

There are two principal shear transfer mechanisms, namely diagonal compression and diagonal tension. The third one would be the dowel effect of the kinking vertical reinforcement associated to the sliding shear failure. The boundary conditions of the present program eliminates the sliding-dowel mode by the construction of the two loading beams through the

shear steps and the diagonal tension mechanism by the lack of vertical reinforcement anchored to the cap beam and by the variable but always in compression axial loads. Consequently, the only mechanism that is permitted is the diagonal compression shear transfer. In these conditions the present boundary conditions can be referred to as a subtype of the restrained rotation, namely diagonal compression dominated shear transfer.

Besides the model-to-prototype issue, the question remains to be addressed is the adequacy of the adopted boundary conditions to reproduce the as-built real situation during a seismic event. The experimental elements are modelling a prototype ground floor wall, part of a large panel building. In general the free behaviour of an element may be significantly altered with respect to the condition when it is restrained/constrained to interact with other structural members connected to it. The boundary conditions adopted in the experimental program were aimed to reproduce the outrigger effect, deemed to be of high importance in the behaviour of lateral load resisting structural systems.

This effect was mentioned by Abrams 1991, but it was abandoned and only recently is gaining wider attention. The core idea is that the either of the extremities of a vertical structural member is restrained from rotation by the counterbalance exerted by the structural members on the uplifting side. This effect can be conveyed by a rigid diaphragm floor or directly through the vertical edges from orthogonal walls, the latter being the case for the large panels. The uplifting end attracts additional axial loads from the nearby elements to the extent which these axial loads are available, for the total amount is finite. It is interesting to note that the dynamic condition may increase the available axial loads due to a vertical uplifting acceleration that may be added or subtracted from the vertical acceleration of the ground motion. The amount of additional axial load available for a specific lateral load resisting element is a matter of structural system configuration and relative stiffness.

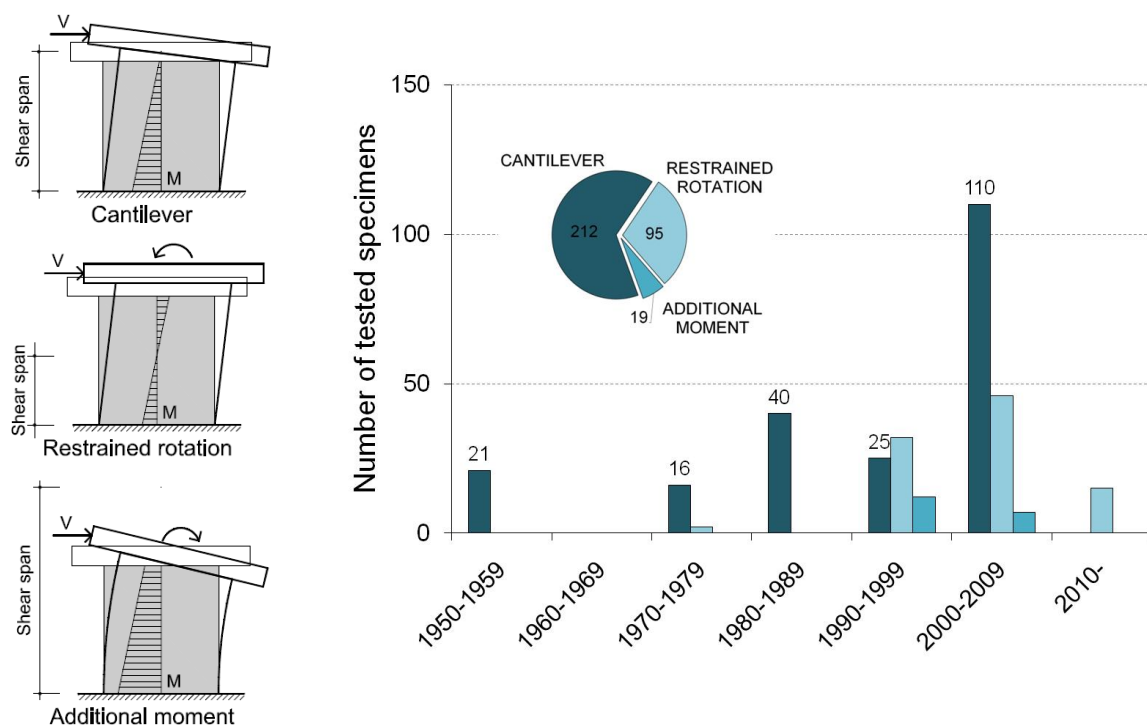


Figure 16. Boundary conditions, their timeline and distribution

### 2.3.4 Experimental program

The objectives of the experimental research were to record the seismic performance of the precast large wall panels considering the outrigger effect of adjacent structural members, to assess the weakening of doorway cut-outs and to investigate the performance of the CFRP-EBR strengthening method. The tests were carried out in the Reinforced Concrete Structures Laboratory of the Department of Civil and Industrial Buildings, Faculty of Civil Engineering, Politehnica University of Timisoara, Romania.

An outline of the test program can be structured in three levels. The first level is represented by a bare solid wall, see Figure 18, which was the reference specimen. The second level comprises two bare walls with cut-out openings, which were identical in all aspects with the solid reference, except the presence of the cut-outs. The difference between the elements of this level was the width of the door opening. The third level is composed by two pairs of strengthened specimens, which corresponded in all regards to the second level walls and were additionally retrofitted. Besides the opening size, the difference between the specimens of the third level consisted in the state of the walls at the time of retrofitting: after sustaining a number of damaging load reversals, the specimens of the second level were upgraded to the third one by repair and post-damage strengthening, whereas their counterparts were prior-to-damage strengthened.

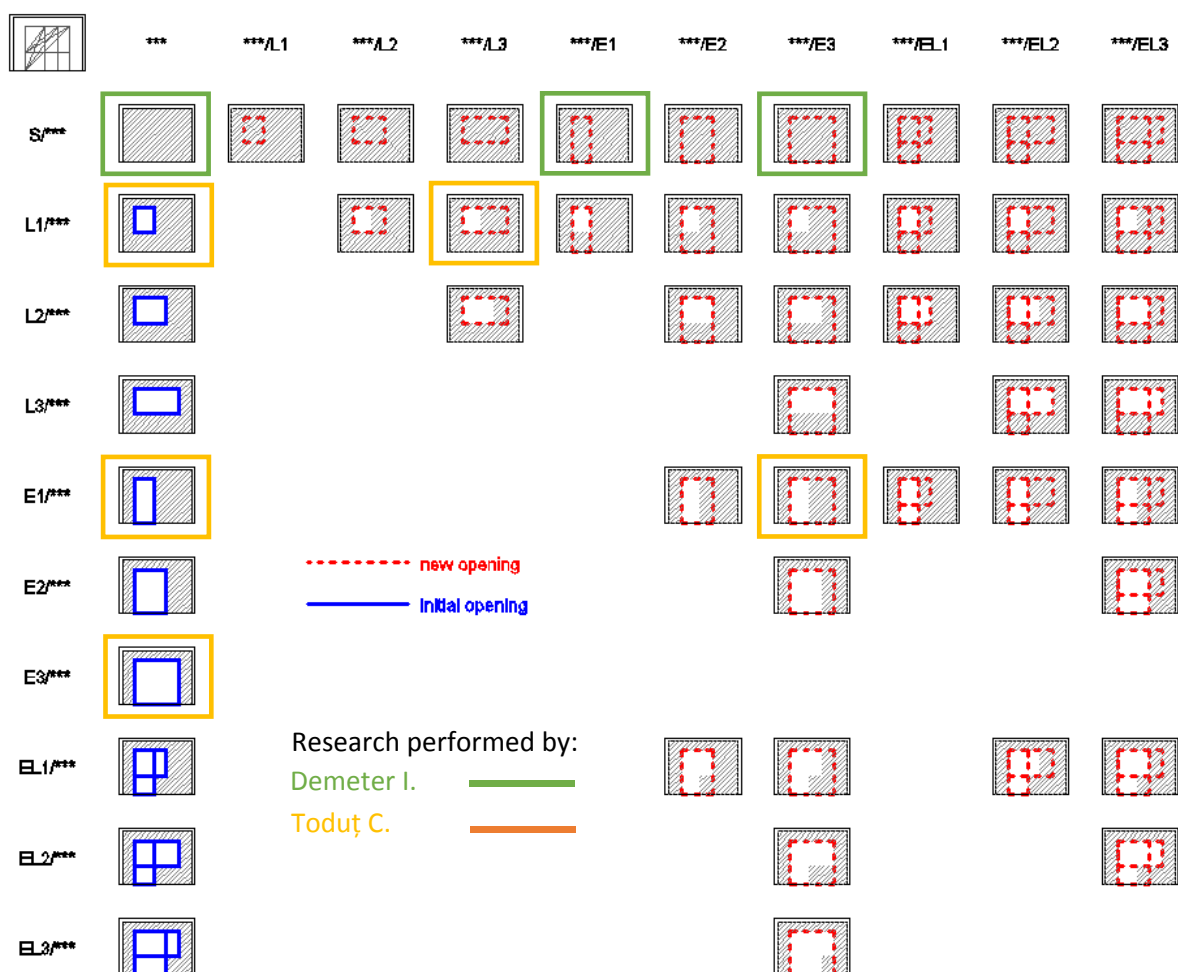


Figure 17. As-built / cut-out opening matrix.

A comparison line is defined as a series of at least two specimens or tests that are identical in all regards except one variable. These lines are set up in order to assess the effect of the investigated variable on the behaviour of the specimens. The present program contains three comparison lines, each of them comprising of three tests. The first comparison line was set to assess the weakening effect of doorway cut-out. The reference specimen of this line is the solid specimen while the variable is the cut-out width. The second and third comparison lines are referred to as strengthening effect of CFRP-EBR, with reference specimens being the bare walls with narrow and wide door cut-out, respectively and the variable being the strengthening condition.

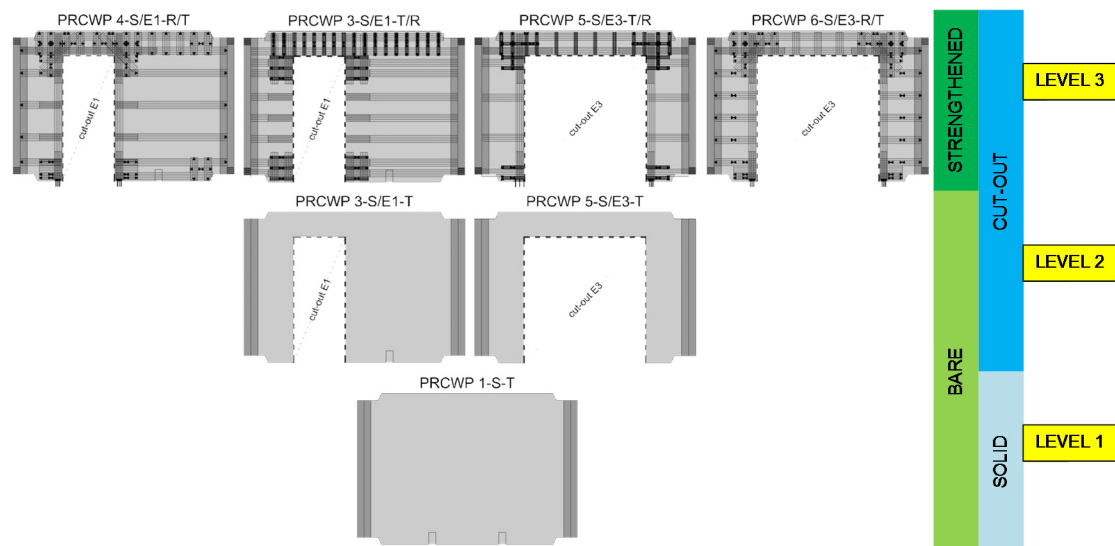


Figure 18. Test matrix for the current presentation

In the experimental part of the program a series of eight, 1:1.2 scaled wall specimens were constructed. The geometric dimensions, reinforcement arrangement and material properties of the wall panels resulted from an actual precast RC large panel building, according to a typical plan. The experimental variables were represented by the opening type (without opening, i.e. solid wall, narrow door, and wide door), the opening nature (as-built and cut-out) and the strengthening state. The discussion was focused on the strengthening strategies adopted for the specimens with both narrow and wide door openings.

The concrete outlines and the reinforcement arrangement of the solid wall (S), as well as the size and position of the cut-out opening are presented in Figure 19. Note that wall reinforcement, comprised of horizontal and vertical deformed bars and a welded wire fabric, was placed only in the mid-plane of the panel. The 750 mm wide by 1800 mm high door opening (E1) was positioned asymmetrically with respect to wall centreline by 500 mm to the left. This resulted in a narrow pier of 500 mm width (pier #1), a wide pier of 1500 mm width (pier #2) and a spandrel beam of 350 mm depth by 750 mm length above the opening (coupling beam). The 1750 mm wide by 1800 mm high door opening (E3) was positioned symmetrically with respect to the wall centreline, resulting two piers of 500 mm width and a beam of 350 mm depth by 1750 mm length above the opening (coupling beam). In order to ensure the out-of-plane stability, the wall panels were constructed with wing elements along the vertical edges, which were reinforced by longitudinal bars and hoops. The horizontal panel-rebars were anchored in the wing element, while the vertical bars (one for each wing) were lap-welded to the foundation.

The test set-up was designed to reproduce the in-situ boundary and seismic loading conditions of a wall panel at the ground floor of an actual PRCLP building. As force transmitter (cap beam) and as foundation (base beam) element two composite steel-concrete beams were used. The horizontal joint gap between the beams and the wall specimen was grouted with high-strength mortar. The axial (gravity,  $N$ ) and in-plane lateral (seismic,  $\pm V$ ) forces were induced by four hydraulic cylinders supported by reaction frames. The test set-up is depicted in Figure 20.

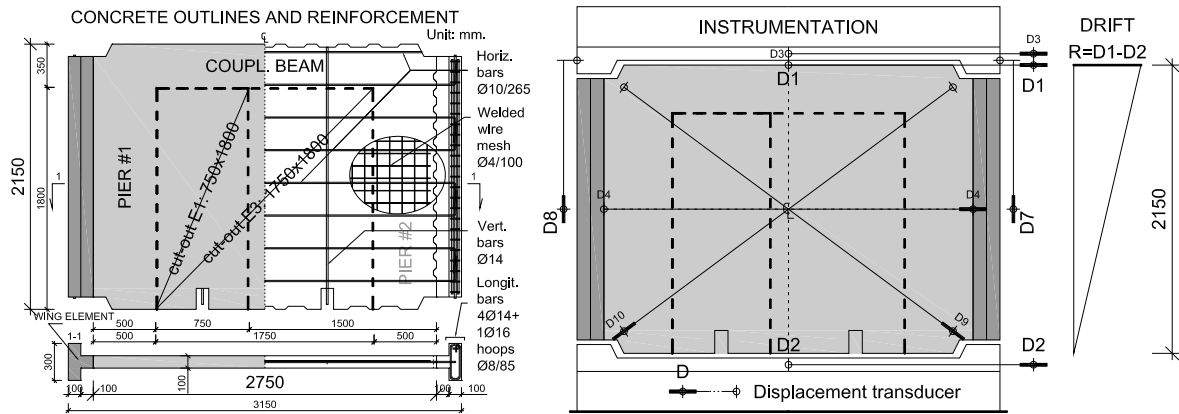


Figure 19. Concrete outline, reinforcement arrangement and instrumentation

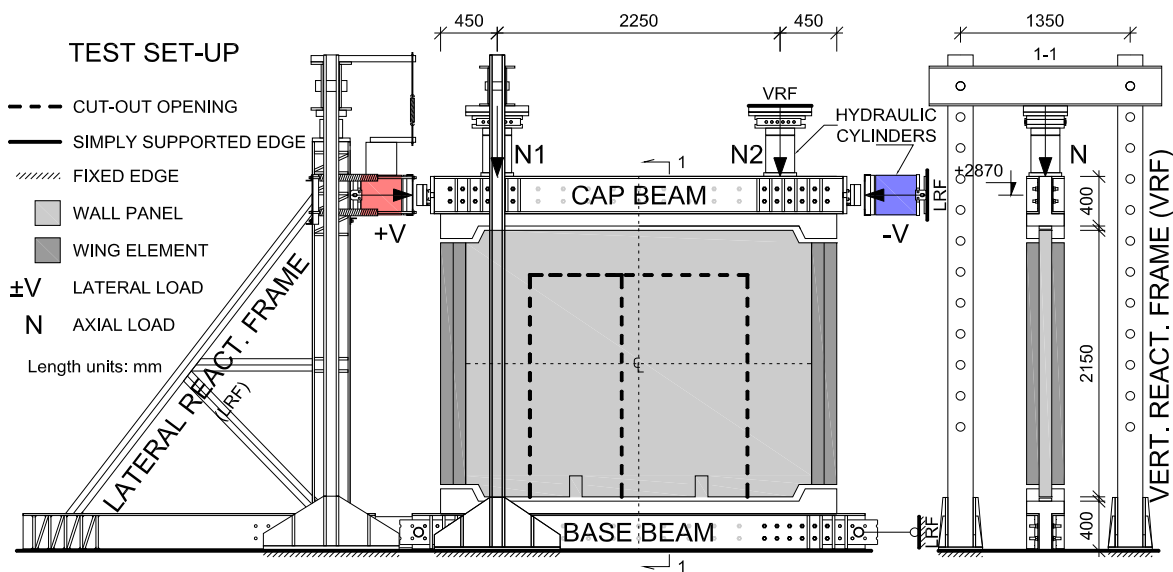


Figure 20. Test set-up

The designation pattern of the specimens, in accordance with the described experimental variables, is indicated in Table 4.

The experimental elements were subjected to pseudo-constant axial and quasi-static in-plane reversed cyclic lateral forces. The initial level of the axial loads was computed considering a normalized axial stress (the ratio of the induced axial stress to the characteristic cylinder strength of the concrete) of 5.1%. In addition, alternating axial loads ( $N1$  and  $N2$ ) were imposed in order to restrain the rocking rotation of the laterally loaded wall, these being controlled by the displacement control of the two vertical hydraulic cylinders, at a rate of 100 kN/mm (Demeter et al, 2008).

Table 4. Variables of the experiment

Element No.	As-built / cut-out opening type	Strengthening state	Element designation
3	solid wall / narrow door (S/E1)	non-strengthened (T)	PRCWP 3-S/E1-T
		post-damage strengthened (T/R)	PRCWP 3-S/E1-T/R
4		prior-to-damage strengthened (R/T)	PRCWP 4-S/E1-R/T
5	solid wall (S)/ narrow door (E3)	non-strengthened (T)	PRCWP 5-S/E3-T
		post-damage strengthened (T/R)	PRCWP 5-S/E3-T/R
6		prior-to-damage strengthened (R/T)	PRCWP 6-S/E3-R/T

Table 5. Wall specimen proportions

Component	L [mm]	H [mm]	b [mm]	$A_c$ [cm <sup>2</sup> ]	A [m <sup>2</sup> ]	$\alpha_s$ [cm <sup>2</sup> ]
Web-panel	2750	2750	100	2750	5.91	0.78
Boundary wing	200	1950	100	400	0.39	N/A
Wall specimen	3150	2150	100	3550	6.69	0.68
Cut-out E1	750	1800	100	750	1.35	2.4
Cut-out E3	1750	1800	100	1750	3.15	1.03
Pier #1	500	2150	100	500	1.08	4.3
Pier #2 E1	1500	2150	100	1500	3.23	1.43
Spandrel E1	750	350	100	350	0.26	2.14
Spandrel E3	1750	350	100	350	0.61	5

Note: L - length; H - height; b - thickness;  $A_c$  - area of cross-section; A - in-plane area;  $\alpha_s$  - aspect ratio.

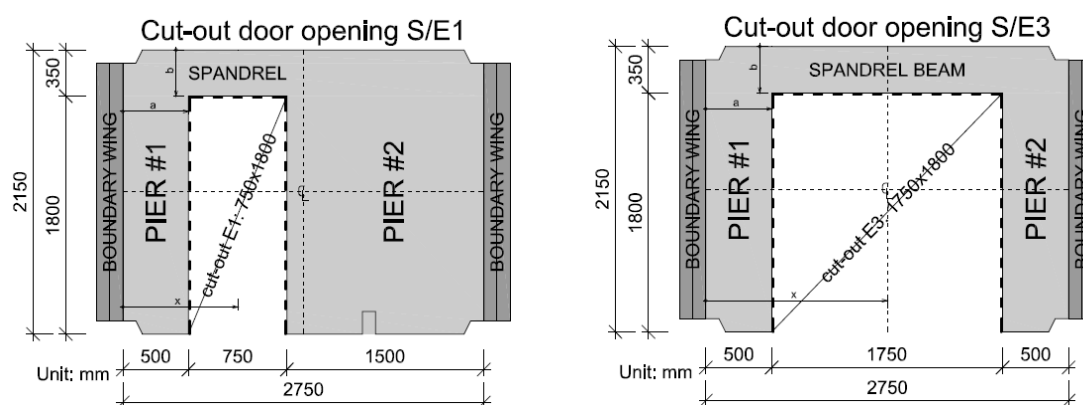


Figure 21. Cut-out openings

The axial loads were composed of two parts, namely a constant and an alternating (variable) part. The constant level was set so as to reproduce the gravity loading conditions at the base of a 5-storey large panel building. For this, a mean compressive stress of 0.9 MPa was considered. In order to account for the differences in the concrete properties, the normalised axial load ( $n$ ) concept was employed. This value yielded 5.1% for the nominally C16/20 as-built concrete. In the experimental program a 6%  $n$ -value was taken for the reference solid wall. The difference is caused by the overlook of the  $\beta_{cc}$  time factor in ciphering the characteristic concrete strengths, which was included later, when the tests were already performed. One can observe that the specimens with cut-out openings had normalised axial loads greater than 6%, namely

7.7% for the E1-cutout and 12% for the E3-cutout openings. The reason for this is that the axial loads correspond to the solid reference and the cross sectional loss caused by the cut-out implies the increase of the compressive stress. The initial compressive stress was in the 0.5÷1.7 MPa range, depending on the cut-out condition and the concrete compressive strength. In Figure 22 the normalised axial load values are indicated considering both the web-panel and boundary wing concrete properties.

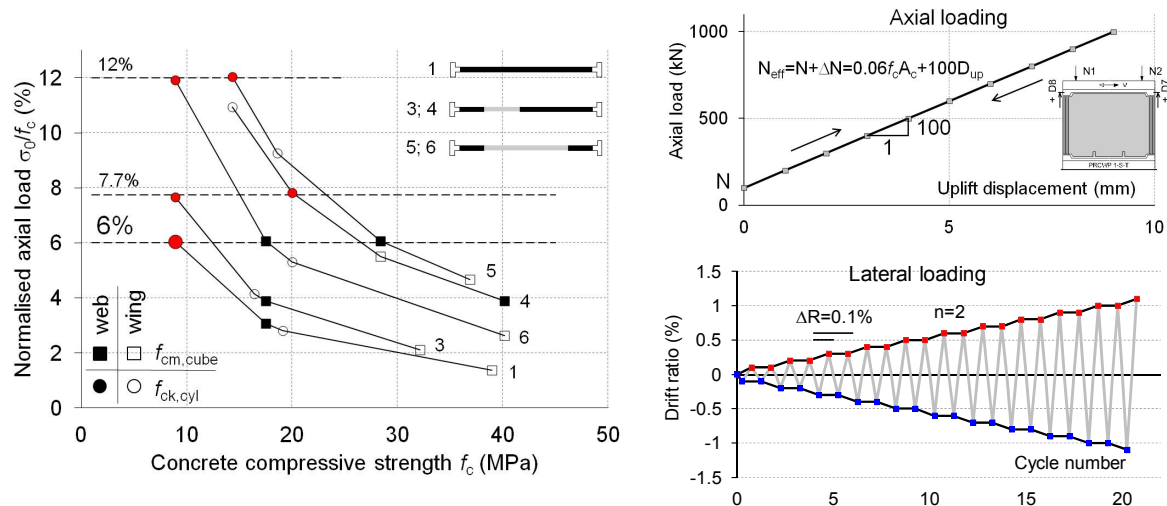


Figure 22. Lateral and axial loading strategy

Except for the first few cycles, the lateral loads were applied in displacement (story drift) control. The loading history was defined in terms of constant displacement increment of 2.15 mm (0.1% drift ratio) and two cycles on each displacement level. The failure criterion was assigned to the displacement level, where a 20% lateral load capacity drop was observed.

The behaviour of the experimental specimens was monitored by displacement transducers, strain gauges fixed on reinforcement bars and CFRP sheets, and pressure transducers. The instrumentation of the specimens is shown in Figure 19.

Structural alterations by doorway cut-outs, impair the seismic performance of a reinforced concrete wall member. According to the common sense of structural engineering the weakening effect should be proportional to the size of the cut-out opening, although this assumption needs further data regarding the shape and position of the opening. Moreover, the weakening should be specified in terms of strength, stiffness, ductility and energy dissipation. Even the assumption of weakening may be subject of investigation with respect to the structure's overall response given that slitted walls were adopted (Muto et al. 1974) as seismic rehabilitation method.

In order to enhance the seismic performance of the cut-out weakened walls retrofitting should be carried out. The strengthening technique of FRP-EBR (Externally Bonded Fibre Reinforced Polymers) was introduced in the past twenty years and gained widespread application for its advantages with respect to conventional/traditional methods primarily for RC beams and column members and masonry elements. As with many other novel techniques, the structural engineering research and design regarding the FRP-EBR strengthening is one step behind technology and application, consequently a series of unaddressed issues are expected. As externally bonded reinforcement (EBR) this technique can be used similarly (emulating) to conventional steel reinforcement, bearing in mind the differences between them in terms of

material and geometric properties. In the case of an RC shear wall the reinforcement, either steel or FRP, should be flexural, shear or confinement and should have corresponding directions at specific locations: vertical concentrated at the extremities, horizontal or diagonal in the web, and transversal, respectively. Furthermore the strengthening should address the behaviour aspects as strength, stiffness, ductility and energy dissipation.

### **2.3.5 Strengthening procedure**

Based on the behaviour and failure mode observed during the test performed on the non-strengthened specimens, the strengthening strategy was divided in three directions: (1) to offer flexural capacity along the edges of the cut-out opening, (2) to increase the shear capacity of the wall piers, and (3) to provide confinement effect at the cut-out opening corners. Before strengthening, the damaged specimens were repaired by replacing the crushed concrete with high-strength mortar. The substrate preparation consisted in grinding the concrete surface, rounding the edges, drilling holes through the wall and vacuum-cleaning.

Strengthening of the walls was carried out with CFRP fabrics, using the Externally Bonded Reinforcement (EBR) technique. Two types of unidirectional Carbon Fibre (CF) sheets (S1 and S2) were applied by dry layup and wet layup method, respectively. The S1 and S2 CF-sheets were utilized in form of strips with 100 mm and 50 mm width, respectively. The strengthening was carried out symmetrically on both faces of the wall. A description of the order, form and position, and the application procedures for the walls are presented below.

#### **Strengthening of the walls with narrow door openings (3-S/E1-T/R and 4-S/E1-R/T)**

The strengthening layout of specimens with narrow door opening is presented in Figure 23 and 24. The flexural strips (f) were placed horizontally on the coupling beam and vertically on the wall piers alongside the opening. Note that for specimen #3 the flexural strips were applied in one layer and the piers were not CFRP-anchored to the foundation, while for specimen #4 the flexural strips were doubled at the opening's corners and CFRP-anchorage was provided. The shear strips (sh) were aligned parallel to the shear forces, i.e. horizontally on the piers and vertically on the coupling beam. The stirrup-like confinement (c) strips were closed by CFRP tows referred to as through-wall anchorages.

#### **Strengthening of the walls with wide door openings (5-S/E3-T/R and 6-S/E3-R/T)**

The strengthening layout of specimens with wide door opening is presented in Figure 25 and 26. Alongside the opening, tensions resulted from bending was transmitted by the sheets type S1 (f1 and f3), supplemented at the corners with a second layer (f4, f5 and f6), while on the upper part of the coupling beam horizontal sheets (f2) were applied.

Anchorage of the sheets at the base of the piers was resolved using two methods. At pier #1 the vertical sheets (f3' and f6') were laid into a groove cut in the foundation, then filled with a resin and covered with an L-shaped steel profile fixed to the foundation with chemically anchored steel bolts. For pier #2 anchorage of the vertical sheets (f3 and f6) was realized using CFRP spikes inserted in the foundation and then spread on the wall.

The shear strips (sh) were aligned parallel to the shear forces, i.e. horizontally on the piers and vertically on the coupling beam. On the piers U-shaped S1-type sheets (sh1) were applied. For the coupling beam the S2-type sheets were disposed similarly as steel stirrups. At the middle of the span these were like opened stirrups, while at the ends were closed through overlapping

of the leg (sh3), or using transversal anchorages of short sheets (sh2) drawn through the holes performed in the preparing phase.

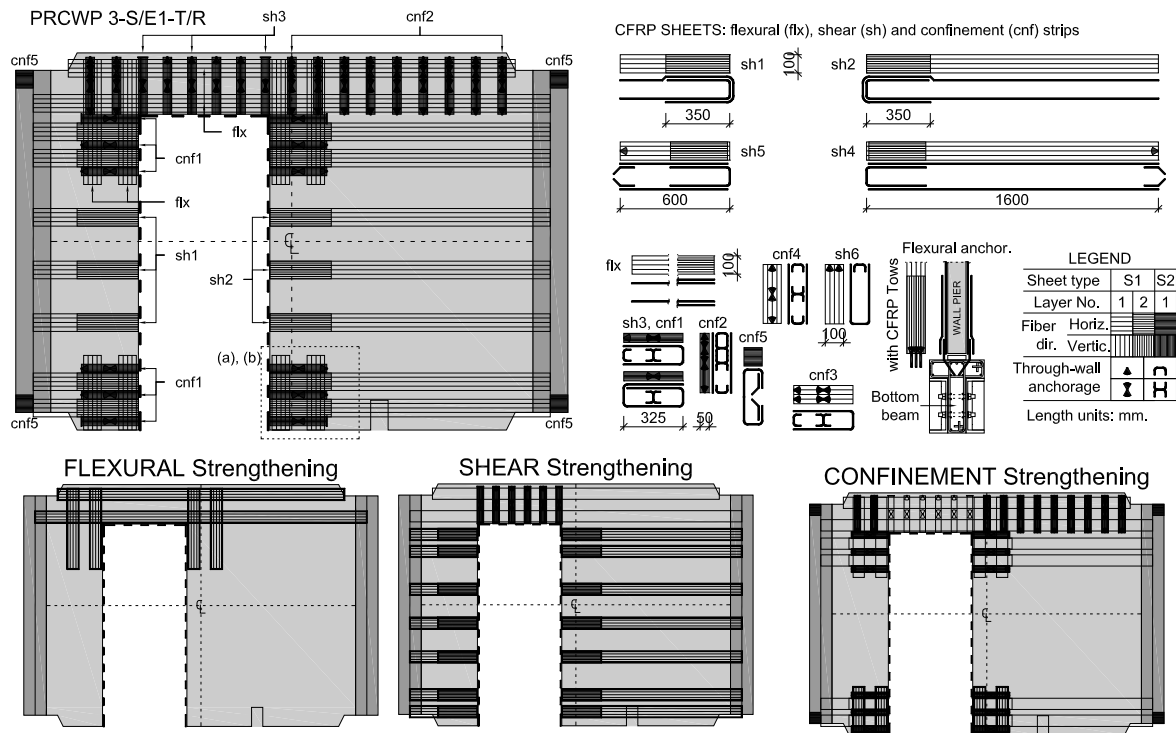


Figure 23. Strengthening layout for the specimen 3-S/E1-T/R

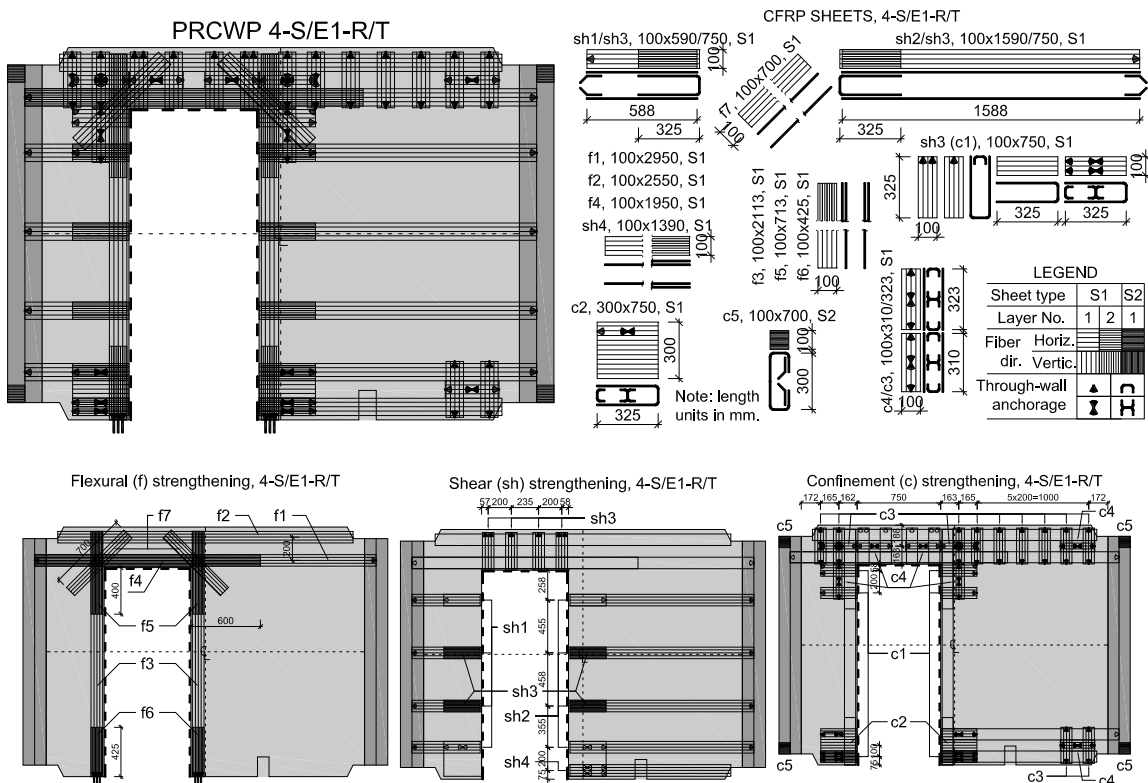


Figure 24. Strengthening layout for the specimen 4-S/E1-R/T

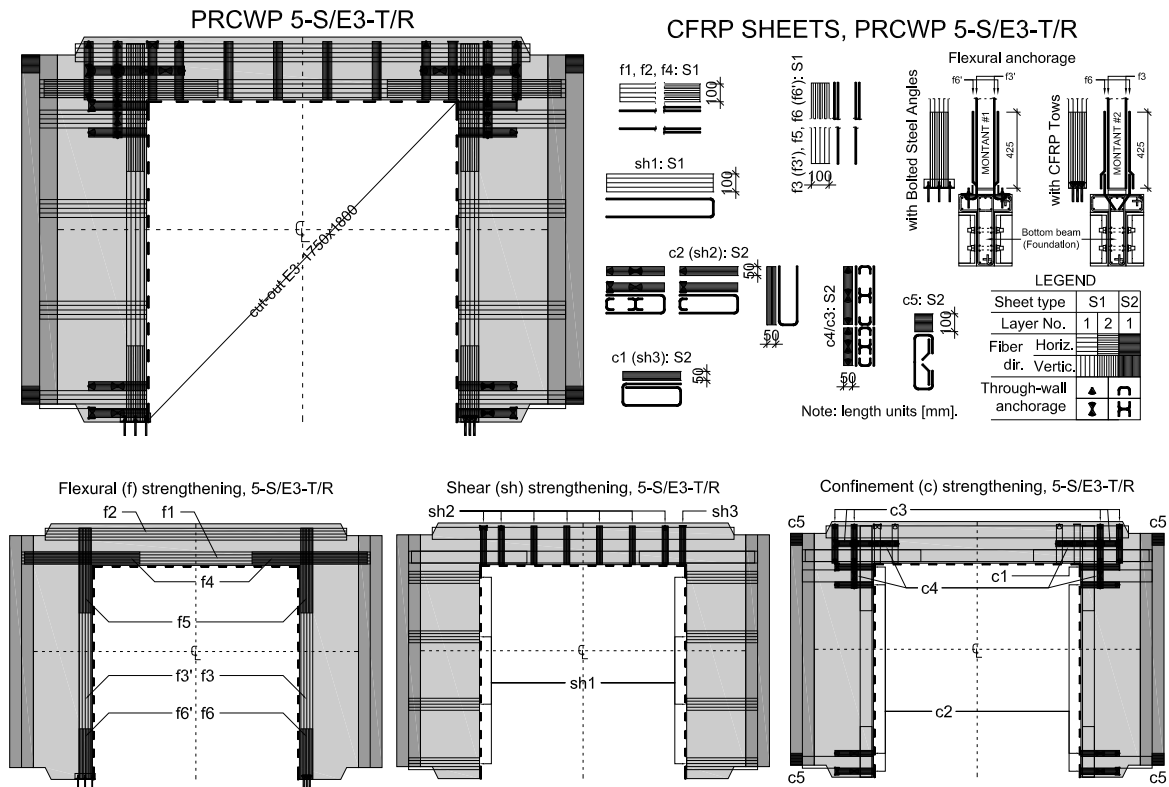


Figure 25. Strengthening layout for the specimen PRCWP 5-S/E3-T/R

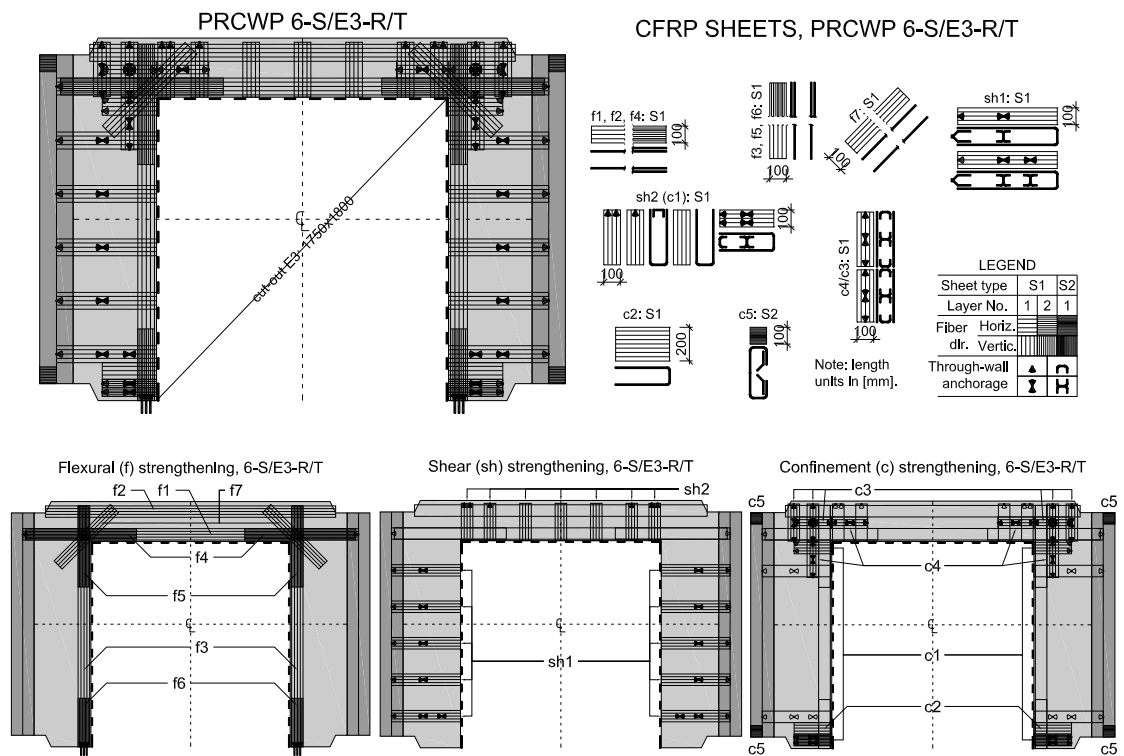


Figure 26. Strengthening layout for the specimen PRCWP 6-S/E3-R/T

For the confinement of the concrete at opening corners, stirrup-like sheets from type S2 were applied in similar way as presented above (c1 and c2) or using two independent strips closed in the middle and at the ends (c3 and c4). The inferior and superior parts of the wing element were confined with 100 mm wide sheets, type S2 (c5). The strengthening principle, procedure and phases for the PRCWP 6-S/E3-R/T wall was identical with the above presented, however some details were changed.

The specific usages were ciphered with reference to the gross wall area composed of two times the in-plane areas (inclusive the in-plane parts of the wings) and the transverse area of the pier edges at the openings. The specific CF-usage ranged between  $0.8 \dots 1 \text{ m}^2 \text{ CF/m}^2 \text{ wall}$  or  $230 \dots 300 \text{ g CF/m}^2 \text{ wall}$  while the resin amount was  $1.2 \dots 1.8 \text{ kg/m}^2 \text{ wall}$ . The number of cross-ties was 50 to 80 per wall.

### Detailing of the anchorage

Strengthening details are provided for the base anchorages in Figure 27. At the inside toes of the piers the anchorage of the vertical flexural strips was resolved by two methods: with bolted steel angles and with CFRP fingers.

In the first case in the base beam a channel was made with approx. 20 mm depth 150 mm length and 50 mm width. In the next step three vertical  $\phi 10$  mm holes were drilled. The channel and the holes were vacuum cleaned. Prior to the application of the CFRPs the holes were filled with resin. The CFRPs were laid on the bottom of the channel which was subsequently filled to the level of the beam with resin. A previously drilled 50 mm equal wing steel angle was then placed over the resin-filled channel which was gripped to the foundation through three  $\phi 8$  mm threaded bolts pushed to the vertical holes. After curing the bolts were tightened by nuts.

In the second case preparing phase consisted in drilling three  $\phi 10$  mm inclined holes 100 mm deep in the base beam at the edge of the pier toes after which the holes were vacuum-cleaned. Preceding the application of the flexural strips the holes were filled with resin and 50 mm wide by 250 mm long S1-type CFRPs were squeezed inside the holes the other end of these being laid and spread on the toe of the pier overlapping the flexural strips. The former anchorage was used only for pier #1 of specimen 5-S/E3-T/R, all the other being the latter type.

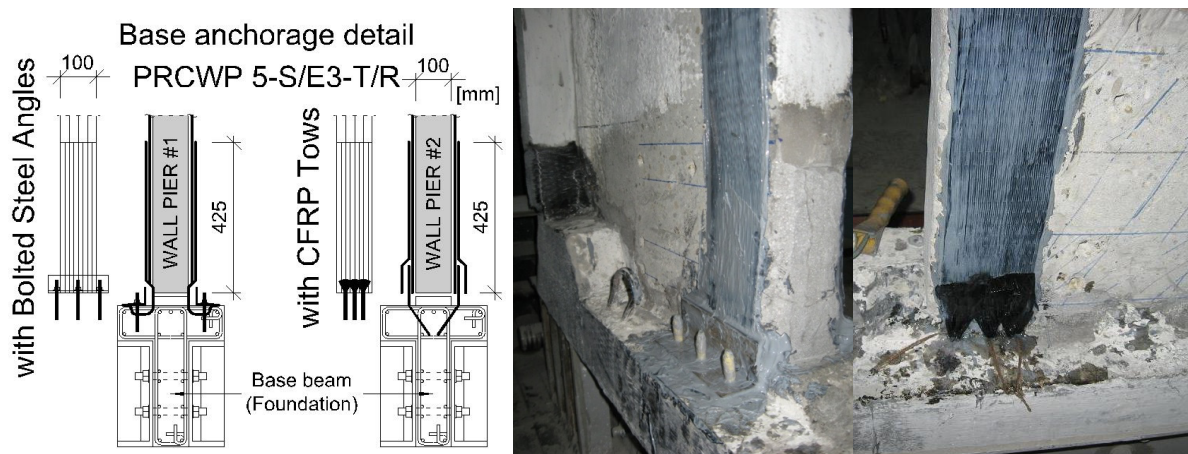


Figure 27. Base anchorage details with bolted steel angles and CFRP tows

The strengthening details of the pier-to-spandrel connection regions were the most difficult due to the congestion of the flexural, shear and confinement strips (see Figure 28). During the

preparatory works a series of  $\phi 10$  mm holes were drilled through the wall typically in a grid-like pattern at 150 mm centres. The ingress and egress portions of the holes were rounded by shallow drilling with larger diameter. The holes were cleaned from dust by vacuum and air blasting.

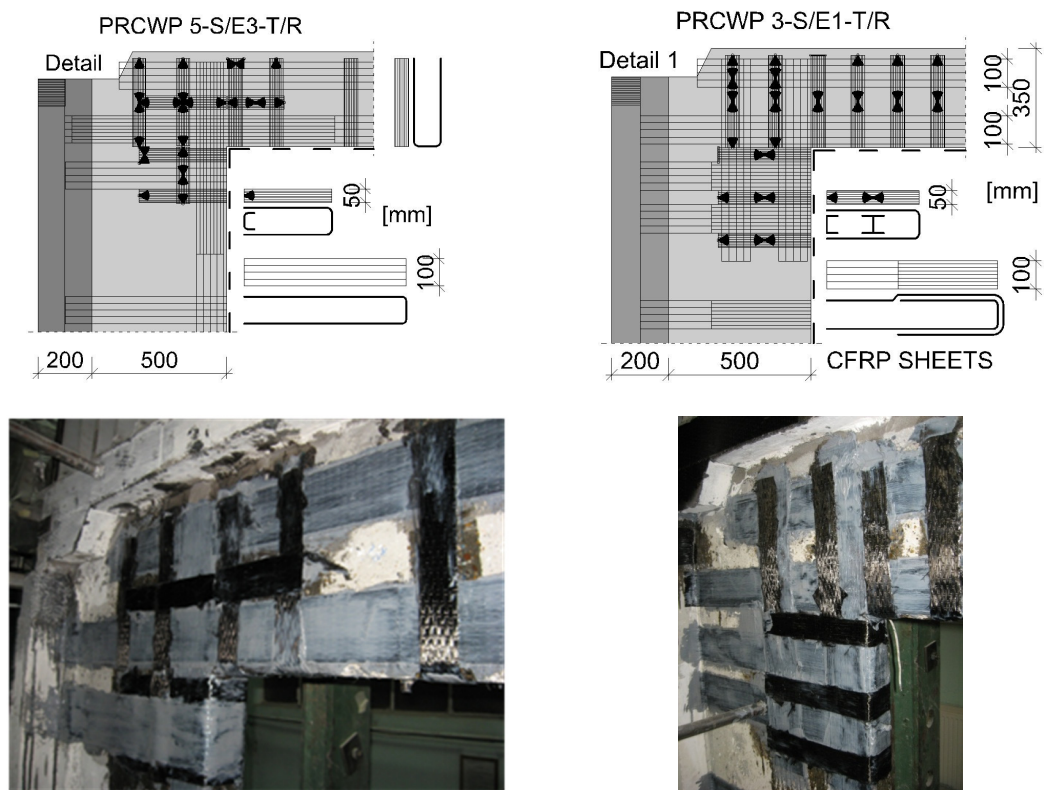


Figure 28. Pier-beam connection details

### 2.3.6 Experimental results

#### General commentary on the results

In the presented part of the experimental program the RC walls failed predominantly by concrete crushing, as presented on Figure 30. The tests on the bare specimens with cut-out openings (refer to Line 1 in Figure 30) showed that the critical regions are the pier-to-spandrel connections and the pier toes, that is, the extremities of the diagonal compression struts. At these locations the reduced concrete section with no transverse reinforcement couldn't withstand the increasing diagonal compression forces which resulted in spalling and crushing of concrete. It is noteworthy that one can construe this type of failure as flexural compression; however, one should bear in mind that the cracking pattern substantiates typical shear behaviour by diagonal compression (refer to the above discussion on the cracking pattern); therefore, the flexural failure interpretation is not acceptable.

Looking at Lines 2 and 3 in Figure 30, it can be remark that the failure mode of the FRP-strengthened specimens was mainly similar to their bare counterparts'; it is noteworthy however, that the FRP confinement and the highstrength mortar repair significantly improved the load transfer response at the critical regions. In three cases (3-T/R, 4-R/T and 6-R/T) the failure of the walls was triggered by the fracture of the FRP confinements, whereas the 5-S/E3-T/R specimen failed by sliding shear along the pier-to-wing joint; this latter failure mode can

be attributed to the reduction of the internal reinforcement due to the welded wire mesh cut-off (refer to Figure 3.6) and to the peeling-off of the horizontal shear strips. In relation with the test on the 5-S/E3-T/R specimen it is also important to note that the post-test investigation revealed crushed concrete inside the FRP confined cores at the pier toes, even though the confinement itself was apparently undamaged.

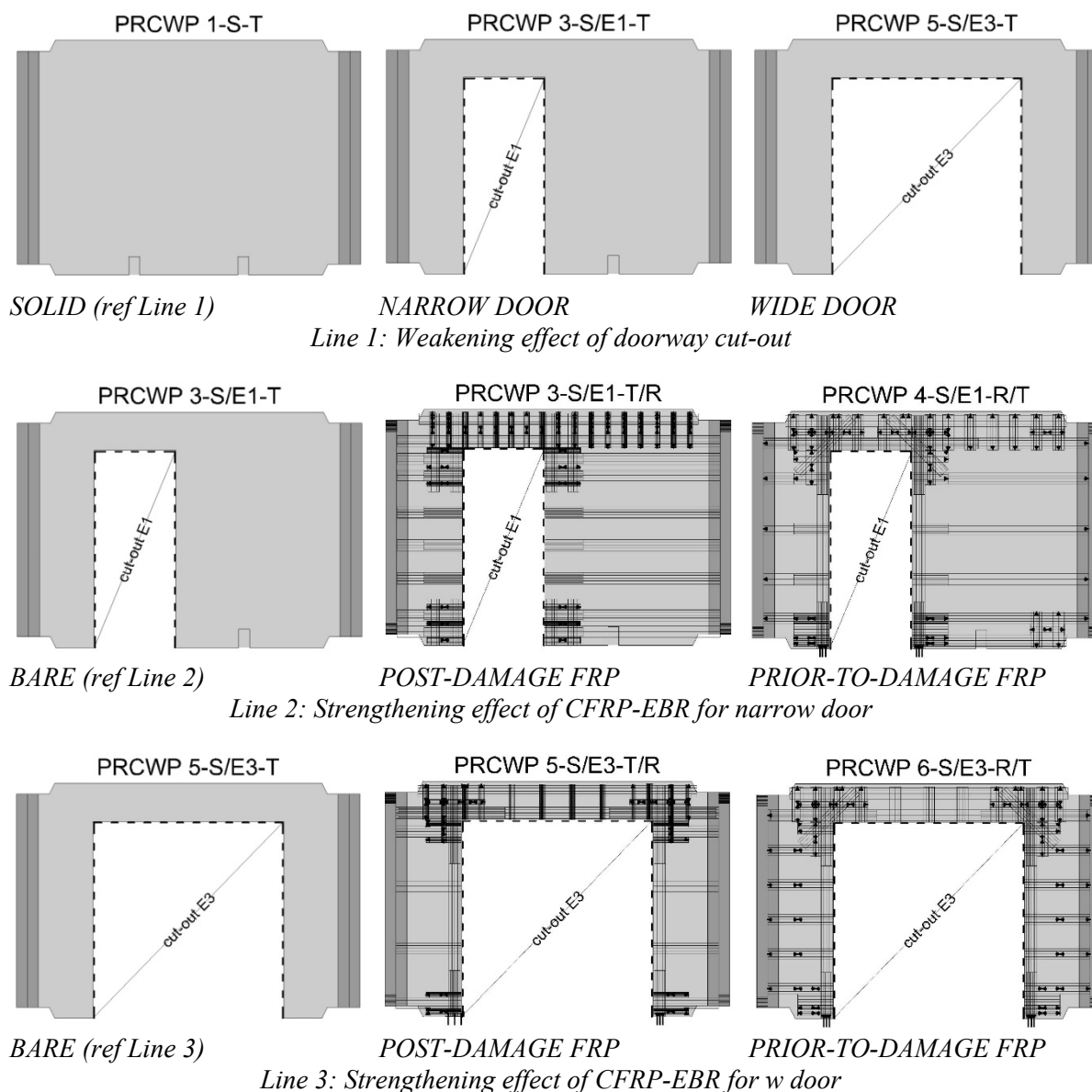


Figure 29. Comparison lines with strengthening layouts

In Figure 31 the responses were plotted to adequate load and drift limits along the three comparison lines of the experimental program. As presented earlier the first comparison line was aimed to assess the weakening effect of the doorway cut-outs. It is impressive the loss of load resistance of the specimens with cut-out door with respect to the solid reference. Comparison lines 2 and 3 were meant to assess the performance improvement achieved by CFRP-EBR strengthening for the narrow and wide door cut-out conditions, respectively. Both lines comprised a bare, a post-damage strengthened and a prior-to-damage strengthened wall test of the same opening condition. One can remark the increased load and displacement

capacity and the enlarged hysteresis loops of the strengthened specimens with respect to the bare references.

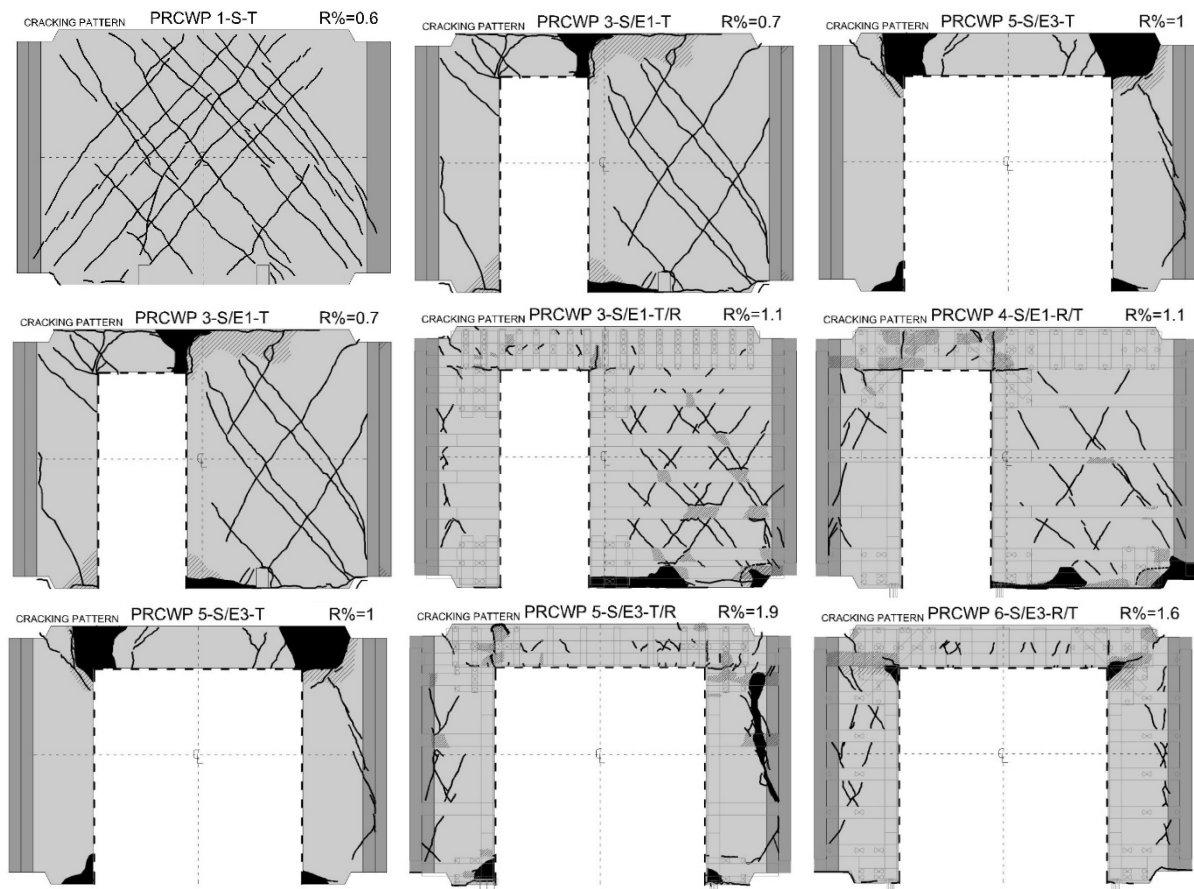


Figure 30. Cracking patterns and failure details

The performance of the shear CFRP strips can be exhibited by a comparison in terms of stiffness degradation. After shear cracking, the non-strengthened specimen's stiffness decreased significantly. Although the post-damage strengthening resulted in the complete recovery of the initial stiffness, the existing shear cracks opened at low displacement levels because the CFRP strips were applied on the already loosened wall portions, consequently the stiffness degradation took place similarly as for the non-strengthened specimen. The shear cracks of the prior-to-damage strengthened specimen were closed firmly by the CFRP strips at each unloading, therefore the wall's stiffness decreased in a smaller degree in comparison to the previous cases.

The tests performed on the non-strengthened elements revealed that the critical zones are the coupling beam to pier joints. In the absence of transversal reinforcements the failure is produced through crushing of concrete, in this way limiting the force transfer from the beam to piers.

The retrofitting technique by means of CFRP EBR yielded in improved behaviour characteristics, yet certain limitations were identified on the use of this strengthening system in reversed cyclic loading conditions. CFRP sheets with fibres parallel to tension-compression reversals are likely to fail prematurely. In order to develop the full shear capacity of the wall piers, adequate confinement should be provided at the corners.

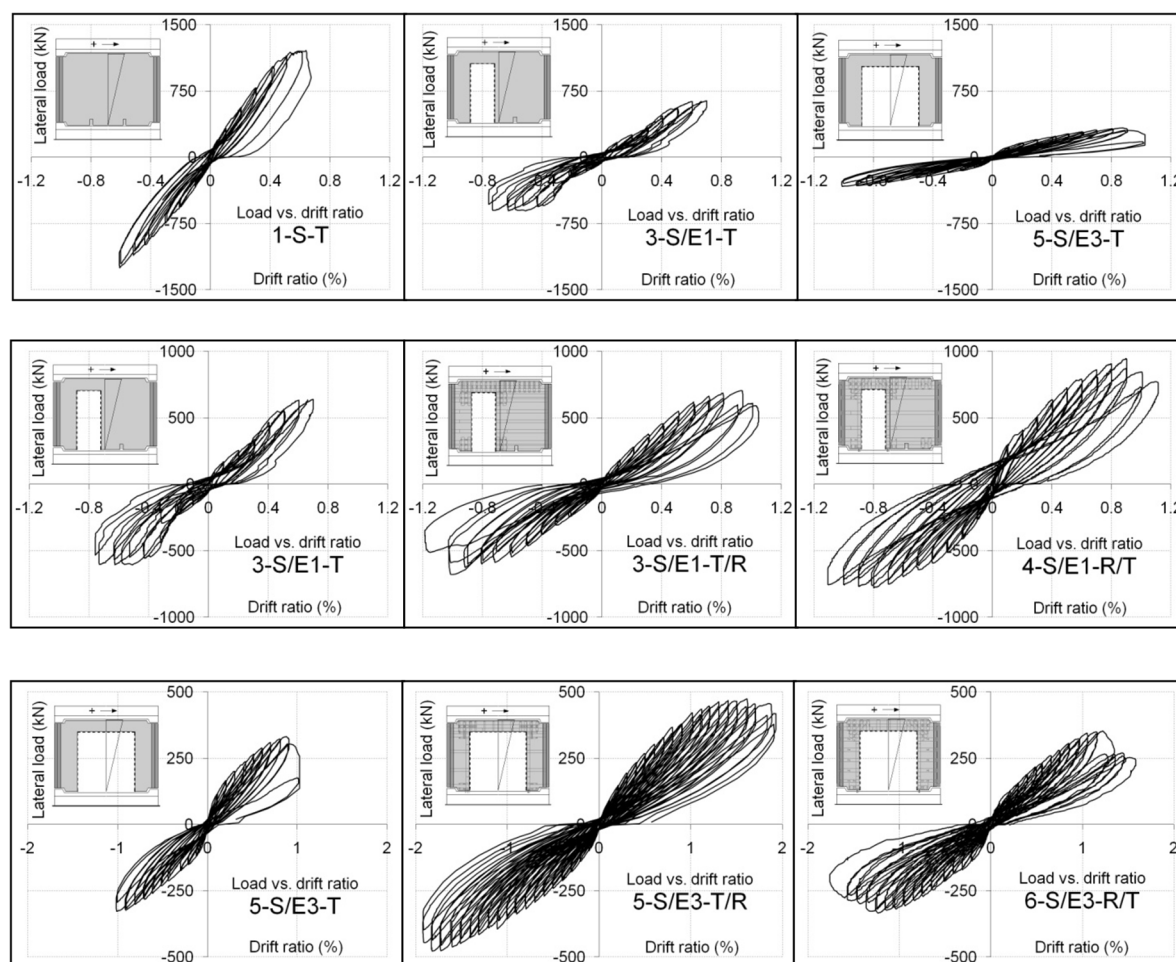


Figure 31. The load-displacement responses arranged along the comparison lines.

### Analysis of the results

In the first step of the analysis the envelope curves were constructed, by interconnecting the peak points through the consecutive displacement levels.

In the second step the cyclic load envelopes for each specimen were drawn, considering the main characteristic of the two axial loads during the lateral loading (it is noteworthy that the increase rate of the axial loads is strongly affected by the) (Figure 32). In similar way the strain-drift and displacement-drift envelopes were also represented.

In the third step the monotonic envelope curves were processed only for the lateral load-drift responses. These envelopes were obtained from the average cyclic envelopes by computing the mean ordinates between the positive and negative direction branches, taken as absolute values. In other words the monotonic envelopes were drawn by connecting the average peak loading points, taken as absolute values, through each drift amplitude (Figure 33).

In the fourth step a tri-linear backbone curves were constructed based on the cracking point, peak load and failure. The first point was based on the observed cracking history by using the criteria of either diagonal cracking across the piers or significant cracking development. The second load-displacement point (peak load) of the backbone corresponded to the maximum load on the monotonic envelope, while the third point (failure) was defined on a 20% post-peak load drop basis (Figure 34).

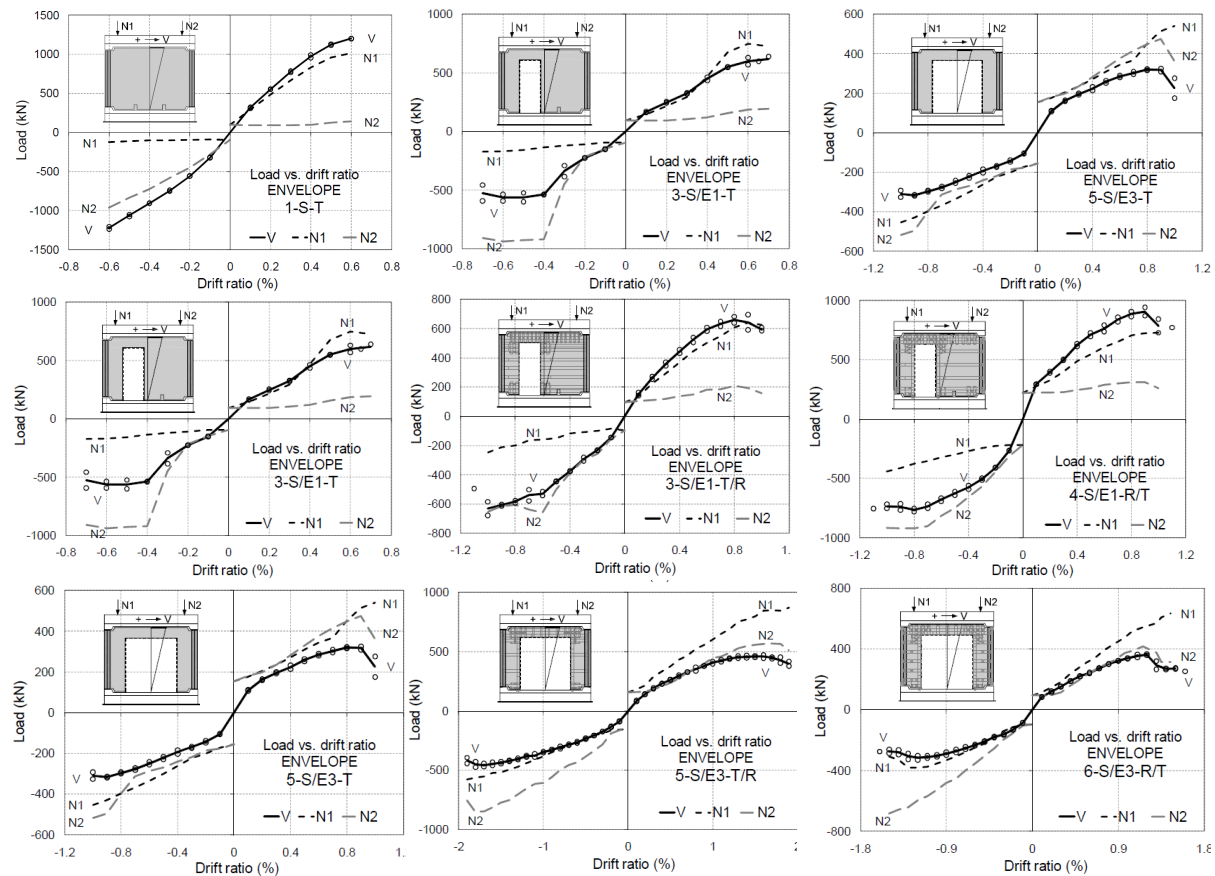


Figure 32. Cyclic load envelopes of the specimens

- **Strength analysis**

The shear strength was defined as the maximum load on the monotonic envelope curve or in other words as the peak load point on the backbone envelope, denoted by V2. As can be seen, the highest load sustainability (or inversely the lowest cracking strength ratio) was exhibited by the solid wall. However, there is no clear correlation between the cut-out size or strengthening condition and the variation of the load sustainability (Figure 35).

- **Stiffness analysis**

On the average loading curve is pointed out the tangent stiffness for each line segment between two subsequent drift levels up to the target drift amplitude. The variation of the secant stiffness along the monotonic envelope curve is referred to as stiffness degradation and it can be displayed by plotting the subsequent stiffness values against the drift ratio. It can be observed that the degradation curves are grouped in three clusters according to the cut-out condition, while the influence of strengthening was quiet small (Figure 36).

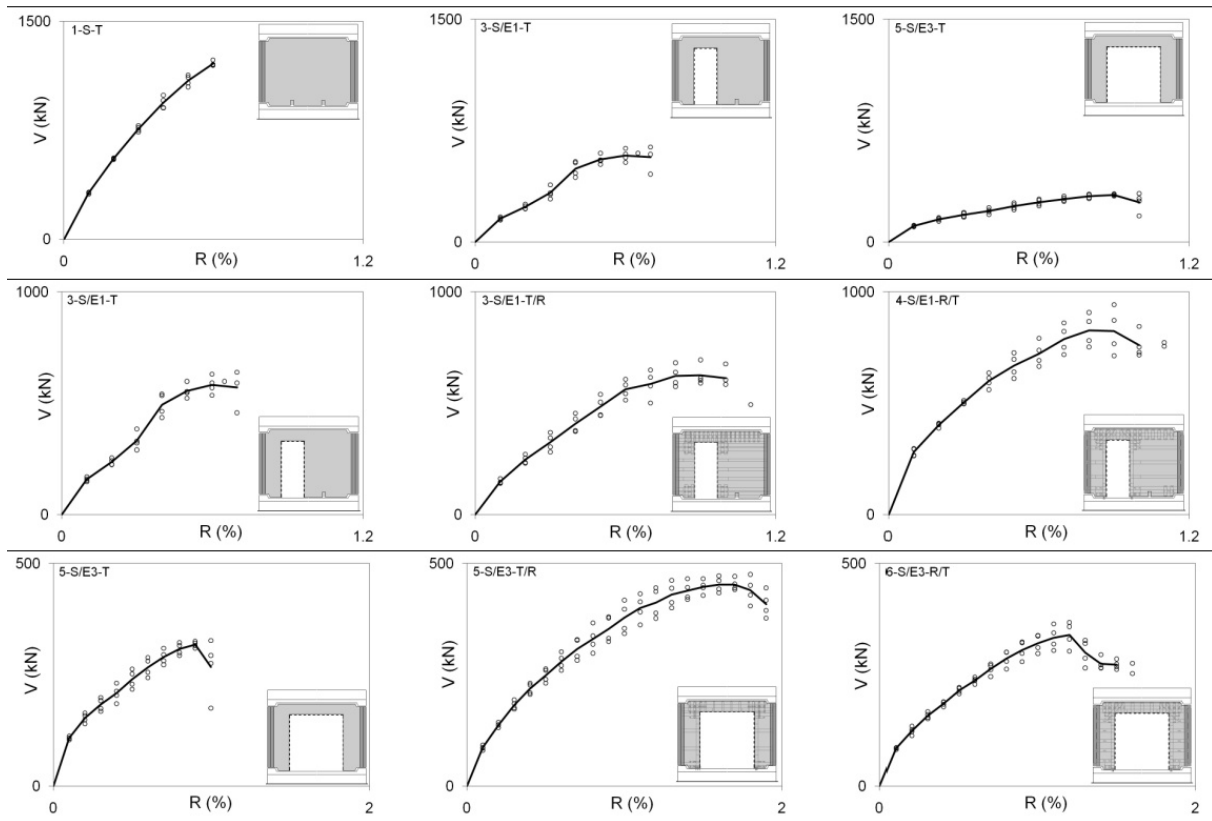


Figure 33. Monotonic load-drift envelope comparison lines

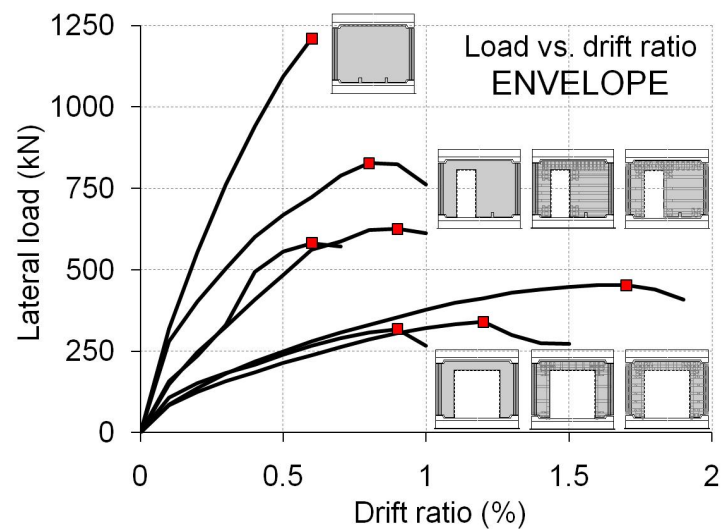


Figure 34. Load-drift tri-linear backbone envelopes

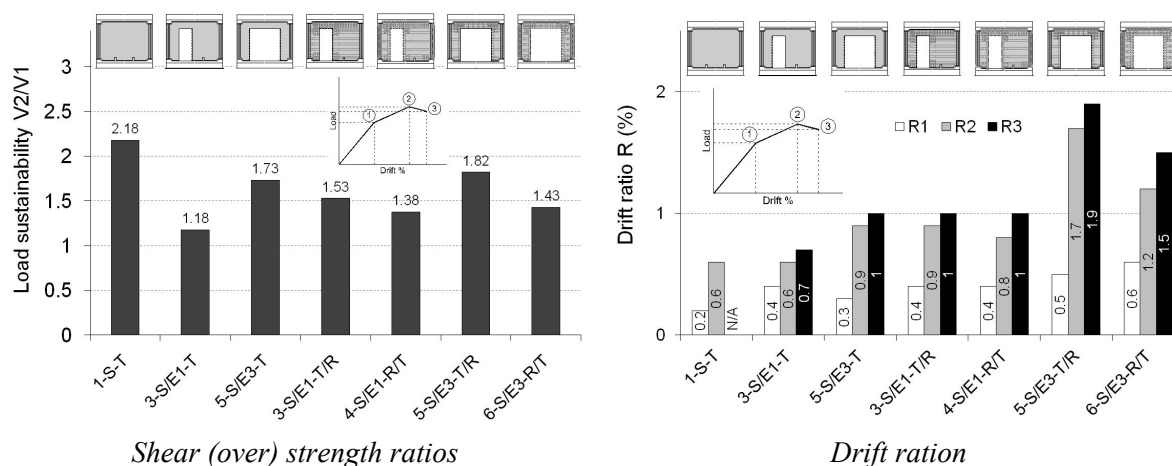


Figure 35. Strength analysis

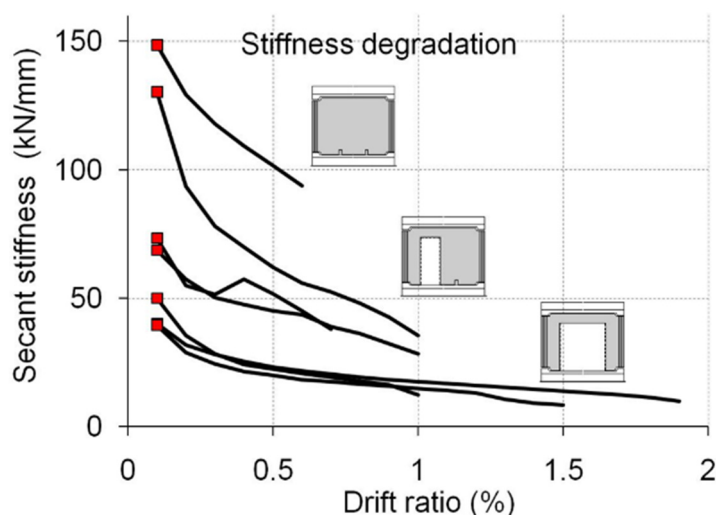


Figure 36. Normalized Stiffness degradation

- **Energy dissipation analysis**

In order to assess the degree of pinching one should compare the energy dissipated during a complete load-displacement cycle (the area bounded within the hysteresis loop) with the energy which could have been theoretically dissipated within the same load-displacement limits assuming perfectly plastic behaviour (the area of the rectangle defined by the positive and negative peaks). This ratio was referred to as energy dissipation ratio.

On the Cumulative Energy Dissipated (CED) vs. cyclic drift plot the envelopes are constructed by connecting one by one the local maximum points separately, whereas on the CED vs. cumulative drift graph the envelopes are drawn by connecting the local maximum points in one continuous series and the local minimums in another (Figure 37).

The cumulative dissipation ratio of the experimental specimens varied in the (8.5÷13)% range; it is noteworthy that neither the cut-out nor the strengthening condition affected significantly the dissipation ratio. Consequently, the value of 10% dissipation ratio can be considered as a general response characteristic of the wall panels in this experimental program (Figure 38). Similar, however not identical, definition was reported by other researchers, too.

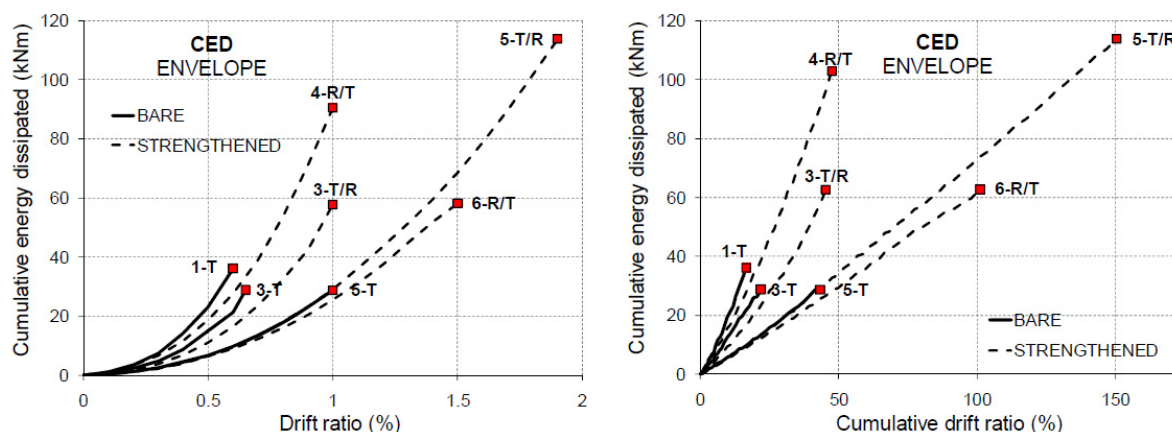


Figure 37. Energy dissipation envelopes

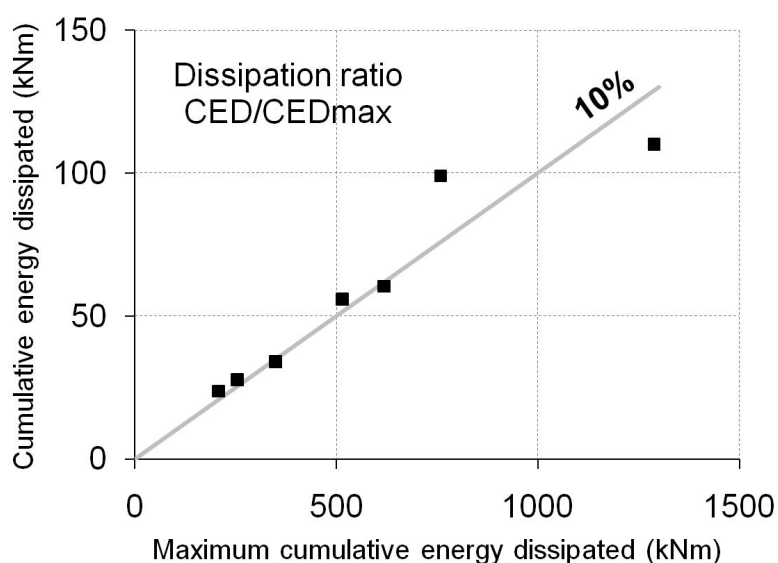


Figure 38. Ultimate dissipation ratio

### 2.3.7 Conclusions

#### Weakening caused by cut-out door openings

The experimental results regarding the weakening effect of the door cut-outs on the seismic response of the solid reference wall are presented in Figure 39; the cut-out ratio is a measure of the opening size relative to the solid reference wall calculated either as the horizontal cross section ratio or as the square root of the in-plane area ratio (peripheral ratio); the performance ratio indicates the response characteristic of the weakened specimen normalised to the corresponding characteristic of the sound (solid) reference; the situation of complementarity between the performance ratio and the cut-out ratio is represented by the dashed line joining the unities of the two axes. One can observe that there is experimental evidence on the complementarity relationship between specific performance and opening ratios: the strength and stiffness performance ratios are the complement of the peripheral ratio, whereas the energy dissipation rate performance ratio is the complement of the cross sectional ratio.

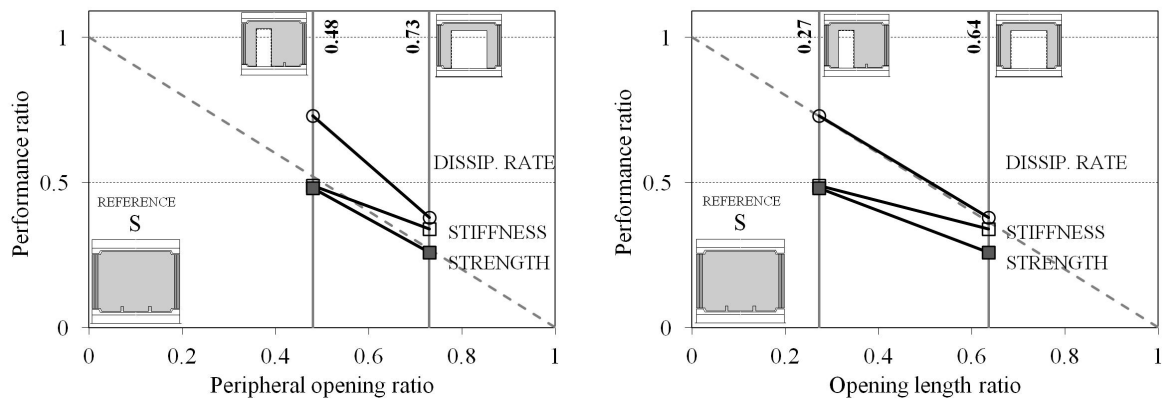


Figure 39. Weakening effect of the cut-out openings.

Practicing engineers can use the experimental results to quickly approximate the response characteristics of the precast RC walls weakened by doorway cut-outs according to the following equations:

$$R_{weak} = R_{sound} \cdot \alpha_p$$

where  $R_{weak}$  is the response characteristic of the weakened member in terms of shear resistance, initial stiffness or energy dissipation rate;  $R_{sound}$  is the response characteristic of the sound (solid, as-built) member in terms of shear resistance, initial stiffness or energy dissipation rate;  $\alpha_p$  is the performance ratio, given by

$$\alpha_p = 1 - \eta$$

The opening ratio  $\eta$  is given by:

$$\eta = \begin{cases} P = \sqrt{A_0/A_w} & \text{for } R: \text{shear resistance and stiffness} \\ l_0/l_w & \text{for } R: \text{dissipation rate} \end{cases}$$

where  $P$  is the peripheral ratio,  $A_0$  and  $A_w$  is the in-plane area of the opening and the wall, respectively; and  $l_0$  and  $l_w$  is the length of the opening and of the wall, respectively.

This expression was derived from the AIJ recommendation (AIJ 1999); however, the AIJ equation is reportedly applicable only for peripheral opening ratios less than 0.4 and it refers only to the shear strength and stiffness. In the present research the above equation was experimentally verified for two opening ratios (0.48 and 0.73); in-between these values one can assume linear performance ratio-to-peripheral ratio relationship. Moreover, it is important to bear in mind that the relationship given in equation was validated for the specific loading and boundary conditions applied in the present experimental program (outrigger effect by additional axial loads); further investigations are required to widen the loading and boundary conditions range.

## Strengthening attained by CFRP-EBR

The effect of the FRP-EBR strengthening on the seismic response of the cut-out weakened specimens is presented in Figure 40; the performance ratio indicates the response characteristic of the FRP-strengthened specimen normalised to the corresponding characteristic of the cut-out weakened bare reference. It can be remarked that the response characteristics were differently influenced by the CFRP-EBR strengthening (generally in the range of 0.8÷1.9 performance ratio); outstanding improvement was achieved in terms of energy dissipation (2.2÷2.2 performance ratio). Furthermore, one can assess the differences the timing of the strengthening (post-damage or prior-to damage) had on the response. Note that the results should be viewed in the light of the concrete strength performance ratio (in the range of 0.62÷2.3) and of the loading and boundary conditions. As regards the contribution of the three components (flexural, shear and confinement) of the FRP strengthening to the above performance, it can be concluded that the confinement FRP strips show the most stable response; the shear FRP strips debond in the vicinity of the inclined cracks; and the flexural CFRP-strips subjected to alternating tension-compression reversals parallel to fibre direction are likely to fail prematurely. In order to assess more clearly the components' contribution further subject-oriented investigations are necessary.

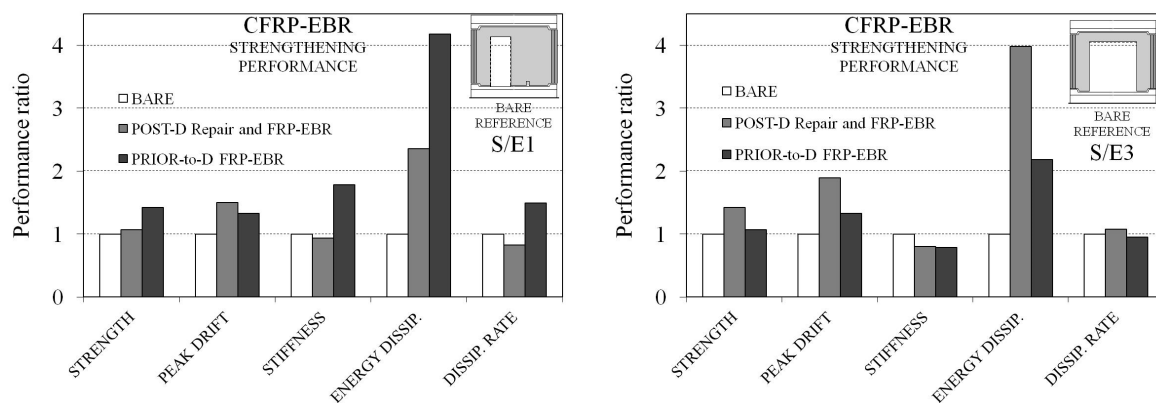


Figure 40. Strengthening attained by CFRP-EBR strengthening.

Practicing engineers can use the experimental results to evaluate the seismic response modifications which can be expected by CFRP-EBR retrofitting of the cut-out weakened precast concrete wall panels. CFRP layouts similar to the ones presented in this thesis would yield the following results: the shear strength increases in average by 25%; the peak drift increases by 50%; the initial stiffness and the energy dissipation rate remain roughly the same; and the cumulative energy dissipation at ultimate increases by 2÷4 times. One should bear in mind that in reversed cyclic applications the flexural CFRP-EBR is susceptible to premature failure; thus is recommended to use a safety factor of 3 for the flexural FRPs.

## Acknowledgement

The presented research received financial support from the Romanian National University Research Council (CNCSIS) through a number of research grants and contracts, as follows:

- Retrofit of RC walls and slabs with cut-out openings using FRP composites (Consolidarea cu compozite polimerice armate cu fibre a pereților și a planșeelor structurale din beton armat cu goluri create ulterior), Grant CNCSIS type A, 2006 - 2008. Coordinated by Prof. Stoian Valeriu, Politehnica University of Timisoara.

- Advanced strengthening systems of RC members, as beams, columns, walls and slabs, using FRP composites (Sisteme avansate pentru consolidarea elementelor structurale din beton armat de tip grinzi, stâlpi, pereți și planșee folosind materiale compozite polimerice armate cu fibre), Grant CNCISIS CEEEX type ET, 2006 – 2008. Coordinated by Dr. Nagy-György Tamás, Politehnica University of Timisoara.
- Reinforced concrete walls strengthened by composite materials (Pereți din beton armat consolidați cu materiale composite), Grant CNCISIS - UEFISCSU, PNII-RU-TD8, 2007. Coordinated by Demeter István, Politehnica University of Timisoara.

My special appreciation and thanks to Dr. Demeter István.

## **2.4 Theoretical and experimental study of precast reinforced concrete slabs with cut-out openings retrofitted using FRP composites**

### **2.4.1 Introduction**

It is quite hard to imagine important renovation of existing buildings without interventions on the floors and slabs of such structures. Whether the need of structural interventions is caused by increased load demands, degradations or changes in functionality, the requirements and the outcome are the same.

The research program that is discussed in this chapter was conducted at the Politehnica University Timisoara and covers theoretical and experimental investigations on two-way Reinforced Concrete (RC) slabs with and without cut-out openings strengthened/retrofitted using Carbon Fiber Reinforced Polymer materials (CFRP). The study was focused on effectiveness assessment of the proposed solutions for the particular case of cut-outs created in the corners and on the edges of the slabs.

Even though researchers were preoccupied previously with reversible solutions suitable for structural renovation of RC slabs, similar studies to those proposed within the above mentioned research program were quite scarce in literature. Given the reversibility of the technique as well as the fact that it is architecturally compatible (at some extent) with old buildings, it could represent an interesting solution for historical constructions. Using of FRP strengthening/retrofitting methods is also justified by its un-laborious appliance. A drawback of these materials/techniques in structural strengthening of RC members is their brittleness that can cause a decrease in their stiffness and unwanted failure mechanisms.

Two-way RC slabs supported on their entire contour are mostly subjected to flexure, with insignificant shear stresses. This being the case, clearly they are susceptible to flexural failure rather than shear one, strengthening them by means of FRP materials being able to provide an efficient solution. The strengthening method for all RC elements presumes applying lamellas or fabrics (in the required amount and direction) by bonding those using resins on the tensioned side of the member.

For slabs with cut-out openings strengthened using FRP, the available research is scarce, only several research programs being reported in literature, as work conducted by Tan & Zhao in 2004, Vasquez & Karbhari in 2003, Enochsson in 2005 or Smith in 2009 being of high importance. The solution applied by all of these researches consisted in laying up CFRP or

GFRP strips or sheets of fabrics along the edges of the cut-out and bonding them to the concrete surface, on the tensioned side, using epoxy based resins. Different configurations for the layout of the strengthening materials were used, the most common being the one in which the material is placed parallel to the edges of the cut-out.

## 2.4.2 Experimental program

The program consisted in twelve tests performed on six RC two-way slab panels. Even though all six experimental specimens were identical in terms of geometry and material specifications (full scale 3950x2650x120mm prismatic elements) they were split into 2 groups. The first 4 elements were included in the 1<sup>st</sup> group while the 2<sup>nd</sup> group consisted of the last 2 specimens.

The 1<sup>st</sup> group of experimental elements consisted in a homogeneous slab (full slab, without any opening) and three slabs with rectangular cut-out openings. The full slab served as reference and was referred to as RCS-FS-01 (standing for Reinforced Concrete Slab-Full Slab). The second slab, denoted RCS-RSC-01 (Reinforced Concrete Slab-Rectangular Small Cut-out), had a small rectangular cut-out inserted into one of its corners. Into the third and fourth slabs, denoted RCS-RLC-01 and RCS-RLC-02 (standing for Reinforced Concrete Slab-Rectangular Large Cut-out) a large rectangular cut-out was positioned on an entire width of these slabs.

The 2<sup>nd</sup> group of experimental elements consisted in a homogeneous slab referred to as RCS-FS-02 and one with a circular opening placed at one of its corners denoted RCS-CC-01 (standing for Reinforced Concrete Slab-Circular Cut-out).

All elements in the 1<sup>st</sup> group were cast using concrete with cubic compressive strength of 65N/mm<sup>2</sup>. The slabs were reinforced with steel welded wire meshes at the inferior side (4 mm in diameter with spacing of 100 mm) and with steel rebar at the superior one (6 mm and 10 mm bars). The bars in the steel welded wire meshes had average yield strength between 537 MPa and 597 MPa.

The specifications for the elements in the 2<sup>nd</sup> group were identical to those in the 1<sup>st</sup> group, however, some differences have occurred. Thus, elements in the 2<sup>nd</sup> group were cast using concrete with cubic compressive strength of 38N/mm<sup>2</sup>. The layout of reinforcement was identical to that of the specimens in 1<sup>st</sup> group.

For all specimens (both 1<sup>st</sup> and 2<sup>nd</sup> group ones) the inferior reinforcement was laid on the entire surface of the slab, while the superior one was placed only along the edges. Since the reproduced situations involved simple supported slabs, the superior reinforcement was designed mainly due to constructive reasons.

The testing protocol was to test all elements in their as-build state up to a stage that would impose the need of applying strengthening/retrofitting interventions. For all of the slabs, this stage was considered as the maximum allowable deflection ( $L/250=2400\text{mm}/250=9.60\text{mm}$ ) according to EN 1992-1-1.

As this limitation was reached, the test was stopped and a mixed (hybrid) retrofitting solution that involved the use of both Near Surface Mounted (NSM-FRP) and Externally Bonded (EB-FRP) techniques was applied (Figure 41). Finally, after allowing CFRP system to cure, the retrofitted elements were tested up to their complete failure.



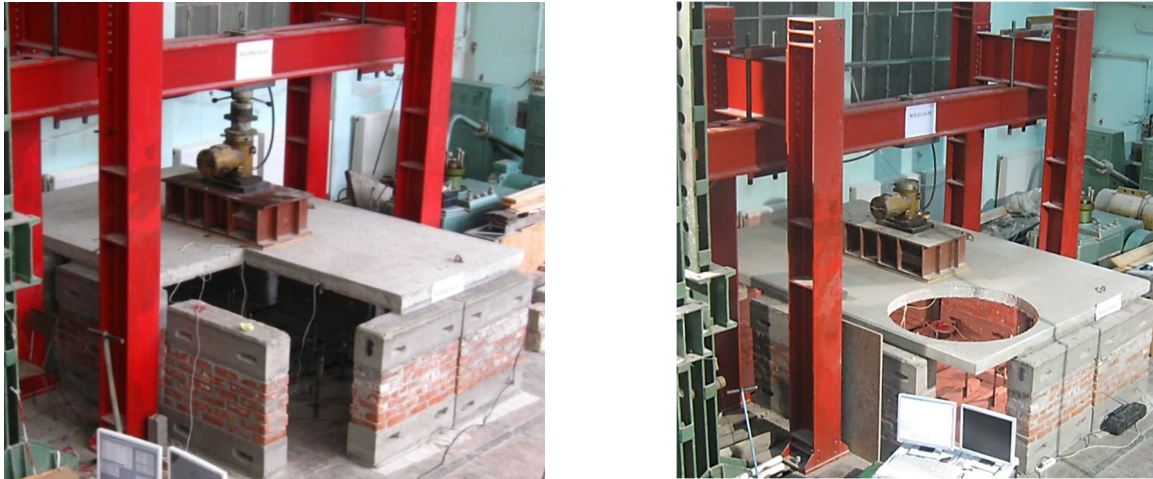


Figure 43. Test setup for RSC-01 and CC-01 slabs

### 2.4.3 Results of tests on bare elements

All tests on bare elements were denoted starting with the reference of the experimental specimens and updated with the mark “UU” standing for Undamaged Unstrengthened (e.g. RCS-FS-01 represents the specimen and RCS-FS-UU-01 represents the test on the bare specimen).

#### Elements in the 1<sup>st</sup> group

One of the most important features of the specimens' behaviour is the small number of cracks that have opened, in conjunction with crack patterns that indicate larger stresses in the area around the cut-outs. Actually, initiation points of all cracks are located in areas around the cut-outs.

In the case of the slab RCS-FS-UU-01, a very predictable behaviour was observed, as four cracks appeared on the direction of the yield lines, at inclinations close to 45° (36°, 44°, 52° and 56°). For all of the other tests, the first crack to appear was a longitudinal one, parallel to long edges of the slabs, located quasi-centrally. In all these tests on slabs with cut-outs, the first crack was always followed by inclined cracks, at various inclinations (ranging from 30° to 73°).

The maximum load level reached during the RCS-FS-UU-01 test was 118 kN. Past this value, the strain in numerous steel reinforcement bars has reached yielding point and the vertical mid-span displacement has reached maximum allowable deflection ( $L/250=9.60$  mm) as provided by EN 1992-1-1. Moreover, deflection increased without a substantial increase of load. During the test, the maximum vertical mid-span displacement had a value of 10.28 mm.

The maximum load level reached during the RCS-RSC-UU-01 test was 87 kN while the maximum vertical displacement had a value of 11.36mm, being larger than the maximum allowable deflection.

During RCS-RLC-UU-01 test the maximum recorded load level was 75 kN while the maximum vertical displacement had a value of 9.59 mm. The first crack (again the one quasi-parallel to the long side of the slab) was visible at a load of 55kN. In total, three cracks appeared.

For the RCS-RLC-UU-02 test the maximum recorded load level was 67 kN while the maximum vertical displacement had a value of 8.88 mm. All of the load-displacement diagrams recorded for the bare elements within the 1<sup>st</sup> group are presented in Figure 44.

The load displacement diagrams recorded for the bare elements (Figure 44 and Figure 45) are represented at a different scale in terms of displacement from the diagrams on the strengthened elements, due to clarity and readability reasons.

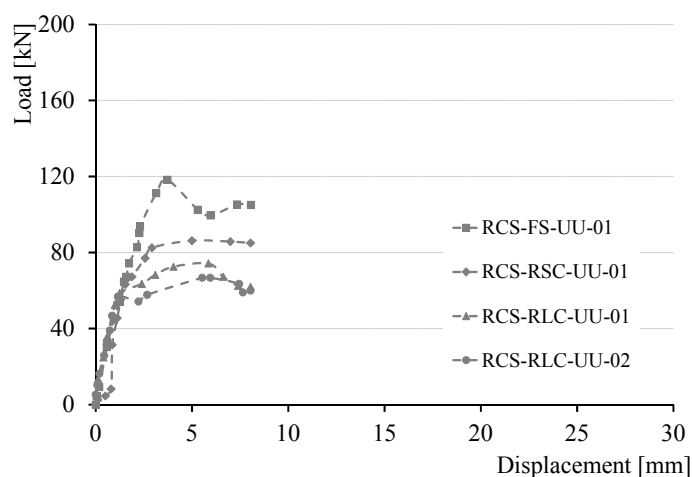


Figure 44. Load-displacement for 1st group of bare elements.

### Elements in the 2<sup>nd</sup> group

An important characteristic of slabs in 2<sup>nd</sup> group that differentiate these specimens from those in 1<sup>st</sup> group is related to the crack patterns. Even though identical materials specifications were provided and required to the manufacturer of the slabs, the results were somehow different. The crack patterns of 2<sup>nd</sup> group slabs show a large number of cracks, opening quite early in the loading stage, in contradiction to the elements in the 1<sup>st</sup> group for which the tests on bare elements disclosed a very small number of cracks.

The maximum load level reached during the RCS-FS-UU-02 test was 101 kN and during test RCS-CC-UU-01 was 76 kN. All of the load-displacement diagrams recorded for the bare elements within the 2<sup>nd</sup> group are presented in Figure 45.

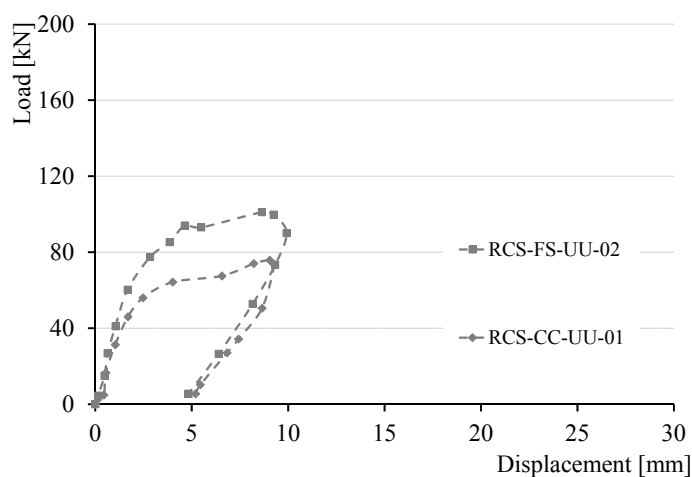


Figure 45. Load-displacement for 2nd group bare elements.

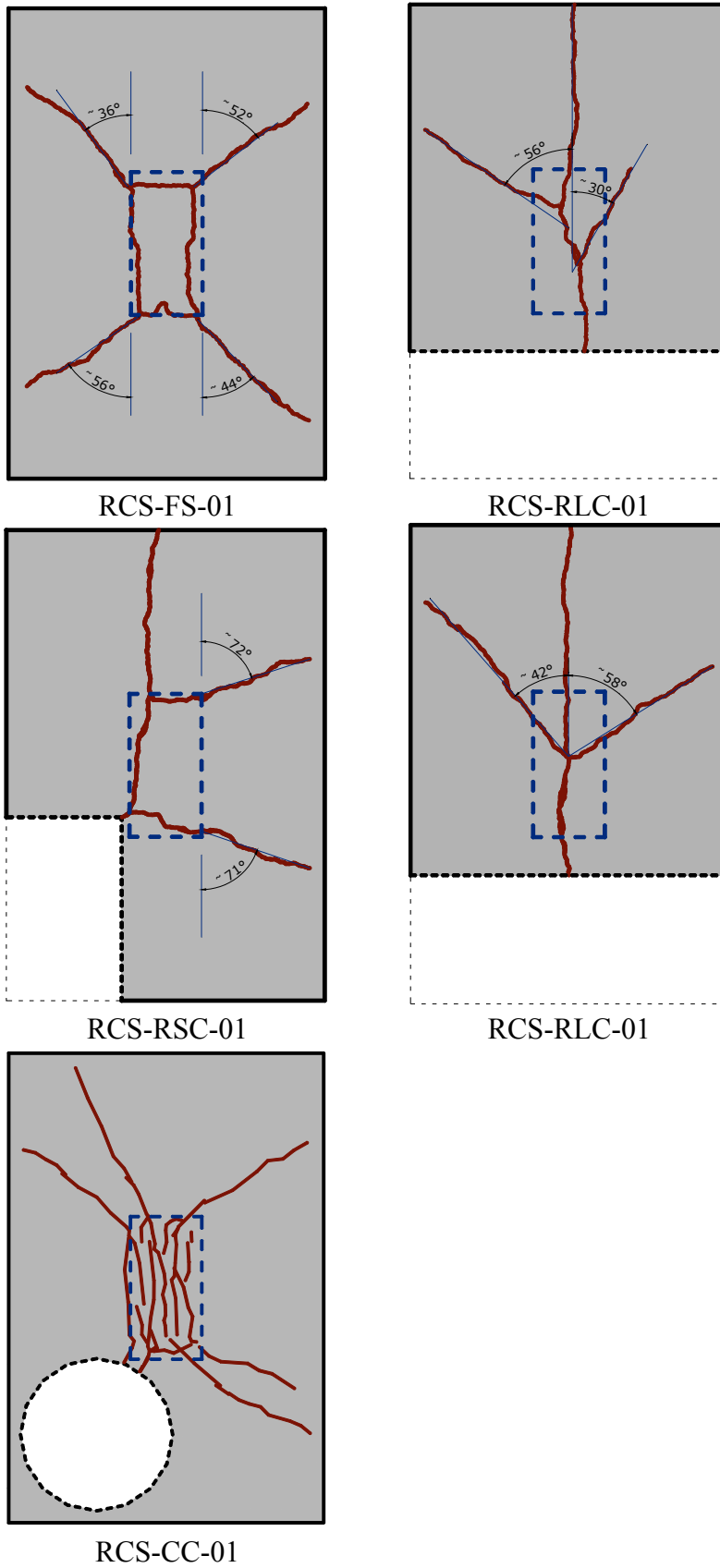


Figure 46. Crack patterns at the end of the tests in bare elements

#### 2.4.4 Design of strengthening solution

As mentioned previously, for all RC elements for which the aim of the strengthening procedure is to enhance performance in flexure, the strengthening procedure consists in applying of the CFRP components on the tensioned side (i.e. the bottom face of the slab in the present cases), in the required direction and quantity. In the case of the present research program, the CFRP elements will be placed on two directions, parallel with the edges of the slab, for all specimens, with or without cut-out openings, regardless of the geometry of the cut-outs.

The required amount of CFRP is determined analytically considering two simplified assumptions. For the full slabs, the tensile force that would have been undertaken by the steel reinforcement (which is yielded at the end of the tests on bare elements) is equalized with the tensile force that will be undertaken by the CFRP components. For the elements with cut-outs, the CFRP strengthening material will be placed around the cut-out, along its edges, parallel to the edges of the slabs. The amount of CFRP is to be determined analytically by equalizing the tensile force that would have been undertaken by the steel reinforcement eliminated by inserting the cut-out opening, with the tensile force that will be undertaken by the FRP, as provided in the following equation. Inside this formula, the strain in CFRP composite is limited to 0.8%, this value being an accepted limit for elements subjected to flexure, according to the strain limitation approach as presented in *fib* bulletin 14. This value is much lower than the ultimate strain provided by the producers, being considered the value at which composite action is lost due to premature failure.

$$F_s = F_f \Rightarrow A_f = \frac{f_{yd}}{E_f \cdot \varepsilon_f} A_s$$

where:  $F_s$  - tension force in steel reinforcement;  $F_f$  - tension force in FRP fibers;  $A_f$  - area of fibers in CFRP composite;  $f_{yd}$  - design yield strength of steel reinforcement;  $E_f$  - modulus of elasticity of fibers of CFRP composite;  $\varepsilon_f$  - strain in fibers of CFRP composite;  $A_s$  - steel reinforcement area.

CFRP lamellas and NSM strips with a modulus of elasticity of 165000 MPa and a thickness of 1.2 mm and CFRP sheets with a modulus of elasticity of 230000 MPa and a thickness of 0.12 mm were used for all strengthening systems. On the direction parallel to the short edges of the slabs, FRP reinforcement was applied by NSM-FRP technique while on the direction parallel to the long edges the EBR-FRP technique was used. Inside Figure 47 the lay-up of CFRP components for all of the tested slabs is depicted.

As it can be observed in Figure 47, for slabs RCS-RLC-01 and RCS-RLC-02 the approach is different (as the goals were quite different) even if the specimens have identical geometry. The RCS-RLC-01 slab was only retrofitted, as the purpose was only to restore the initial capacity of the slab. Thus, the CFRP elements were applied only around the long edge of the cut-out. However, for the RCS-RLC-02 slab the objective was to enhance the behavior and increase of the load bearing capacity, this desiderate being obtained by applying strengthening materials on the entire soffit of the slab.

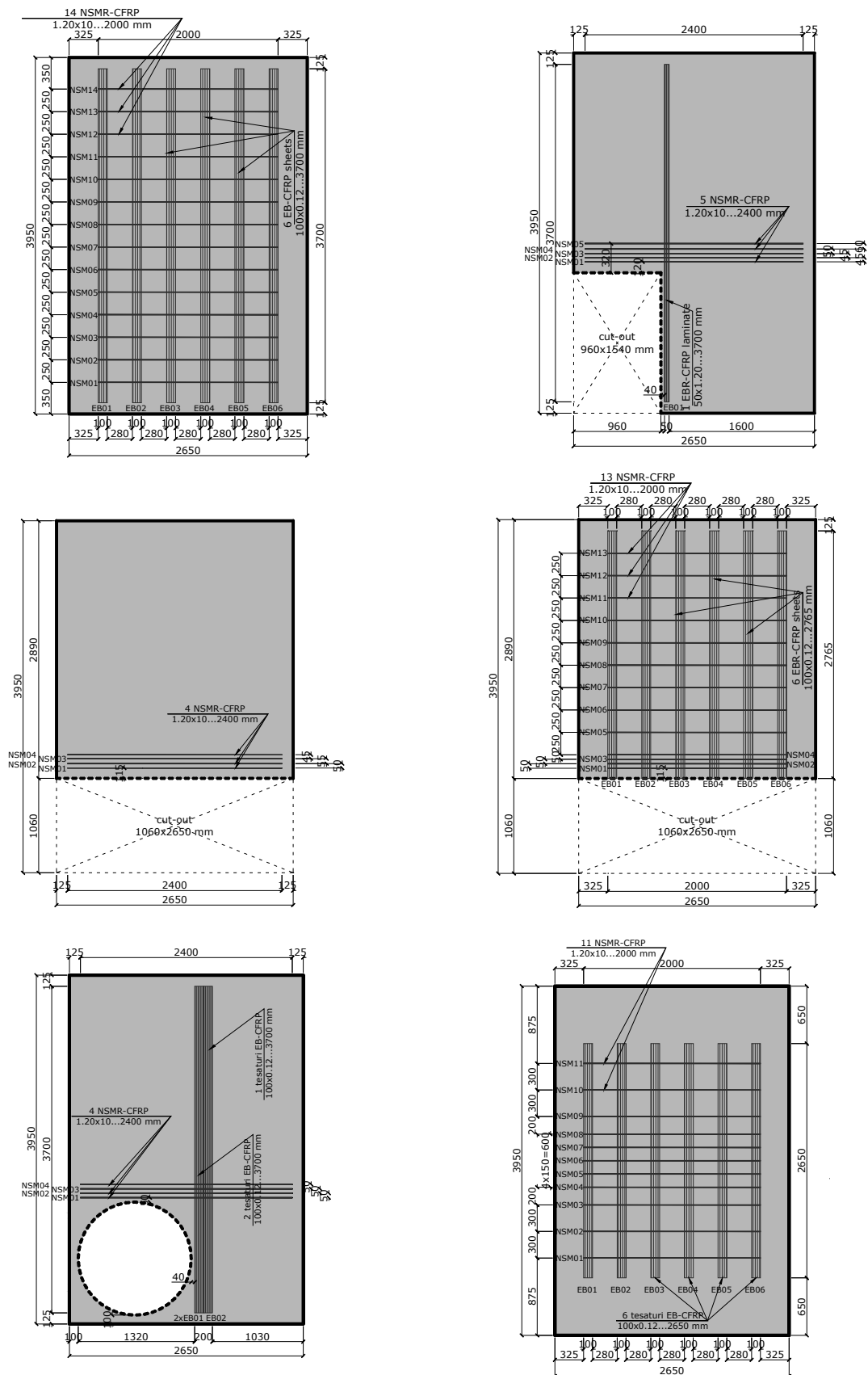


Figure 47. Geometry and retrofitting solution for the slabs

### 2.4.5 Behavior of strengthened elements

All tests on strengthened elements were denoted starting with the reference of the experimental specimens and updated with the mark “DS” standing for Damaged Strengthened (e.g. RCS-FS-01 represents the specimen and RCS-FS-UU-01 represents the test on the bare specimen).

#### Elements in the 1<sup>st</sup> group

The FS-DS-01 slab was tested up to failure, reaching a maximum load of 186 kN that corresponds to a vertical mid-span deflection of 50 mm. After this level, the deflection increased while the load diminished. The slab was able to deflect almost 110 mm before full failure. During the RSC-DS-01 test a maximum load of 86 kN was recorder at a central deflection of 27 mm. Maximum recorded deflection was 33 mm. The RLC-DS-01 test reached a maximum load of 75 kN at a central deflection of 8 mm. Maximum deflection was of 87 mm. The RLC-DS-02 test reached a maximum load of 147 kN at a central deflection of 63 mm. Maximum deflection was of 84 mm. The load-displacement diagrams of 1<sup>st</sup> group slabs are presented in Figure 48.

#### Elements in the 2<sup>nd</sup> group

The RCS-FS-DS-02 slab reached a maximum load of 199kN with a corresponding mid-span vertical displacement of 70 mm. The RCS-CC-DS-01 test reached a maximum load of 109 kN at a central deflection of 27 mm, being however able to deflect up to 85 mm showing a relative uniform plateau in the load-displacement curve after a small drop recorded after reaching the maximum load level. The load-displacement diagrams of 2<sup>nd</sup> group slabs are presented in Figure 48. A partial view of the soffit of the specimen RCS-FS-DS-02 at the end of the test is presented in Figure 49.

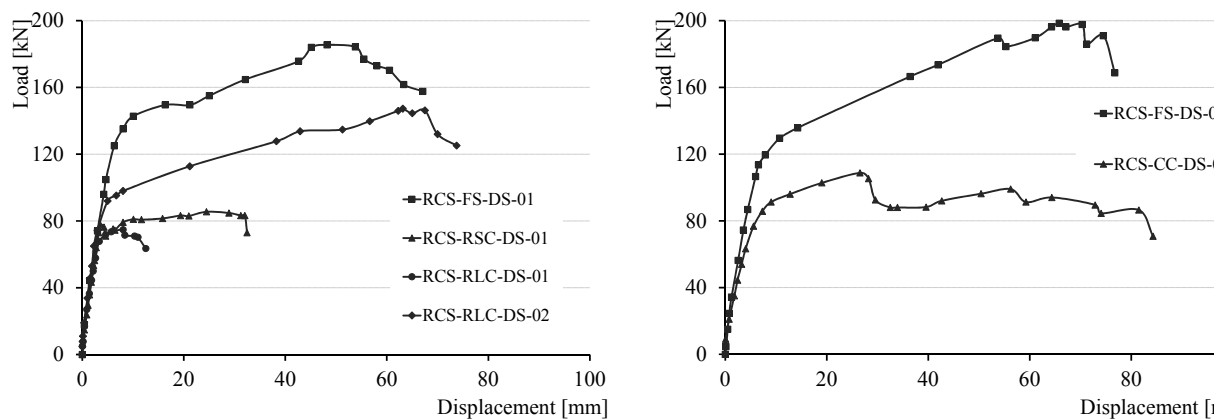


Figure 48. Load-displacement diagrams of the strengthened elements (left-1st group, right-2nd group).

### 2.4.6 Conclusions

The goal of strengthening/retrofitting interventions is achieved as slabs prove a regain or an increase in the capacity after applying the strengthening/retrofitting solutions. The increase of capacity by 58% for slab RCS-FS-01 is an extremely important prove of the effectiveness of the applied solutions. An even larger increase is obtained in the case of full element in 2<sup>nd</sup> group (by 96%) and in the case of slab RCS-RLC-02 (by 119%).

By applying only a retrofitting system, the capacity of the RCS-RSC-01 and RCS-RLC-01 slabs was restored. The amount of CFRP laid-up around the cut-outs was however insufficient for increasing the bearing capacity of the slabs. It is however interesting that by applying the retrofitting system for RCS-CC-01 slab, the capacity increase reached a value of 43%, suggesting the fact that the circular configuration of the cut-out is a much more favourable one.

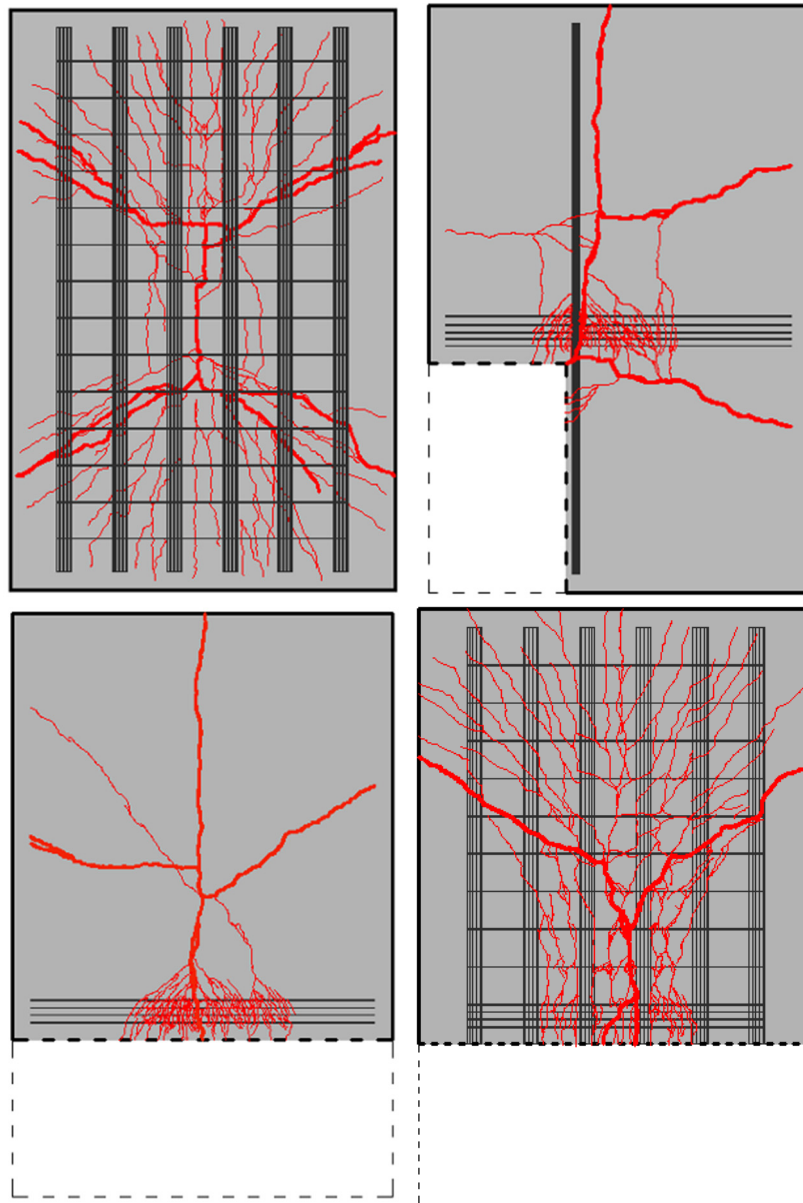


Figure 49. Final crack patterns superposed with the retrofitting system.

An important characteristic of the behavior of strengthened slabs consists in the fact that all of the CFRP components have failed due to fiber rupture; the only situation in which premature debonding had occurred was related to the failure of the laminate mounted by EB-FRP on the RCS-RSC-01 slab.

The crack patterns of all tested elements show a greater concentration of cracks for the retrofitted elements in comparison with the reference bare elements, suggesting a more favorable behavior in terms of cracking and crack width opening.

The behaviour of the full slab was improved significantly after applying the retrofitting system. The load capacity at ULS is improved by 59.3%. However, if the allowable deflection at SLS is considered, the load capacity is improved only by 37.3%, the corresponding load level being 102 kN and 140 kN, prior and after retrofitting, respectively.

By applying the retrofitting systems, the capacity of the slabs with cut-outs was restored. The amount of CFRP laid-up around the cut-outs was insufficient for increasing the bearing capacity of the slabs. The failure of NSMR-FRP by fiber rupture along with the crack patterns, have proved the effectiveness of the CFRP elements.

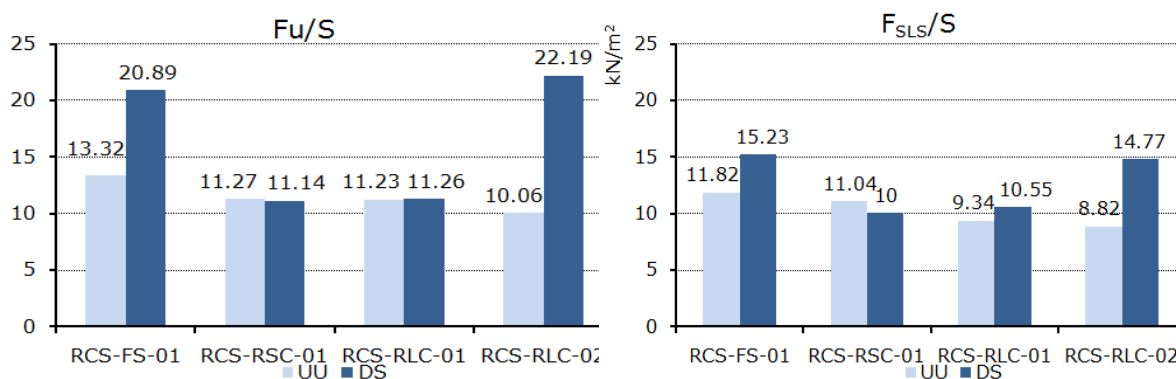


Figure 50. Capacities of all slabs before (UU) and after strengthening (DS)

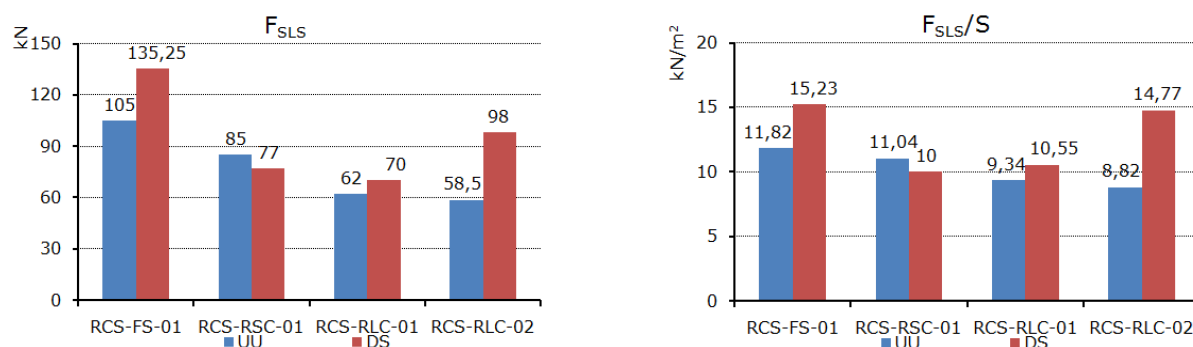


Figure 51. Capacities at SLS of all slabs before (UU) and after strengthening (DS)

## Acknowledgement

The presented research received financial support from the Romanian National University Research Council (CNCSIS) through a research grants, with title Advanced strengthening systems of RC members, as beams, columns, walls and slabs, using FRP composites (Sisteme avansate pentru consolidarea elementelor structurale din beton armat de tip grinzi, stâlpi, pereți și planșee folosind materiale compozite polimerice armate cu fibre), Grant CNCSIS CEEX type ET, 2006 – 2008, coordinated by Dr. Nagy-György Tamás, Politehnica University of Timisoara.

My special appreciation and thanks to Dr. Floruț Sorin-Codruț.

## 2.5 Theoretical and experimental study of precast reinforced concrete dapped-end RC beams' retrofitted using FRP composites

### 2.5.1 Introduction

Precast prestressed concrete (PC) structures have several advantages compared to cast-in-place structures; they can be constructed more rapidly and are generally more robust and durable. They are made of individual elements and assembled with various types of connections. For beams, these connections may require severe reductions of the cross-section at the ends, called dapped-ends. The abrupt change of cross-section in a beam results in a complex flow of internal stresses, which are typically highly concentrated at the re-entrant corner. Such regions in an element are called disturbed regions (D-regions).

According to the PCI Design Handbook dapped-end beams may fail in any of the five modes schematically represented in Figure 52: (1) Flexure (cantilever bending) and axial tension in the extended end; (2) Direct shear at the junction between the dapped and undapped zone of the member; (3) Diagonal tension failure at the re-entrant corner; (4) Diagonal tension failure in the extended end; and (5) Diagonal tension failure in the undapped zone. Numerous researchers have analyzed and experimentally investigated these failure modes. Using the strut and tie method, Reynolds (1969), Mattock and Chan (1979), Mattock and Theryo (1986) and Hwang and Lee (2002) have all proposed equations for predicting these failure modes and presented design criteria for dapped-end beams. Chen (2002) tested four dapped-ends with identical geometry and reinforcement ratio, but different reinforcement layouts. The results showed that the reinforcement arrangement influences the capacity of the elements, and that the provisions given in the ACI 318-08 code are conservative. Lu et al. (2003) theoretically and experimentally investigated the shear resistance of 12 dapped-end beams, again finding that the PCI Design Handbook provisions are conservative, and suggested new design proposals.

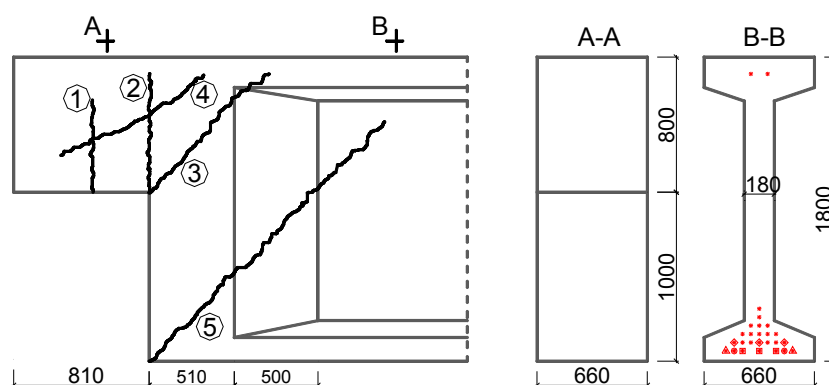


Figure 52. Potential failure modes in dapped-ends, and cross-sections of the original beams in the real application this study is based upon (dimensions in mm)

The load carrying capacity (hereafter capacity, for convenience) of dapped-end beams may be insufficient for reasons such as design errors, code changes, increases in loads, or structural damage. One option to increase the capacity of the dapped-end regions is to use fiber-reinforced polymers (FRP) using the externally bonded reinforcement (EBR) technique. FRPs are viable solutions for strengthening or retrofitting reinforced concrete (RC) elements, and several guidelines for strengthening RC structures with FRPs have been published recently (fib, NRC, ACI).

However, these guidelines do not refer specifically to FRP strengthening of dapped-end beams, partly because the variations in geometry, material and loading conditions at their dapped ends hinder the establishment of clear criteria for robustly classified strengthening configurations.

In a series of tests, Huang and Nanni verified that FRPs can increase the capacity of dapped-end beams with “mild steel and no mild reinforcement”, and proposed a method for strengthening dapped-end beams with FRPs that was found to be “satisfactory and conservative”. They too showed that dapped-end reinforcement designed according to the PCI Design Handbook is very conservative.

Gold et al. strengthened dapped-end beams of a three-story parking garage that were deficient in shear resistance with FRP. Due to the lack of design provisions at that time, they carried out a series of tests to verify the effectiveness of the FRP strengthening and predictive performance of their design approach. The FRP strengthening systems doubled the resistance of the beams, confirming their effectiveness.

Tan experimentally investigated the efficiency of several FRP configurations for strengthening dapped-end beams with deficient shear resistance, varying in both fiber types and mechanical anchorage systems for the FRP. The results showed that glass fiber reinforced polymers (GFRP) provided greater improvements in terms of ultimate load than carbon FRP plates and carbon fiber sheets, and the tested mechanical anchorage devices enhanced exploitation of the FRP systems’ strengthening capacity by preventing their debonding. The empirically based strut and tie model they derived was applied to predict increases in the shear capacity of the dapped-end beams, and proved to be sufficiently accurate for the type of beams tested.

More recently, in a large series of experiments Taher assessed the effectiveness of the following techniques for improving the capacity of dapped-end beams: externally bonding steel angles; anchoring unbonded steel bolts in inclined, pre-drilled holes; externally applying steel plate jackets; and wrapping carbon fiber around the beam stem. Tests with 50 small-scale rectangular beams indicated that the FRPs were the most viable solution for strengthening/retrofitting applications. Using the strut and tie analogy, Taher also derived a regression model to estimate the capacity of the FRP-strengthened dapped-end beams, which reportedly provided “reasonable” predictions, but he did not consider any possible scale effects of the beams tested for deriving the model.

The current study presents an experimental program prompted by a real case application. To the authors’ knowledge, only four experimental investigations on dapped-end beams strengthened with FRPs have been reported (Huang, Gold, Tan, Ther). The specimens tested in the previous four experimental programs and the research presented here are shown (at the same scale) in Figure 53. Clearly, there are major differences in the specimens used in these research programs, in terms of the configuration of the dapped-end, position of the loading, shear spans, and size of the beams (see Table 6). Therefore, the work presented in this chapter enriches the experimental database on FRP-strengthened dapped-end beams and provides both experimental and numerical assessments of the behavior of large, FRP-strengthened (and unstrengthened reference) dapped-end beams.

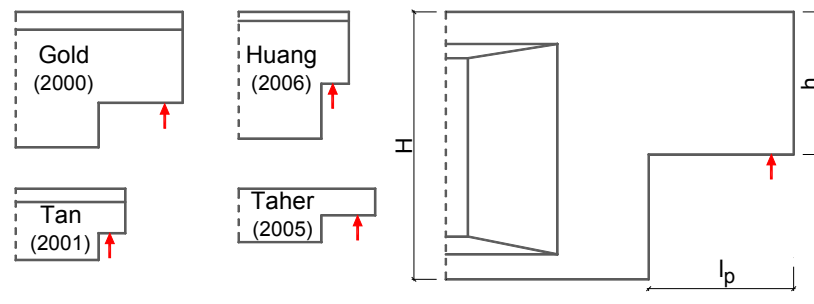


Figure 53. Dimensions of the dapped-end beams strengthened with FRPs tested in current and previous studies.

Table 6. Numbers and types of specimens, and dimensions of FRP-retrofitted dapped-end beams tested in this and previous studies.

Source	No. of tested elements	Type	Specimen height (H) (mm)	Cross-section web width (B) (mm)	Dapped-end H/recess (h/l <sub>p</sub> ) (mm)	Shear span (a) (mm)
Gold	16	Double T	760	97	510/470	880
Tan	7	T	400	150	250/150	320
Taher	52	Rectangular	300	200	150/300	350
Huang and Nanni	5	Double T	711	114	403/153	460
Current study	4	Rectangular	1500	660	800/810	940

### 2.5.2 The context of the study

A single-storey industrial hall was constructed using 20 m long identical precast/prestressed beams, with 1800x660 mm cross-section, serving as supports for the roof purlins (Figure 52). Immediately after assembly of the structure eight beams had diagonal cracks corresponding to the third mode of failure, see Figure 52. The inclination of the crack angle varied between 40° to 50° with respect to the longitudinal axis of the beam. Initially the dapped-ends were designed using the strut and tie method according to the Romanian codes (1990) and EC2 (2004) for a reaction force of 800 kN positioned 400 mm from the re-entrant corner.

An inspection revealed that the dapped-ends were not in full contact with the supporting columns. Consequently, the position of the reaction force was displaced by an additional 275 mm, resulting in the diagonal cracking. Hence, the dapped-end beams were re-assessed, considering the new lever arm (675 mm). At this stage, the reaction force in the beam was about 500 kN. The widely used strut and tie models proposed by Schlaich et al. and Martin (Figure 54 a, b), indicated that the dapped-end beams' capacity was 600 and 590 kN, respectively, based on the prescribed safety factors for the materials and the loads. Therefore, they had a deficit in capacity of ca. 200 kN, and a strengthening solution using EBR carbon fiber reinforced polymer (CFRP) plates was proposed to meet it. The International Federation for Structural Concrete's guideline (Bulletin 14), recommends a strain limitation of 4‰ for FRP plates. However, due to the variations in FRP strengthening applications, there are serious doubts about the suitability of this limit; thus a further aim of the presented research was to assess its validity under the examined conditions.

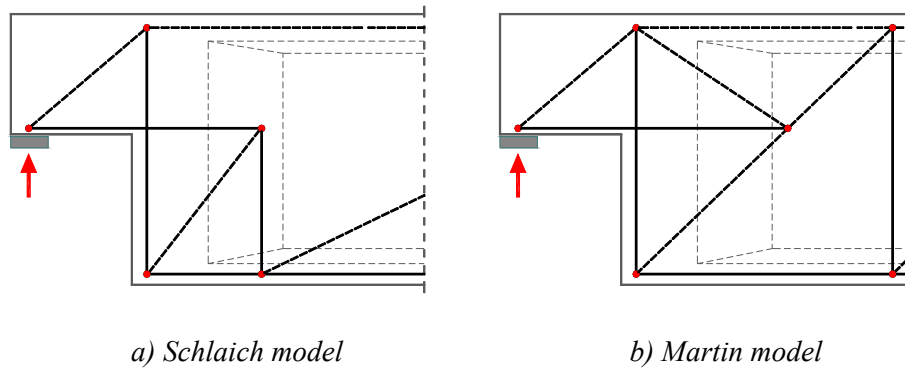


Figure 54. Schematic diagrams of the strut-and-tie models used to evaluate the capacity.

### 2.5.3 Research program

#### Experimental investigations

Two beams, each with two dapped-ends, were cast. Since the investigations focused on the dapped-ends, the total length of the element was reduced from 20 m to 6.24 m by removing the flexural span of the beam; the tensile prestressed reinforcement was replaced with an equivalent steel reinforcement area; and the height of the cross-section of the beam was reduced from 1.8 m to 1.5 m. These modifications should have had no significant influence on the failure mode, as observed at the job site (mode 3, in Figure 52). The arrangement, spacing, diameter and strength class of the reinforcements were identical to those of the original beams (Figure 55).

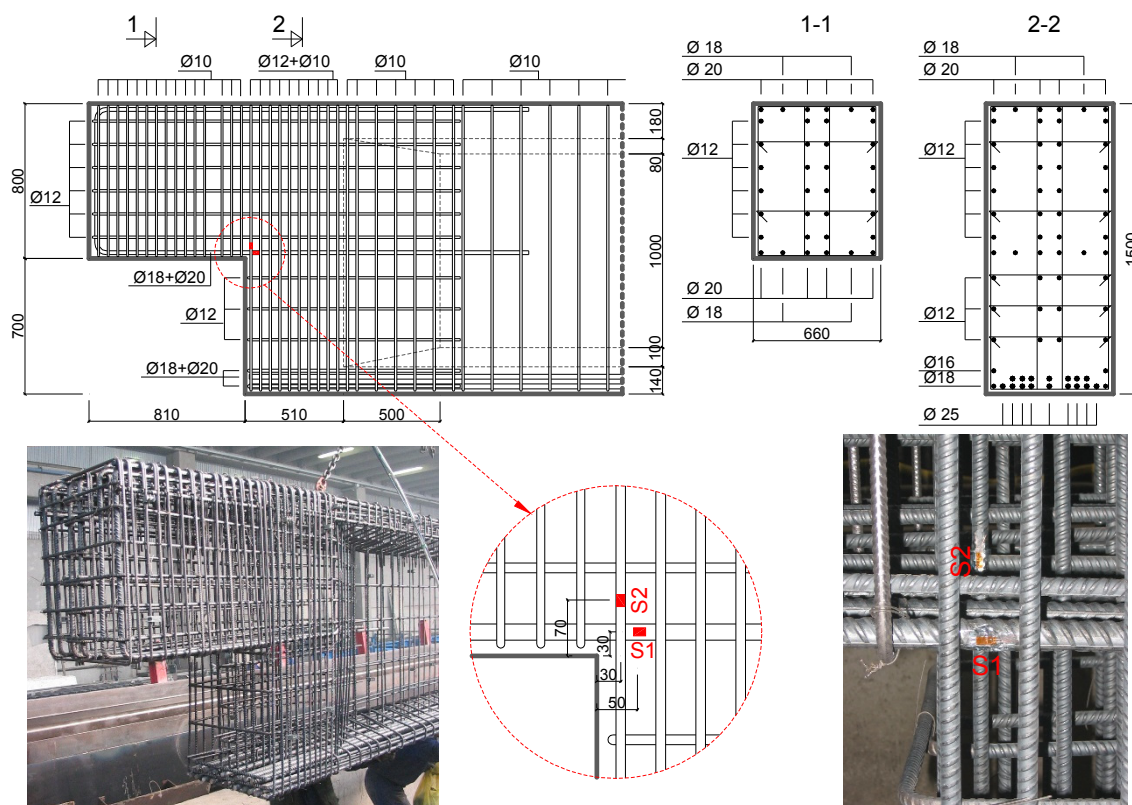


Figure 55. Reinforcement details, position of the strain gauges and casting of the elements (dimensions in mm).

## Material tests

The material properties were determined from laboratory tests, in conformity with SR EN 12390-1-4:2002 for concrete and SR EN 10002-1:2002 for steel. A concrete with a maximum aggregate size of 16 mm and mean compressive cube strength of  $56 \text{ N/mm}^2$  was used, corresponding to a C45/55 concrete strength class. Characteristic values of the tensile properties of the steel reinforcements are presented in Table 7.

## Test setup, instrumentation and test procedure

The dapped-end specimens were tested according to the schematic test configuration shown in Figure 56, by applying a monotonic force in increments of 50 kN by a hydraulic jack. After each step the loading was maintained and the cracks were mapped.

Table 7. Properties of the steel material, determined in laboratory tests

Diameter (mm)	$f_y$ ( $\text{N/mm}^2$ )	$f_u$ ( $\text{N/mm}^2$ )	$\varepsilon_y$ (‰)	$\varepsilon_u$ (‰)	$\varepsilon_{ult}$ (‰)
10	780	922	3.6	14.9	15.5
12	522	600	2.5	23.1	24.0
16/18/20	460	600	2.2	19.9	21.0
25	440	625	2.2	18.9	20.0

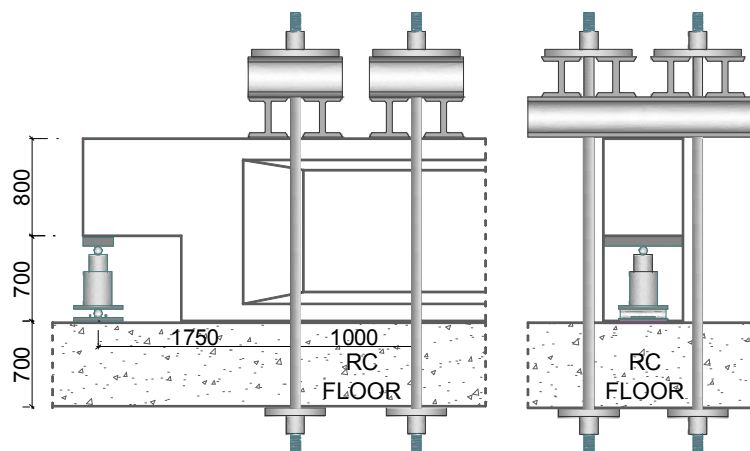


Figure 56. Schematic diagram of the test setup – side and front views (dimensions in mm).

Before casting, one strain gauge was applied in the horizontal bar closest to the re-entrant corner (S1), and another was glued in the vertical bar nearest the re-entrant corner (S2), Figure 55. The strains recorded by the gauges are classified as illustrated by the following example: S1-RC2-T is the strain registered in steel reinforcement (S) in vertical (1) direction for the retrofitted (R) concrete element 2 (C2) during the experimental test (T).

The horizontal displacements of the specimens were monitored using four linear variable differential transducers (LVDTs): one at the top (M7) and one at the bottom (M4) of the nib; plus one at the top (M5) and one at the bottom of the undapped portion (M6). Three LVDTs were also used to measure the vertical displacements: one placed in the front face at the bottom of the nib (M1), one on the edge of the dapped-end at the re-entrant corner (M2), and one on the bottom edge of the undapped portion (M3), Figure 57. The “displacement” term in the presented load-displacement diagrams is defined as the difference in positions recorded by the LVDTs at points M1 and M3.

In the experimental program, the four dapped-end specimens were tested in the following sequence. First, the C1 element was tested to failure, to obtain reference measurements of the capacity of the in situ dapped-end beams before strengthening. Then the remaining three dapped-ends (C2, C3 and C4) were tested up to 800 kN; the design load of the original dapped-ends. Finally, the C2, C3 and C4 elements were repaired, strengthened as described below and retested to failure.

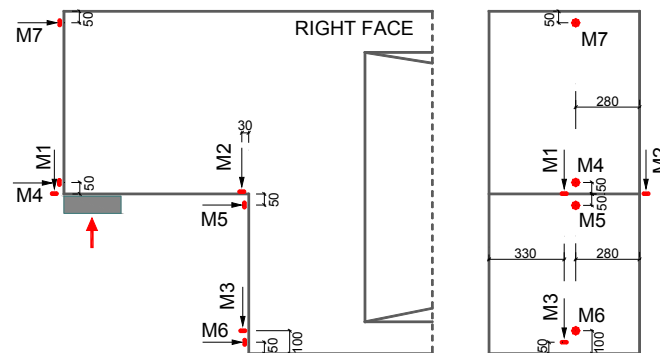


Figure 57. Positions of the displacement transducers (dimensions in mm).

### Strengthening of the elements

The pre-cracked elements were strengthened by using two systems of EBR CFRPs, in three different solutions. The aims of the strengthening solutions were to increase the capacity up to the design load and to delay the yielding initiation of the steel reinforcement. After the initial tests of the C1-C4 elements the surface of the concrete was ground, the dust and impurities were removed with compressed air, the strengthening systems were applied and cured during seven days. New strain gauges (labelled G in Figures 61c, 65c and 68c) were installed to monitor the strains developed in the FRPs. An identical test setup was used for both the unstrengthened (C) and retrofitted (RC) specimens. Table 8 presents mechanical and geometrical properties of the FRPs. For the field application, strengthening Systems 1 and 2 were used. Since the  $0^\circ/90^\circ$  layout (RC4) provided the longest anchorage length this configuration was preferred in an attempt to avoid premature debonding. However, in some cases the purlins obstructed application of this layout (RC4, Figure 68), hence the  $45^\circ/90^\circ$  layout (RC2, Figure 61) was adopted.

For comparison, strengthening System 3 was also applied in the experimental program. The amount of carbon fibers (CFRP) used in System 3 was modified to provide equivalent strength to that of Systems 1 and 2.

*Table 8. Characteristics of the CFRP composite systems used (as specified by the producer).*

System	Components	Tensile modulus [N/mm <sup>2</sup> ]	Strain at failure [%]	Thickness [mm]	FRP width [mm]	FRP layout	Retrofitted element designation
1	Plate	165000	17	1.2	2 x 100	45°/90°	RC2
	Resin	11200	10	N/A			
2	Plate	165000	17	1.2	2 x 100	0°/90°	RC4
	Resin	11200	10	N/A			
3	Fabric	640000	4	0.19	300	45°/0°/90°	RC3
	Resin	3500	15	N/A			

## 2.5.4 Numerical investigation

### Modeling strategy

The numerical analysis was carried out a posteriori to the tests. Due to malfunction of some of the installed gauges, it was not possible to register the corresponding strains during the tests. Therefore, to better understand the failure progress of the tested elements in general, and the behavior of the FRPs in particular, the tests were simulated in 2D using ATENA software. The aim of this analysis was to obtain information regarding the development of strains in the steel reinforcement after strengthening and in the FRP up to failure.

The numerical modeling was carried out in two steps. First, several full geometry FE models were constructed and analyzed using characteristic values reported by the manufacturers for the concrete, steel and FRP reinforcement in order to calibrate the experimental test setup. In the second step the specimens were modeled using average values of the material properties, determined from standardized tests. In the latter phase the boundary conditions were also calibrated, to account for elastic deformations in the upper supports of the reaction frame of the test setup. Here, only the results from the second modeling phase are presented. Due to software limitations it was not possible to simulate the phased process of the strengthening intervention (as the CFRP systems were applied when the specimens had already cracked). Therefore, in the numerical modeling the CFRP systems were considered to have been applied to uncracked specimens. This limitation has certain drawbacks for modeling the strain development in the CFRP systems. However, as will be shown, its consequences are of minor significance in the context of the field application. In a similar manner as for the laboratory tests, the displacement plotted in all the diagrams was computed as the difference between the M1 and M3 measuring points presented in Figure 57.

The standard incremental and iterative Newton-Raphson method for material nonlinear structural analysis was used in the numerical simulations, based on the finite element method (FEM). The specimens were modeled with a mesh of 8-node serendipity plane stress finite elements. A Gaussian integration scheme with 2x2 integration points was used for all the concrete elements. The steel bars, CFRP laminates and CFRP sheets were modeled with 2-noded perfectly bonded embedded truss elements (one degree of freedom per node) (Cervenka, 2011).

The strains monitored during the analysis are labeled similarly to those from the experimental tests, but the character N is added to distinguish the experimental from the numerical results. For instance, the designation S1-RC2-N refers to strains obtained numerically at the position

coinciding with the S1 strain gauge, in the numerical simulation of the specimen strengthened with the RC2 configuration.

### Properties of the materials in the simulations

#### Concrete

The constitutive model for concrete used in the analysis is a fracture-plastic model that combines constitutive sub-models for tensile and compressive behavior, as presented in the ATENA user manual. This fracture model employs the Rankine failure criterion and exponential softening, with the hardening/softening plasticity component based on the Menétrey-William failure surface. The concrete post-cracking tensile behavior was simulated by the softening function illustrated in Figure 58a in combination with the crack band theory.

#### Steel bars and carbon fiber reinforced polymer systems

The reinforcement was modeled using discrete bars, whose tensile and compression behavior were simulated using the stress-strain relationship illustrated in Figure 58b. After the peak strength,  $f_u$ , the stress was reduced to 10% of  $f_u$  so that internal stress redistribution could be assured in the numerical computations. Table 7 presents values used for characterizing the stress-strain relationships of the different types of bars composing the reinforcement.

FRP materials exhibit linear-elastic behavior until failure. In a similar manner as for the steel bars, a descending branch was also modeled, so that after the peak strength was reached (Figure 58c), the FRP material could not support further loads. The FRP material was introduced using several discrete lines (modeled as bars perfectly bonded to the substrate), each equivalent to a 50 mm wide strip. The same procedure was used for the plates, except that the strips were 25 mm wide. The values of the mechanical properties of the CFRP systems are indicated in Table 8. The predictive performance of the simulations, described in Section 4, show that this simplified approach is acceptable for the purposes of the presented numerical analyses.

#### Boundary conditions

To allow eventual separation of the bottom surface of the specimen in contact with the supporting RC floor, contact elements without tensile capacity were adopted. The elastic deformation of the test supporting system was calibrated based on the experimental results obtained for the reference specimen, and then integrated in all the numerical simulations.

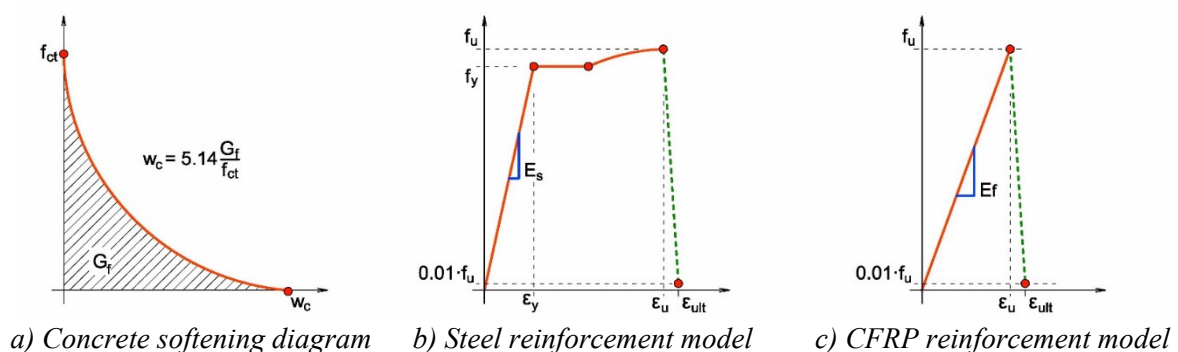


Figure 58. Material models used in the numerical analysis.

### 2.5.5 Results of the experimental program

The research focused on the strengthening system used in a practical application. Results are presented for two loading scenarios: the first for loadings up to 800 kN, for which the dapped-ends were designed, while the second simulates the ultimate limit state (ULS) loading condition of each strengthened element. Results from both experimental and numerical investigations are reported and discussed in terms of: load-displacement behavior, strain distributions in the steel and FRP reinforcements, the increase in capacity of the dapped-ends provided by FRP strengthening, crack patterns and failure modes. Strains in the extremities of the FRPs were not monitored during the tests, but estimates of their values were obtained from the numerical analysis. The numerical analysis accurately predicted the load-displacement responses of all specimens up to the failure load recorded in the tests. After this load, the models for elements RC2 and RC4 overestimated the FRP contribution, because the peeling-off mechanism could not be simulated in the 2D analysis. Up to the yielding strain of the horizontal steel rebars, the strains in the steel and FRPs computed from numerical analysis agreed well with values recorded in the tests. Between the yielding load and failure load, the strains in the steel bars determined by FEM analysis show some differences from those recorded in the tests. These differences may be attributed to the tension stiffening effect present in the beams but not implemented in the numerical models. Furthermore, the strains recorded experimentally only represent the strains in the zones where the strain gauges (SG) were installed, while the FEM analysis provided average strains for the steel bars.

#### Test results for the C1 specimen

The C1 (control) element was tested to failure. Up to 700 kN just a single crack formed, starting from the re-entrant corner at an angle of  $60^\circ$  with respect to the longitudinal axis of the beam. As the load increased, several additional cracks formed, and finally cracks were uniformly distributed around the re-entrant corner, as shown in Figure 59a. The test was stopped at 1600 kN, when a displacement of 30 mm was registered. This relatively high deformation was due to yielding of the tensile reinforcement and local crushing of the compressed concrete under the supports. At that moment the major measured crack was 3.5 mm wide, see Figure 59b. The strain gauges attached to the reinforcements did not function during this test. However, the FEM analysis (Figure 60) indicates that yielding of the vertical (S2-C1-N) and horizontal (S1-C1-N) steel reinforcements occurred at loads of about 865 and 970 kN, respectively. At the design limit, i.e. 800 kN, the strains were 1.75 ‰ in horizontal (S1) and 2.20 ‰ in vertical (S2) reinforcements, as subsequently confirmed in the tests of C2, C3 and C4 specimens. The FEM analysis indicated that failure occurred at 1573 kN (Figure 60a) by crushing of the concrete in compression and yielding of the tensile reinforcement as indicated in Figure 60b.

#### Test results for the C2 and RC2 specimens

Specimen C2 was tested up to 800 kN. The first crack (1), occurred at 600 kN and started from the re-entrant corner at  $42^\circ$  angle with respect to the longitudinal axis of the beam (Figure 61). Between 600 and 650 kN three other cracks (2, 3, 4) formed near the first crack. From 650 kN until the target load two additional cracks (5, 6) formed (Figure 61a). The strain gauge attached to the horizontal steel reinforcement (S1-C2-T) recorded 1.75 ‰ strain at 800 kN, close to the yielding strain (2.2 ‰). The strain gauge installed on the vertical reinforcement only recorded values up to 200 kN, therefore these recordings will not be commented upon. After the test the specimen was unloaded, retrofitted with FRP, and retested (Figure 61b).

Compared with the reference specimen (C1), this retrofitted element (RC2) had a higher capacity and stiffness, especially above the deflection corresponding to a loading of 800 kN (Figure 63a), due to the FRP systems delaying development of the cracks in the concrete and decreasing the strain in the reinforcements (Figure 63b).

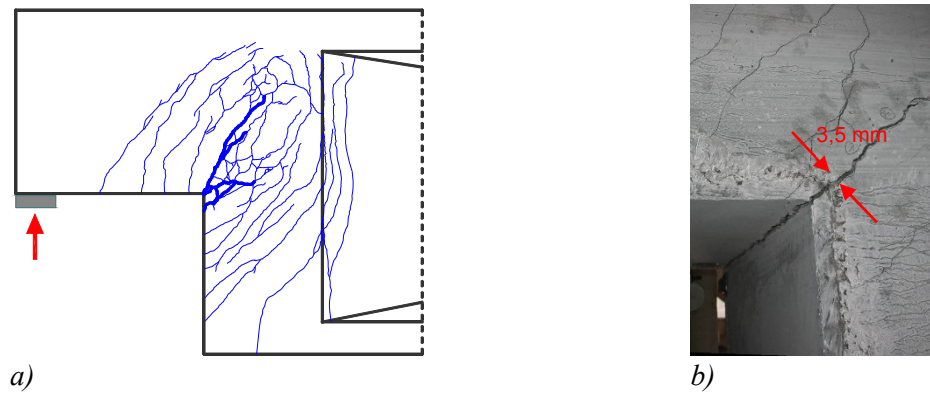


Figure 59. (a) Schematic representation of the crack pattern in the C1 specimen and (b) photograph, showing the major crack.

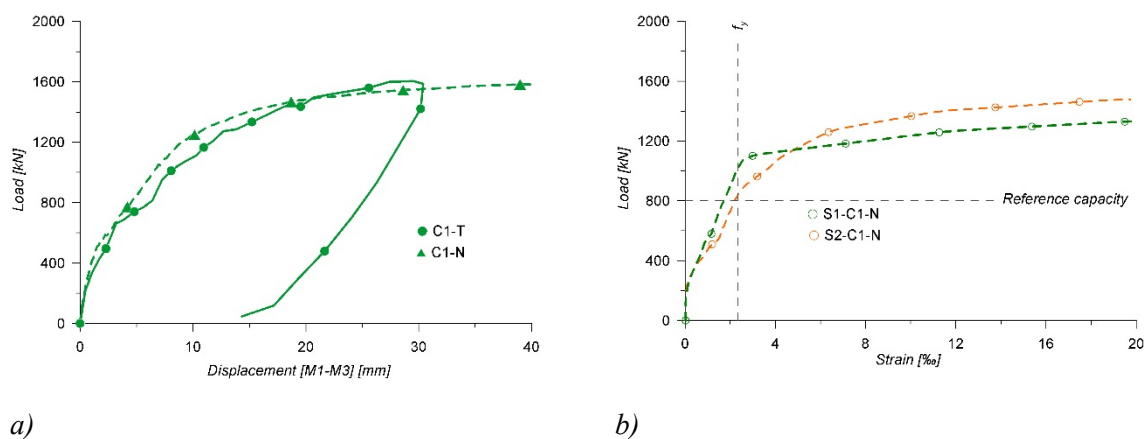


Figure 60. (a) Load-displacement curves obtained experimentally (C1-T) and numerically (C1-N), and (b) load-strain relationship determined numerically at the positions of the strain gauges S1 and S2 for the C1 specimen.

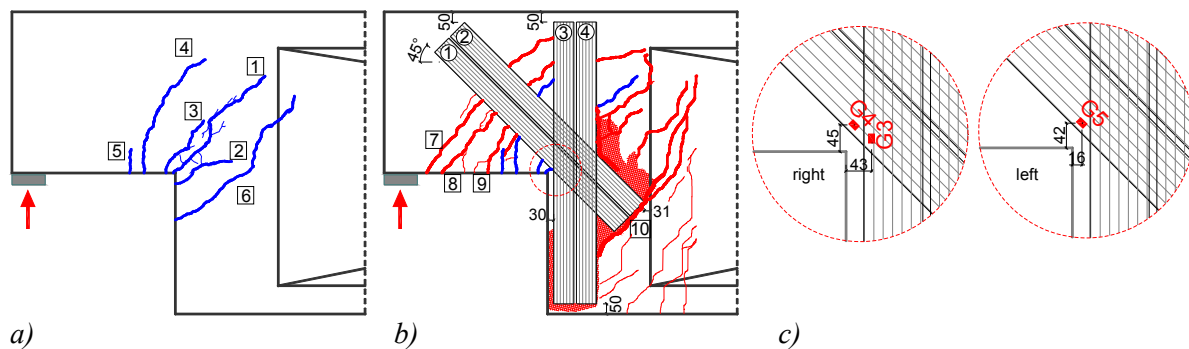


Figure 61. Schematic representation of the crack patterns in: a) C2 specimen at 800 kN b) RC2 specimen at failure; c) Locations of the strain gauges.



Figure 62. Photographs showing the vertical and inclined CFRP plates peeling-off from element RC2.

The stress-strain relationship of the RC2 element was almost linear up to 1300 kN. Up to this load the existing cracks did not develop further, but new three cracks (7, 8, 9) formed in the nib (Figure 61b). This shows the capacity of the applied FRP systems to limit damage that occurred in the C2 test phase, promoting stress redistribution. Between 1300 and 1350 kN a new crack (10) formed around the inclined FRP plates and extended towards the bottom part of the vertical plates (Figure 61 and 62). The element started to fail at 1670 kN, by the inclined plates on the right face of the strengthened dapped-end successively peeling-off (Figure 62). At this load the strain in the FRP was 5.5 ‰ (G5-RC2-T, see Figure 61c); 32 % of the FRP's ultimate strain. The failure ended in a brittle manner at 1760 kN, when the inclined FRP plate on the left face of the dapped-end peeled-off, and caused the vertical FRP to peel off (Figure 62). At failure the strains measured in the inclined (G4-RC2-T) and vertical (G3-RC2-T) FRP plates were 7.2 and 4.9 ‰, respectively (Figure 63c). The strain measured in the steel reinforcement (S1-RC2-T in Figure 55) at a load of 800 kN was 1.20 ‰; 31 % less than the strain at this load in the reference specimen (S1-C2-T).

The strain distribution along the FRP, determined from the numerical simulations, for a load of 1620 kN, just before the peeling-off process started, is shown in Figure 64. For this load the maximum strain recorded at the bottom-end of the inclined plates was 4.1 ‰, while at the bottom-end of the vertical plates only marginal strains were recorded. This confirms observations from the experiments that the inclined plates initially debonded and subsequently the vertical plates.

The FEM analyses also indicated that if the FRPs had been mechanically anchored, the capacity of the dapped-ends could have been increased to 1917 kN. The maximum strain in the inclined FRP (17 ‰) was reached at 1845 kN, just before peak load. After the first strip reached its ultimate strength, the remaining FRP bands failed consecutively up to the point at which the peak load was reached. At peak load a strain of 9.50 ‰ in the vertical FRP was obtained. This suggests that a debonding failure could have been avoided if the inclined FRP plates had been mechanically anchored. If so, the numerical analysis indicates that the failure mode could have been changed from FRP peeling-off to yielding of the horizontal reinforcement together with failure of the inclined FRP and crushing of the compressed concrete.

### Test results for the C3 and RC3 specimens

Specimen C3 was tested up to 800 kN. The first crack (labeled 1 in Figure 65), started at 400 kN and developed at a 45° angle from the re-entrant corner. Between 400 to 600 kN three other cracks (2, 3, 4) formed near the first crack, followed by two additional cracks (5, 6) by the time the target load was reached (Figure 65a). At 800 kN the strains recorded by the gauges attached to the horizontal steel reinforcement (S1-C3-T) and vertical steel rebar (S2-C3-T) were 1.81 and 1.76 ‰, respectively. Hence, the reinforcement was close to the yielding level (2.2 ‰). At this loading the specimen was unloaded, retrofitted according to the FRP configuration illustrated in Figure 65b, and retested.

The stress-strain relationship of the RC3 specimen was almost linear up to 900 kN but above 450 kN the existing cracks (1, 4, 6) reopened, and at each 50 kN load increment the cracks gradually widened, and the fibers of the sheets started rupturing progressively, with an accompanying typical loud noise. The strain gauges bonded to the composite (Figure 65c) became damaged at a load of about 500 kN. However, at 800 kN the strain gauges installed on horizontal (S1-RC3-T) and vertical (S2-RC3-T) steel reinforcements indicated strains of 1.20 and 1.50 ‰, respectively. Thus, the FRP system reduced strains in these reinforcements, relative to those in the reference specimen, by 33% and 15%, respectively.

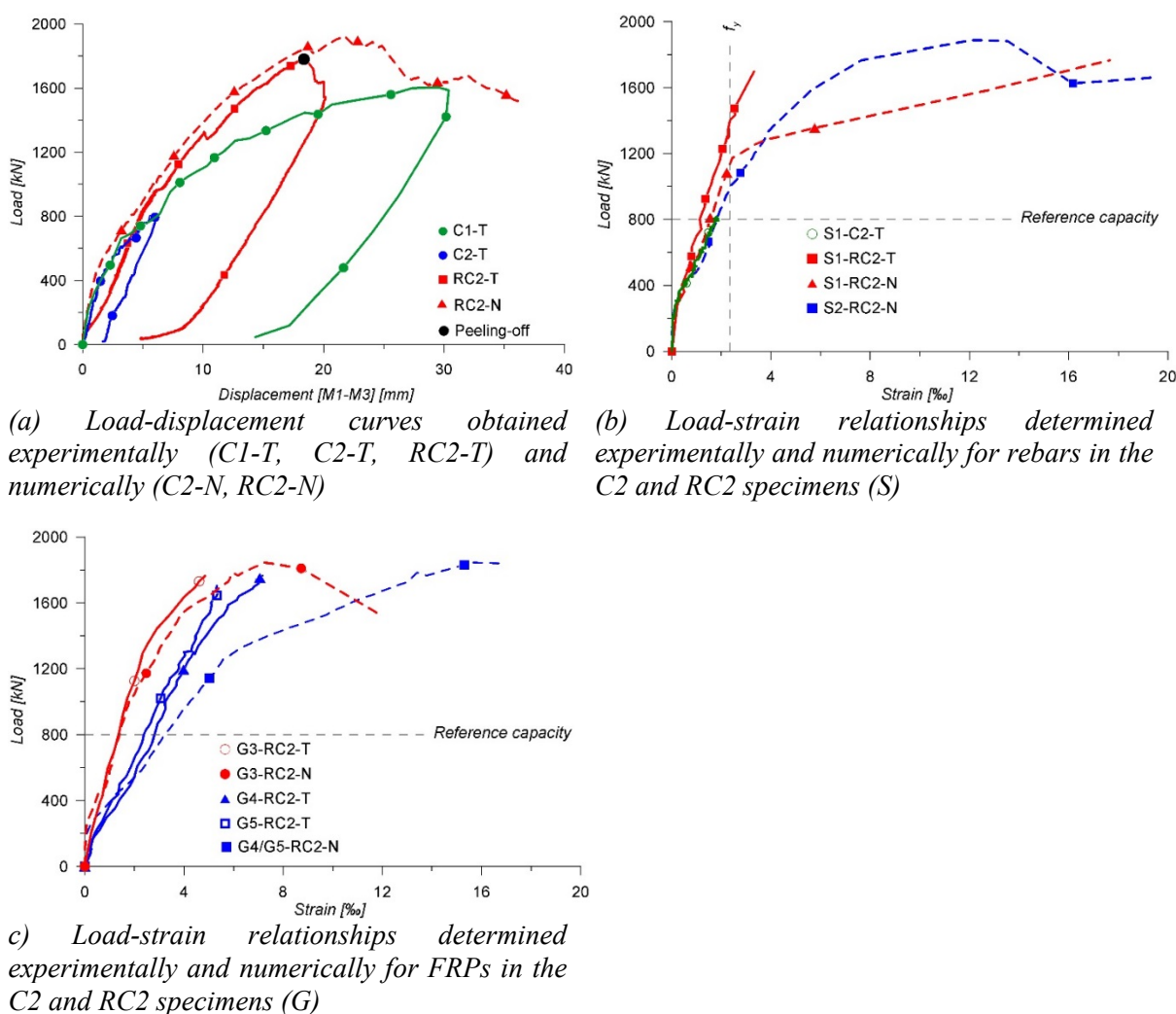


Figure 63. Behavior of the C2 and RC2 elements.

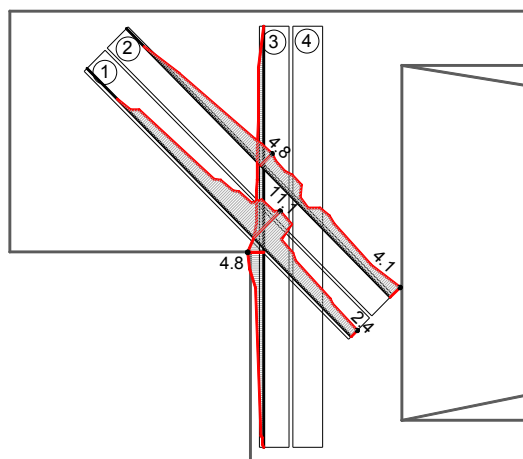


Figure 64. Strain distribution along the FRPs at a load of 1620 kN for specimen RC2-N.

The RC3 specimen had marginally higher ultimate capacity and higher stiffness up to 900 kN than the C1 element, due to the delayed cracking.

The numerical analysis accurately predicted the behavior of the RC3 specimen up to the maximum load recorded in the test (1587 kN vs 1618 kN), see Figure 66a. The strains in the horizontal and vertical steel rebars obtained by the FEM analysis were in good agreement with the strains recorded in the tests up to 1100 kN, at which the rebars started yielding (Figure 66b). The strains recorded by the G3-RC3-T and G4-RC4-T gauges (Figure 66c) correlated well with the strains predicted by the numerical simulations while these strain gauges were working properly, see Figure 66c. However, the deviation of the strains predicted at the position of the G5-RC4-T gauge from the measured values were relatively high, possibly because of its impairment after it was crossed by the principal crack during early loading stages.

The strain distribution along the FRP (Figure 67) clearly indicates its failure mode; fiber rupture of all the sheets along the plane of the principal crack, with values tending to zero at sheet-ends, and local crushing of concrete in the most compressed zone of the dapped-end.

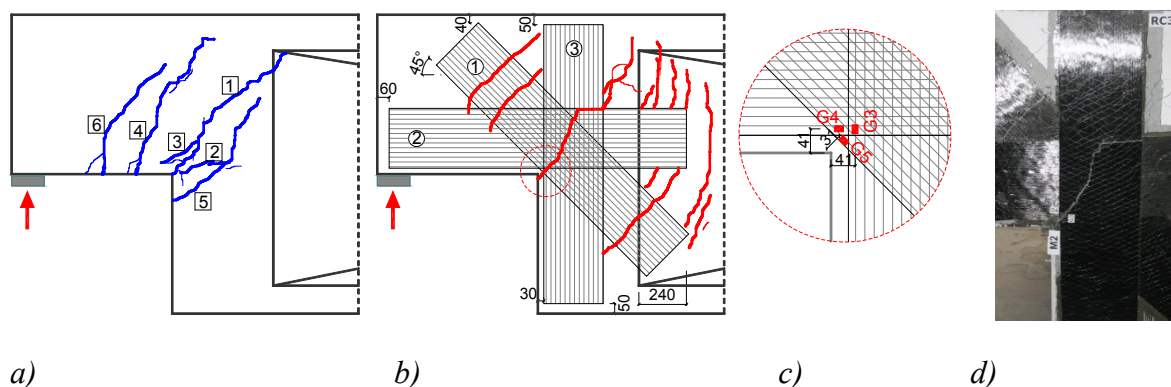
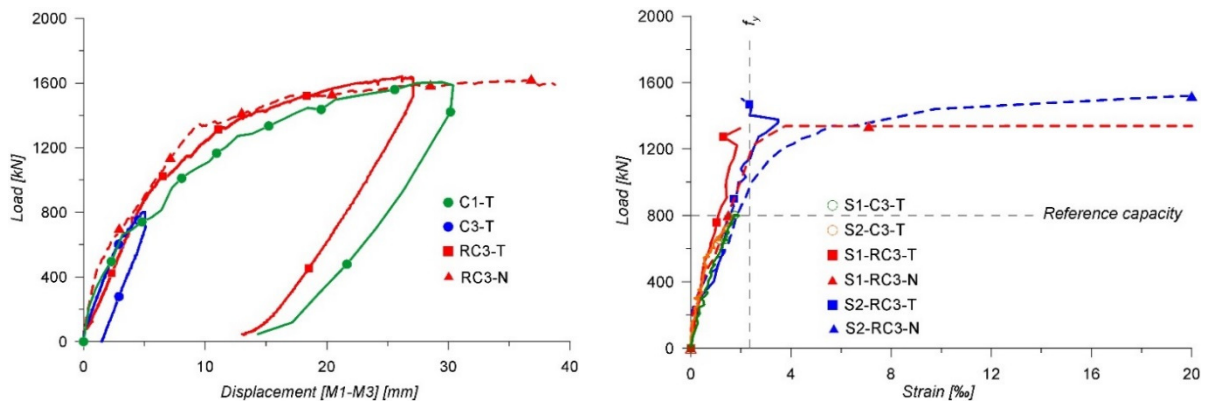
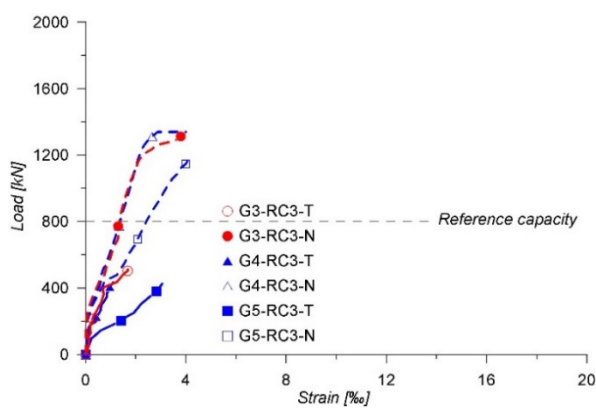


Figure 65. Schematic representation of the crack patterns in a) C3 specimen at 800 kN b) RC3 specimen at failure; c) Location of the strain gauges; d) failure detail.



(a) Load-displacement curves obtained experimentally (C1-T, C3-T, RC3-T) and numerically (RC3-N).  
 (b) Load-strain relationships determined experimentally and numerically in rebars (S) of C3 and RC3 specimens.



(c) Load-strain relationships determined experimentally and numerically in FRPs (G) of the C3 and RC3 specimens

Figure 66. Behavior of the C3 and RC3 elements.

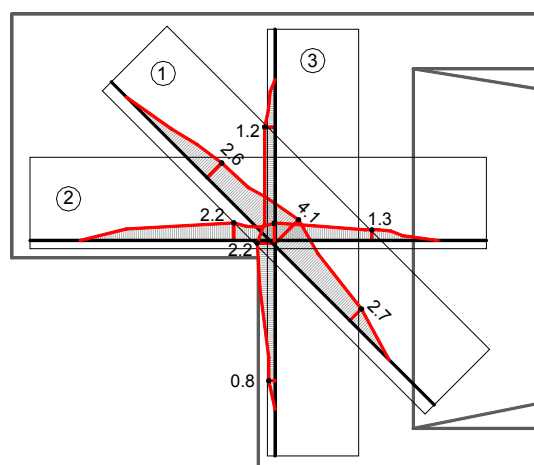


Figure 67. Strain distribution along the FRPs at 1177 kN loading for RC3-N.

### Test results for the C4 and RC4 specimens

Specimen C4 was also tested up to 800 kN. The first crack (labeled 1 in Figure 68), occurred at 600 kN and started from the re-entrant corner at  $46^\circ$  angle with respect to the longitudinal axis of the beam. At 650 kN two other cracks (2, 3) formed near the first crack, followed by four additional cracks (4, 5, 6, 7) by the time target load was reached (Figure 68a). The strain gauge attached to the horizontal steel reinforcement (S1-C4) recorded 1.44 ‰ strain at 800 kN. Due to malfunctioning of the gauge attached to the vertical reinforcement its strains were only measured up to 500 kN. At the target load the specimen was unloaded, retrofitted according to the FRP configuration represented in Figure 68b, and retested.

The stress-strain relationship of the RC2 element was almost linear up to 1300 kN. Up to this load the existing cracks did not develop further and no other new cracks formed. Between 980 and 1000 kN a new crack (8) started around the horizontal plates, extending towards the vertical plates. In the next load steps several new cracks (9, 10, 11) appeared, distributed concentrically with respect to the re-entrant corner.

The specimen started to fail at 1670 kN, by the horizontal plates successively peeling-off from both faces of the strengthened dapped-end (Figure 69). The maximum measured strains in the FRP at this load were 4.12 ‰ on the left face (G4-RC4-T) and 6.65 ‰ on the right face (G5-RC4-T), see Figure 68c and 70c; 24 ‰ and 39 ‰, respectively, of the FRP's ultimate strain. The failure ended suddenly, at 1680 kN, when the vertical plates on both faces failed by debonding, preceded by the horizontal plates peeling-off (Figure 69). At this load the strain measured in the vertical FRP plate was 6.72 ‰ (G3-RC2-T).

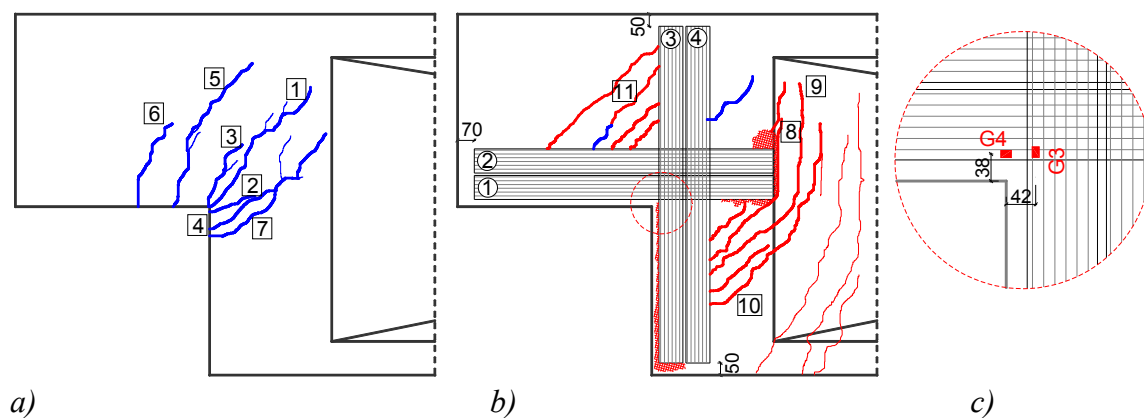


Figure 68. Schematic representation of the crack pattern in: a) C4 specimen at 800 kN, b) RC4 specimen at failure; c) Location of the strain gauges.

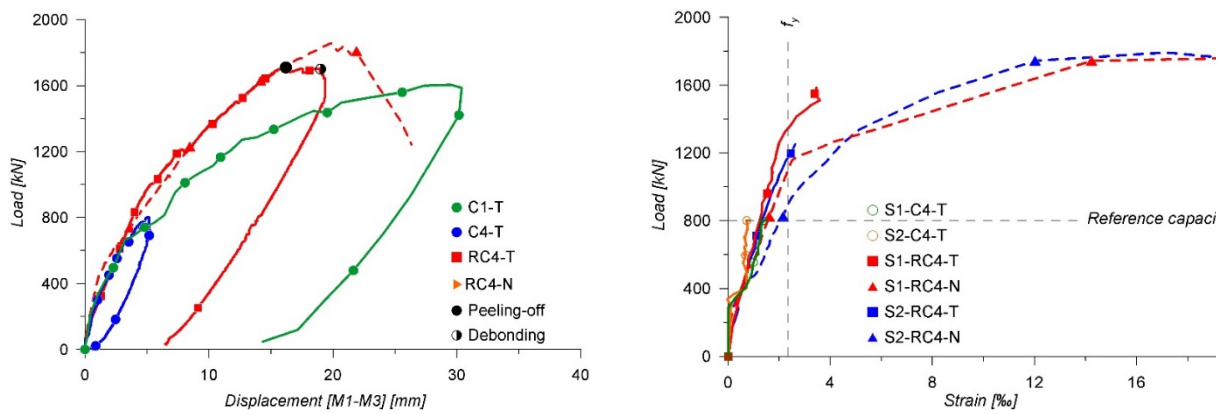
The strain measured in the steel reinforcement (S1-RC4-T) at 800 kN was 1.20 ‰, 15% lower than the strain recorded in the reference specimen (S1-C4-T) at this load. Compared with the reference specimen (C1), the retrofitted element RC4 showed a higher capacity and stiffness, especially above the deflection corresponding to a load of 800 kN (Figure 70a). Its overall behavior was similar to that of the RC2 specimen.

As shown in Figure 70a, the numerical analysis accurately predicted its load-displacement behavior up to the failure load recorded in the experimental test. Similarly to the results for the RC2 element, the model overestimated the final resistance of the specimen, for reasons already mentioned. Up to the yielding limit of the horizontal rebars, the strains in the steel and FRP reinforcements computed by the FEM agreed well with those recorded in the experimental tests.



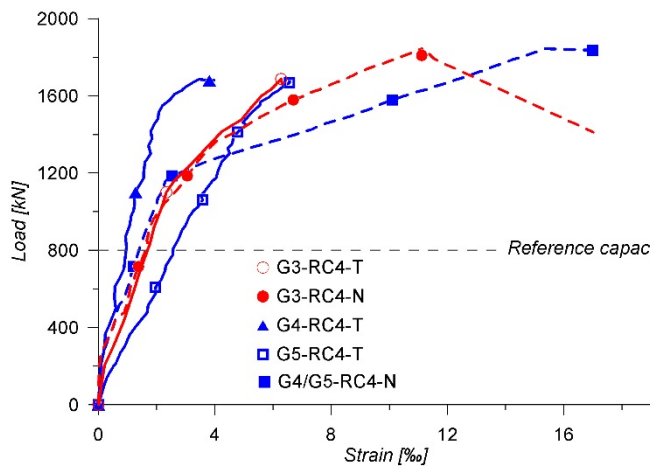
Figure 69. Vertical and horizontal CFRP plates peeling-off from the RC4 element

After yielding started and up to the failure load the strains in the steel determined by the FEM started diverging from (but remained similar to) those recorded in the tests, see Figure 70c.



(a) Load-displacement curves obtained experimentally (C1-T, C4-T, RC4-T) and numerically (RC4-N)

(b) load-strain relationships determined experimentally and numerically in C4 and RC4 specimens for rebars (S)



(c) load-strain relationships determined experimentally and numerically in C4 and RC4 specimens for FRPs (G)

Figure 70. Behavior of the C4 and RC4 elements.

Figure 71 shows the strain distribution along the FRPs obtained from the numerical analysis at failure load. At 1680 kN, just before the first peeling-off recorded in the test, a maximum strain of 2.01 ‰ was recorded at the ends of the horizontal strips, while the strains near the ends of the vertical strips were about 1 ‰.

Similarly to the findings for RC2, the FEM analysis also indicated that if the FRPs had been mechanically anchored (to prevent peeling-off failure), the capacity of the dapped-end could have been increased up to 1844 kN. The maximum strain in the horizontal FRP (17 ‰) was reached at 1830 kN, just before peak load. After the failure of the first strip, the other horizontal strips failed sequentially up to the attainment of the peak load. The vertical FRP developed a maximum strain of 11.12 ‰ at the peak load.

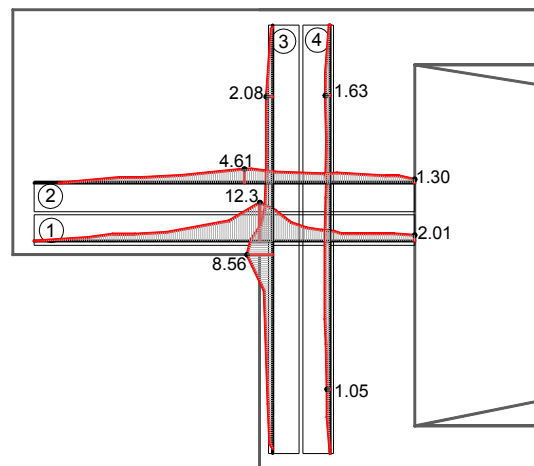


Figure 71. Strain distribution along the FRPs at failure load for RC4-N.

### 2.5.6 Numerical optimization of the strengthening using NSM and EBR CFRP

This study was motivated by the lack of experimental investigations into strengthening dapped-end beams using FRPs. The performed FEM improves understanding of how EBR CFRPs contribute to the capacity of dapped-ends, and highlights critical FRP design aspects such as the choice of FRP material and orientation of the fibers. The numerical modeling identifies the most effective CFRP-based strengthening system and layout for the above field application. Effectiveness is discussed in terms of the ultimate capacity of the dapped-end beam and the strain reduction in the steel reinforcement.

The design variables that were investigated using FEM were chosen based on observations during the experimental work and preliminary numerical computations. These variables are:

- (a) The inclinations of the CFRP with respect to the longitudinal axis of the beam. Alignments of  $0^\circ$  and  $45^\circ$  were selected, in accordance with both the field application and experimental program.
- (b) The mechanical properties of the CFRP materials. The experimentally tested beams were strengthened with high modulus (HM) and high strength (HS) FRPs. However, CFRP behavior with HS fabrics and HM plates was also included in the FEM study to obtain a more complete description of potential FRP strengthening.

(c) CFRP layout application. Owing to the considerable increase in the use of NSMR strengthening over the past decade the FEM investigation was extended to test the use of NSMR strengthening with both HS and HM fibers. Two types of NSMR cross-sections were selected, one rectangular and the other square, see Figure 72, based on the prescriptions given in ACI 440.2R-08 guidelines.

The fabrics, plates and NSM strengthening components are designated F, P and N, respectively. The mechanical properties of these components are named S for high strength and M for high modulus. The orientation of the applied CFRPs is denoted 00 for longitudinal and 45 for strengthening applied at 45° to the longitudinal direction. For example, FM45-N1M00 refers to a strengthening system composed of high modulus CFRP fabrics and type 1 high modulus NSMR bars applied at 45° and horizontally, respectively (see Table 9).

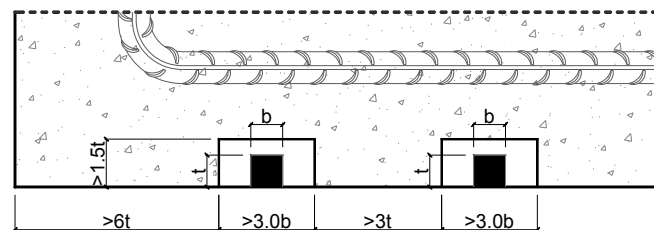


Figure 72. Minimum geometrical requirements for NSMR application

Table 9. Mechanical properties and quantities of CFRPs used in modeling.

Material	$PS^a$	$FM^b$	$FS$	$PM$	$N1S$	$N1M$	$N2S$	$N2M$
Width $b$ [mm]	100	340	340	100	10	10	2.5	2.5
Thickness $t^c$ [mm]	1.2	0.19	0.17	1.4	10	10	20	20
No. of FRPs	4	2	2	6	6	6	10	10
No. of FRP layers [-]	1	4	3	1	1	1	1	1
FRP area/system [mm <sup>2</sup> ] [ $n \cdot b \cdot t$ ]	480.0	516.8	346.8	840.0	600.0	600.0	500.0	500.0
Young modulus $E$ [N/mm <sup>2</sup> ]	165000	640000	231000	350000	165000	265000	165000	210000
Fracture strain $\varepsilon$ [-]	0.0170	0.0040	0.0170	0.0045	0.0135	0.0085	0.0165	0.0130
Variation vs. $PS^a$ [%]	0.00	-1.74	+1.15	-1.74	-0.74	+0.38	+1.10	+1.38
Strain at debonding $\varepsilon_d$ [-]	0.0037	0.0023	0.0048	0.0023	0.0075	0.0059	0.0116	0.0103
Anchorage length $l_a$ [mm]	238	373	183	374	173	220	130	146

<sup>a</sup> Strengthening system applied in the real field application and tested in laboratory

<sup>b</sup> Strengthening system tested in laboratory

<sup>c</sup> represents the depth embedded into the concrete cover

The CFRP fabrics and NSMR components used in the modeling were designed to have equivalent nominal strength along each direction to the CFRP strengthening systems used in the field application and laboratory tests. The number of CFRP layers (for fabrics), or elements (for plates and NSM), applied symmetrically to both faces of the element, designated  $n$ , and the required cross-section areas were obtained using. The Young-modulus ( $E$ ) and the ultimate strain ( $\varepsilon_u$ ) correspond to the mechanical properties of the CFRPs reported by their

manufacturers.  $E_{PS}$ ,  $A_{PS}$  and  $\varepsilon_{PS}$  are, respectively, the Young-modulus, cross-section area and ultimate strain of the CFRP strengthening system used in the field application and laboratory tests (PS in Table 9). Due to geometric limitations of the strengthened elements, the nominal strengths of CFRP sheets and NSM components are not identical to those of the CFRP plates, but the differences are minor (see Table 9).

$$n \cdot b \cdot t = \frac{A_{PS} \cdot E_{PS} \cdot \varepsilon_{PS}}{E \cdot \varepsilon}$$

A two-stage strategy was applied to identify the optimum strengthening configuration. In the first stage, models for specific components of the strengthening systems were constructed and combined in all permutations. The results obtained for these simple cases allowed the construction of models covering the full range of feasible strengthening configurations.

In the second stage, the individual CFRP components, applied at  $0^\circ$  and  $45^\circ$ , were combined (see Figure 73). Owing to technological limitations imposed by the thinness of the concrete cover, the NSM bars can only be used in combination with either plates or fabrics. Thus, some solutions comprise a mix of EBR and NSM components, but are identified with N1 or N2 to facilitate distinction from the EBR systems.

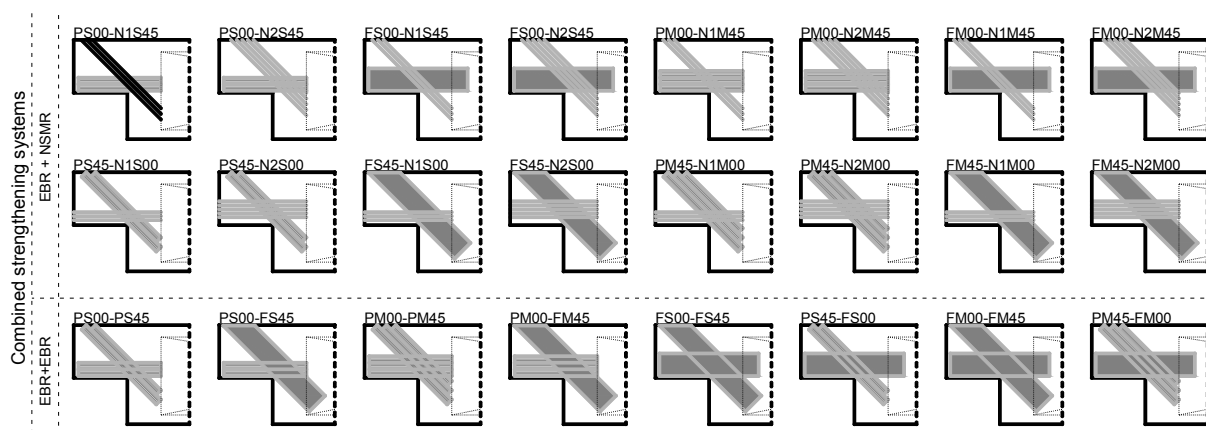


Figure 73. Schematic illustration of the combined strengthening solutions

### 2.5.7 Assessment of the strengthening systems based on the numerical modeling

The results of all analyzed models are presented in Figures 74 to 76, in form of load-displacement diagrams generated from the numerical analysis. For clarity the general characteristics of these diagrams are described below. They are grouped according to the material properties of the FRP (HS vs HM) and type of CFRP strengthening technique used (EBR vs NSM). In order to facilitate comparisons of general strengthening behavior between groups, the envelope corresponding to the region between the maximum and minimum load curves has been highlighted. The point at which debonding is predicted to occur is indicated in each diagram.

After this point the load increases to the maximum capacity of the CFRP strengthening system, and the corresponding part of the diagram simulates behavior in the region in which the CFRPs should be mechanically anchored. The debonding load represents the lowest bound capacity of the dapped-end beam, while the rupture load represents the highest bound capacity. When

ultimate strain in the CFRP was reached, distributed over its entire width, the CFRP was considered to have failed by rupture. The results of the numerical analysis for each strengthening system are compared to the results obtained from the numerical analysis of the reference specimen (C1-FEM).

#### *EBR: HM vs HS*

The behavior of the EBR HM and HS systems is presented in Figure 74 (a) and (b). As expected and confirmed through laboratory tests on specimen RC3, the HM fibers have limited capacity for deformation. Consequently, the elements strengthened using HM fiber systems, at ultimate strain, are able to provide modest gains in capacity compared to the reference specimen (C1-FEM, 1515 kN), about 13% in the best case scenario (specimen PM00-PM45), and no increase in debonding load. Note, for specimens FM00-FM45 and PM00-FM45 the load at debonding is smaller than the ultimate capacity of the reference specimen. This inaccuracy is attributed to the conservative nature of the EBR model of Sas et al.

The HS fiber systems were found to increase the capacity by up to 23%, with small variations in capacity, suggesting that the choice of fabrics and plates does not have a significant influence. However, there is a larger predicted variation in debonding load (14–28%). For systems composed solely of HS fibers no debonding occurs. For the other three systems, containing plates, debonding always starts in the horizontal components, as they have shorter anchorage lengths than the 45° components. In terms of service limit both EBR HM and HS systems delay the yielding of the internal reinforcement and can increase the yielding load by up to 45% compared to the reference specimen.

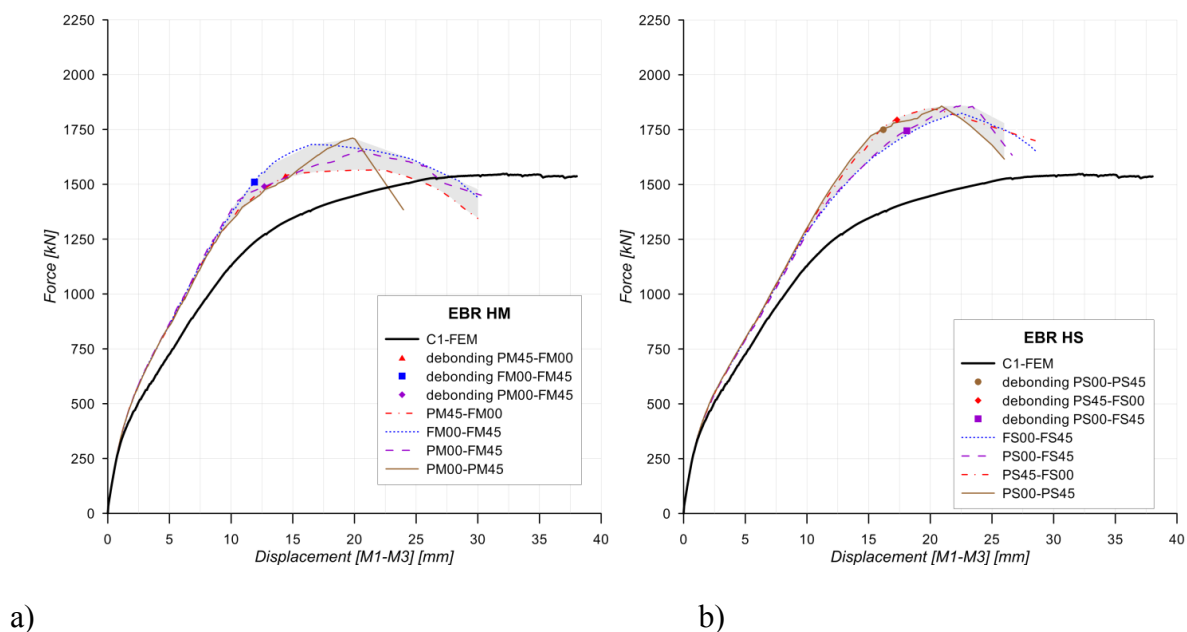


Figure 74. Load displacement diagrams for the group type: a) EBR HM and b) EBR-HS group.

*NSM: HM vs HS*

The behavior of the N1 HM, N1 HS, N2 HM and N2 HS systems are presented in Figures 75(a) and (b), 76(a) and (b), respectively. Generally, their behavior is similar to that of the EBR systems. In terms of ultimate failure load the HS NSM fibers outperform the HM fibers, for both types of cross-section investigated. Increases in debonding and rupture loads, relative to those of the reference specimen, of up to about 36% and 27% respectively, were recorded for element PS00-N2S45, while the reinforcement yields at loads up to about 50% higher.

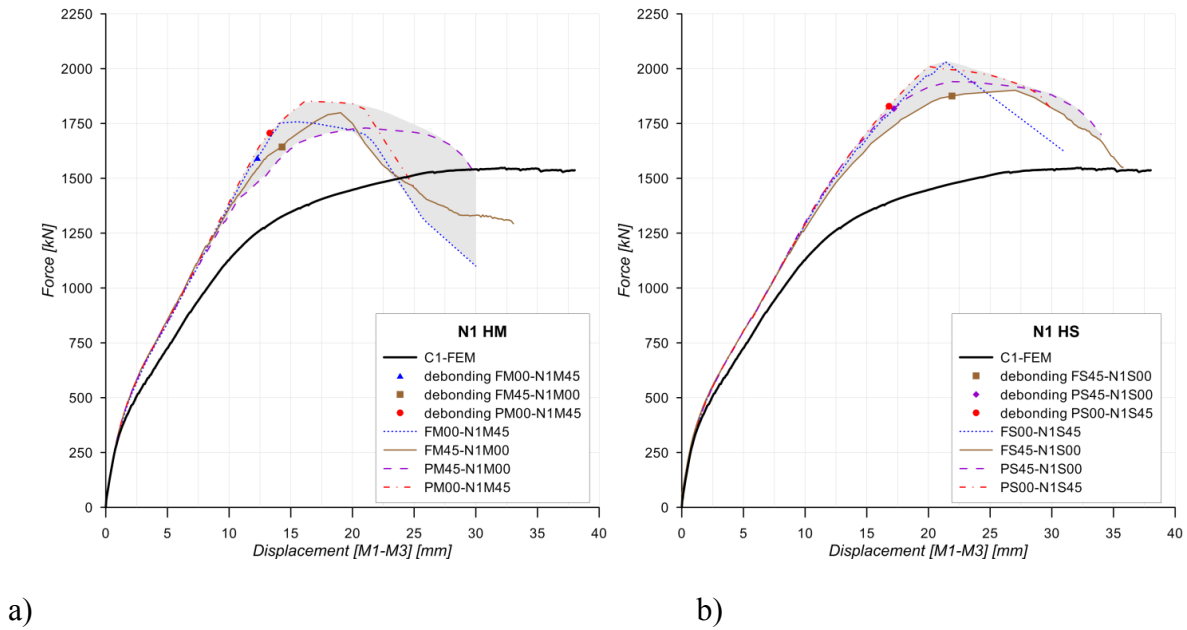


Figure 75. Load displacement diagrams for the group type: a) N1-HM b) N1-HS group.

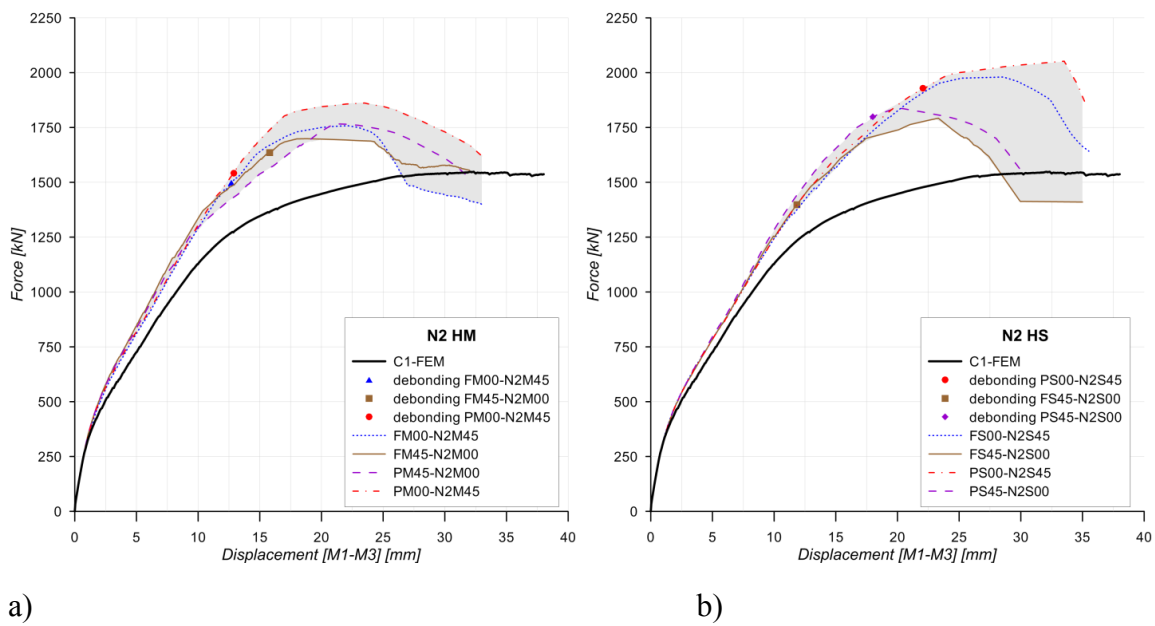


Figure 76. Load displacement diagrams for the group type: a) N2-HM b) N2-HS

### *EBR vs NSM*

The HM NSM systems (Figures 75a and 76a), can provide higher increases in capacity than the HM EBR systems (Figures 74a), but the HS EBR (Figure 74b) systems provide the highest increases in ultimate capacity. The trend is similar for debonding loads. The loading of the first yielding in the reinforcement does not seem to be influenced by the type of strengthening system. In terms of debonding loads, the HS EBR and HS NSM systems provide similar increases relative to the reference specimen (14–23% and 16–27%, respectively), while the HM EBR and HM NSM systems provide marginal increases (–3% to 2% and – to 13%, respectively). In terms of maximum force, the HS EBR and HS NSM systems provide significant increases (20–23% and 18–36%, respectively), the HM NSM systems provide a moderate increase (13–23%), and the HM EBR systems marginal increases (3–13%). In terms of delaying the first yield the increase was similar across the strengthening groups (except for PM45-FM00, PS00-N1S45 and PS00-N2S45), ranging from 12% to 45%. An early failure was recorded for the PM45-FM00 strengthening system (1711 kN), but the PS00-N1S45 and PS00-N2S45 systems provided the highest capacity gains (+33% and +36%, respectively) due to the yielding of the steel reinforcement (vertically aligned), which allowed advantageous stress redistribution.

### *N1. vs N2*

The type of NSM cross-section used, governs the positioning of the CFRP with respect to the most heavily loaded section of the dapped-end and the number of bars used. The results show that differences in ultimate capacity loads between systems with the two types of cross-section are marginal. Element PS00-N2S45, with the rectangular cross-section N2S (2.5 x 20 mm<sup>2</sup>), provided the largest gain (36%), while the best performing element with a square cross-section (N1S, 10 x 10 mm<sup>2</sup>) provided a 33% gain. Nevertheless, all of the HS NSM systems provide both greater capacity gains than the HM NSM counterparts (18–36% and 12–23%, respectively) and debonding load gains (16–27% and –1% to 13%, respectively). However, in terms of delaying the first yield, the HM NSM systems (except PM45-N1M00, as discussed above) can provide a more consistent increase than the HS NSM systems (except PS00-N1S45 and PS00-N2S45, 19–49 and 16–33% gains, as also previously described).

## **2.5.8 Discussion and conclusions**

This part of the study describes experimental and nonlinear numerical analyses of dapped-end beams strengthened with different FRP configurations. This research program was designed to identify the most suitable FRP strengthening configuration among those used in a real field application. The beams to be strengthened on-site were designed to resist a load of 800 kN. Due to an error during the building phase, the lever arm of the support system increased, and diagonal cracking appeared, starting from the re-entrant corner of the dapped-ends of these beams. Using the design methods for dapped-ends described in the PCI handbook, in the Romanian and European standards resulted in conservative values for the capacity of these elements. The cited methods predicted a load of about 600 kN for the yielding initiation of the steel reinforcement, considering the prescribed safety factors for both the materials and the loads. However, the test with the C1 dapped-end reference specimen indicated a yielding load of 865 kN, and in tests with the other (C2-C4) dapped-end specimens yielding did not occur up to 800 kN. There were two reasons for these differences between the design and empirically determined values. The first was the presence of real material in the tests, with significantly higher strength than the design values, especially for the reinforcement. The second was the influence of the shear span and the element cross-section dimensions. The procedure applied

to generate the abovementioned standards does not seem to have been optimized for the design of large dapped-end beams, such as those investigated in this work, hence the conservative nature of the predictions. Therefore, further research is needed to improve the existing design methods for large dapped-end beams.

After subjection to the target load (800 kN), three specimens were retrofitted with different CFRP strengthening configurations, and then retested. The strengthening configurations applied in the RC2 and RC4 specimens were those applied to real beams on-site. Compared to the control element C1, the strengthened dapped-ends exhibited a slight increase in ultimate load capacity. For elements RC2 and RC4 the capacity increases (4 % and 10%, respectively) were limited by the failure mode, i.e. debonding of the FRP. The numerical analysis showed that if mechanical anchorages had been used to avoid this premature failure the capacity could have been increased by up to 20%.

However, at a loading of 800 kN the strengthening configurations applied to the RC2 and RC4 specimens reduced the stress in the reinforcement by 31% and 16 %, respectively, and increased their stiffness, resulting in capacity gains of approximately 18% at the first yielding in the reinforcement, with respect to the reference specimen C1.

The strengthening system applied in the RC3 specimen was ineffective in terms of increasing the capacity and stiffness due to the relatively small ultimate strain of the CFRP composites used in this configuration. The gradient of strains in the CFRP section crossed by the main cracks caused local failure of fibers in early stages of loading during the crack opening process. It is believed that higher capacity could be obtained if larger content of FRPs were applied. However, above a certain content of FRP, the failure mode might change from tensile rupture of the fibers to debonding; if so the capacity could only be increased if anchorage devices were used to avoid premature debonding.

As only two strengthening systems were experimentally tested in the field application an important question remained, namely whether an alternative arrangement could further improve the ultimate capacity of the beams. Thus, in the study presented here all strengthening configurations that could have been applied in practice were investigated in numerical simulations. The modelling approach was to combine CFRPs with different mechanical properties and shapes but similar alignments to tested specimens (0° and 45°). The results indicate that mechanically anchoring the CFRP (as in the PS00-N2S45 arrangement) could have increased the beams' capacity, relative to that of the reference specimen, by up to 36%. The PS00-N2S45 configuration outperforms the two systems used in the field application, RC2 and RC4, with increases in capacity of 20.7% and 16.1% respectively. The debonding process was not modeled, because the modelling was carried out in 2D. In a 3D analysis debonding could be modeled, using a bond slip law or a cohesion–friction model. This was not done due to a lack of the empirical information required to calibrate the constitutive model.

All the results presented above are based on perfect connections and anchorages between the strengthening systems and the concrete element. The occurrence of debonding was simulated by monitoring the strains and the characteristic bond length in the FRP. These parameters were evaluated using existing models available in the literature. Estimating the debonding process in such manner is model-dependent due to the details of the theoretical models used, not because of the numerical modeling. If debonding does occur the maximum load, relative to that of the reference specimen, could be increased by up to about 26% using the PS00-N2S45 system, which outperforms the strengthening configurations used in the case study. Element RC2 failed by debonding at 1760 kN, whereas the PS00-NS245 element could resist a load of

about 1930 kN before debonding. In some cases the debonding load was close to the rupture load of the FRP. This indicates that for these strengthening systems the anchorage length was nearly sufficient to avoid debonding. One objective of the field work was to delay yielding initiation into the steel reinforcement. The numerical analysis has shown that this can be achieved to a certain degree with any of the strengthening configurations investigated. The force at which yielding first occurs can be increased by up to almost 50%, depending mainly on the type of fibers used and their position with respect to the reentrant corner. In this respect high modulus fibers are better than high strength fibers, because of their greater stiffness. In addition, the closer to the edge the FRP is applied the sooner it starts to be loaded.

The results presented here show that the applied strengthening systems, based on CFRP, are viable solutions for improving the capacity of dapped-end beams, especially when, as in the case of NSM, a large part of the strengthening system is applied as close to the beams' reentrant corners as possible. These study helped elucidation of the behavior of the tested specimens and assessment of the strain distribution in the reinforcements. During the tests, it was difficult to see with the naked eye when and where the debonding of the FRP plates started. The numerical analyses also showed that the vertical plates had adequate anchorage length, and that the debonding of the inclined/horizontal plates triggered the debonding of the vertical plates, in accordance with the test observations.

### **Acknowledgement**

The research work was partially supported by research grant type A no. 27688/2005, awarded by the National University Research Council, Romania, as well as by SIKA Romania Corporation, through offering the composite systems used in the experimental tests. Coordinator of the grant was Prof. Stoian Valeriu, Politehnica University of Timisoara.

My special appreciation and thanks to Dr. Dăescu Alexandru Cosmin, Dr. Sas Gabriel and Popescu Cosmin.

### 3. STRUCTURAL HEALTH MONITORING OF ENERGY EFFICIENT STRUCTURES

#### 3.1 Introduction

Energy efficiency as a solution for climate change and climate change generated phenomena represents one of the most important concerns and pursuits of humanity, especially in the economically developed areas of the world, such as European Union. Actually, the EU is aiming for a 20% cut in Europe's annual primary energy consumption by 2020. Thus, The European Commission has proposed several measures to increase efficiency at all stages of the energy chain: generation, transformation, distribution and final consumption. In the same time, based on the Kyoto Protocol to the United Nations Framework Convention on Climate Change (UNFCCC) binding international obligations to reduce emissions of greenhouse gases were set. The European Energy Security Strategy addresses medium and long-term security of supply challenges. It proposes actions in five key areas, one of those being “Increasing energy efficiency and reaching the proposed 2030 energy and climate goals”. Priorities in this area should focus on buildings which use 40 % of total EU energy. At the level of the EU, the residential sector accounts for about a quarter of the final energy consumption according to another important document issued by European Commission. Moreover, in Romania the share of the residential sector represents 36% of final energy consumption, being the largest within the member states, as the smallest is 17% of total final energy consumption in Portugal and Malta. Specialized international bodies also present detailed scenarios on energy demands and climate control which emphasize the need for adopting specific energy efficiency measures, as around 60% of the global savings in emissions are from the buildings sector. Moreover, throughout the entire life-cycle of a building, nearly 80% of the total energy consumption occurs in the usage phase of the building. Therefore, a way of reduce the environmental impacts of a construction is to improve the energy performance of the building (Kashreen et al, 2009). The European Union published the Energy Performance of Buildings Directive EPBD as a legislation regarding the energy performance of the buildings for the European member states and aims to promote improvements in the energy efficiency of a building. There are many different concepts of energy efficient buildings that are generally known as buildings with a lower energy demand than common buildings, such as passive houses, nearly zero energy buildings or, why not, active houses.

In order to achieve the passive house standard, a building must have an annual heating/cooling requirement for at most 15kWh/m<sup>2</sup>/year and a total energy footprint of less than 120kWh/m<sup>2</sup>/year (Feist et al., 2007). A passive house combines high-level comfort with low energy consumption. Passive components like insulation, advantageous orientation, heat recovery, air tight envelope are the key elements. Thanks to the high level of thermal insulation, heat recovery system and solar gains, a passive house doesn't need to be heated actively to a large extent. The low amount of additional heat which needs to be supplied is frequently realized with heat pumps (Ochs et al, 2011). Careful implementation of details and good planning are crucial in obtaining a building with very low energy for heating. A proper design and execution can lead to a high energy efficient building which consistently provides pleasant indoor and surface temperatures. The passive house concept can be adapted to any climate zone; the general approach is the same. Depending on the climatic conditions, the quality and type of components, materials and equipment may vary.

In Romania, passive house concept is a relatively new one and most people are sceptical in approaching it because of the higher initial investment. Currently there are five passive houses built in the whole country (data from 2013). To cover the gap in low-energy residential

buildings, in 2011, a passive house complying with the European passive house standard was designed and built in Timisoara. Located in the west side of Romania, Timisoara is the third largest and economically one of the most important city of the country. Unlike other European countries such Mediterranean and Scandinavian ones that have to deal mainly with one side of the issue (predominant cooling or heating respectively), Romania is situated in an area with a temperate climate with four seasons. The differences between the temperatures in the hot season and the temperatures in the cold season are very high. Therefore, particular attention should be paid to both heating during winter and cooling in summer time, avoiding temperature drop in the elements of the envelope during cold season and also to prevent overheating in the hot season. Moreover, as Romania is a highly active seismic country and since Timisoara is in a zone with peak ground acceleration of  $a_g=0.16g$ , at the concept and design of a building, special structural requirements and detailing are imposed by codes.

In the attempt to push forward energy efficiency of households sector, the European and Romanian legislation require energy certification of buildings. This directive states that the energy performance of a building should consider the amount of energy actually consumed or estimated to meet the different needs associated with a standardized use of the building, which may include, in addition to the heating, hot water heating, lighting (only for non-residential buildings) and cooling. For the evaluation of the standard energy performance of the buildings, the PHPP procedure and the national regulation were adopted. In order to prove the achievement of passive house standard and to assess the deviations in the energy performance evaluation procedures, the house was equipped with extensive monitoring instrumentation, thus the evaluation of the actual performance of the building was made by analyzing the data of energy consumption during an entire year of occupancy.

### **3.2 Performance assessment of energy efficient houses through monitoring**

Energy is the life blood of our society; the well-being of people, industry and economy depends on safe, secure, sustainable and affordable energy. The concept of the project entitled “Performance Assesment of Energy Efficient Houses through Monitoring” - acronym “PASSHOUSE” revolves around two crucial issues for the entire society, both for present and future generations: environment and resources. Subsequently, energy consumption and energy saving are of vital importance in terms of conservation of available resources and enhancement of environmental conditions.

The aim of the project is to conceive and setup a monitoring system through which all the hygrothermal parameters are to be registered. All these parameters can be than after analyzed in order to conclude the efficiency of the system. The target groups of the project are stakeholders who can do something for sustainable energy consumption. Through measuring the energy consumption of a pilot passive house we will have exact data for the controlling the validity of energy consumption calculation methods in this region. With concrete data we can provide cost-benefit calculations for investors, architects, constructors and naturally for private people. Knowledge transfer to people about energy-efficient solutions are crucial.

#### **3.2.1 Background and description of the research program**

In November 2008, the European Commission put forward a comprehensive European Economic Recovery Programme (EERP) to exit from the crisis and coordinate recovery in Europe. Part of the EERP was to mobilise EU sources of funding to accelerate the implementation of major investment projects, notably in the energy sector. Although these

projects are large-scale infrastructural projects the main purpose is the same: provide safe, secure, sustainable and affordable energy and contribute to a sustainable future.

Intelligent Energy Europe Programme partially supported a project titled Passive House Solutions - Promotion of European Passive Houses (EIE/04/030/S07.39990). The project arrives to the conclusion that most frequently encountered barriers in partner countries are: limited know-how; limited contractor skills; and acceptance of Passive Houses in the market. This means that a great deal of attention must be paid to providing practical information and solutions to building professionals, providing practical information and training to installers and contractors and communication about the Passive House concept to the market. PASSHOUSE project tries to link to this concept in the Hungarian-Romanian cross-border area. Energy is also a key priority in Seventh Framework Programme (FP7) research programme, as 137.000.000 Euros was available for FP7-ENERGY-2011-2 call.

The project is developed under aegis of “European Regional Development Fund” within the framework of “Hungary-Romania Cross-Border Co-operation Programme 2007-2013” which aims at enhancing the joint social and economic development of the Hungarian-Romanian border area.

A model passive house was built in Romania in the cross-border region. By conducting the project research (mainly the monitoring of hygro-thermal parameters), answers on the efficiency of the German model in local cross-border Romanian-Hungary climatic conditions will be provided. Furthermore a comparison with data measured in a semi-passive house and traditional house circumstances. By evaluation of measured data the system may be easily understood, and a cost-benefit analysis of passive house solutions may be compiled. This can encourage further investment in passive house building in the region, and that will contribute to the energy consumption efficiency of both countries. Furthermore if the passive system will prove its efficiency, the monitoring system setup proposed within by the present HU-RO project, can be used elsewhere. The project is justified by the similar solutions of building construction which can be applied within the area designated into the HU-RO cooperation. The monitored Passive House is presented in Figure 77 alongside a photograph taken during the site visit in the 3rd Workshop.

### **3.2.2 Impact of the program**

Two partners were involved in the project implementation: “Politehnica” University of Timisoara as Lead Partner and Solartech South Plain Nonprofit Company for Development and Production as Project Partner.

Politehnica University of Timisoara is one of the biggest and most well-known technical universities from Central and Eastern Europe, having the recognition of a first class actor on Romanian scientific research scene, with remarkable results both on the national and international level. In the PASSHOUSE project, “Politehnica” University of Timisoara had conducted research and monitoring of energy consumption and disseminated results.

Solartech South Plain Nonprofit Company for Development and Production is the background organization of a cluster network called Archenerg Regional Renewable energy and Construction Industry Cluster. Solartech were responsible for workshops and conferences organization and for disseminating results for the public.

The project's impact on mid and long-term refers to a series of crucial sectors and issues as: the control of global warming by reducing of CO<sub>2</sub> emissions; channelling research into knowledge and solutions for sustainable development, influencing consumption decision, improve the quality of life, increase investments in human capital through better education and training; improvement of the life quality by sustainable development of regenerating resources and diminishing the climate changes effects, improving knowledge and innovation for economic growth, reduction of pollution, improvement of efficiency in the use of energy , cooperation in research and technology development and human resources development.



Figure 77. *Pilot Passive House - Dumbrăvița, Timișoara, Timiș (pictures taken during the 3<sup>rd</sup> Workshop organized in the PASSHOUSE project)*

### 3.2.3 Materials and methods

The Passive House built in Romania, near the city of Timisoara has approximately 144 m<sup>2</sup> living space and fulfils the space need of an average family. From architectural perspective, the passive house has an advantageous south orientation of the facades with large windows and presents a very compact form (Figure 78). These features help reducing heat losses. The south orientation of the windowed facades avoids overheating during summer times and ensures sunshine penetration during winter times.

The infrastructure system of the house consists in isolated concrete blocks connected with foundation beams in order to ensure sufficient stiffness. The foundation system reduces the amount of used concrete and facilitates the thermal insulation of the entire ground floor, the polystyrene plates being applied from the foundation beams upwards (Figure 79).

The house is built on masonry system of vertical hollow ceramic blocks of 25 cm thickness, confined by RC columns and belts (Figure 80). The traditional house has a continuous foundation system under the resistance walls but the structural skeleton is identical with the one that the passive house was built.

A significant difference between the two houses is the level of thermal insulation. The exterior envelope of the passive house has a thermal insulation of 300 mm thickness for the vertical areas (Figure 81) and 150 mm for the upper part of the parapet. In return, for the traditional house was considered a layer of thermal insulation of 80 mm thickness.



Figure 78. The studied passive house



Figure 79. Thermal insulation of the foundations



Figure 80. The structural system



Figure 81. Thermal insulation of the facade

The high level of thermal insulation is a key point when considering building a passive house and one of the reasons of the higher prices. The roof of the passive house is a non-traffic terrace that has a 425 mm thickness of thermal insulation. The layers of the roof are the same for both buildings, passive and traditional, the only difference consists in the thermal insulation thickness which is 100 mm for the traditional house.

All the elements of the envelope of the passive house must have a heat transmission coefficient  $U$  of maximum  $0.15 \text{ W/m}^2\text{K}$ . Besides the good thermal insulation, windows used in the passive house should have  $U$ -values for around  $0.70 - 0.90 \text{ W/m}^2\text{K}$ . For the discussed passive house, the used windows are not quite at passive house level but they have an appropriate heat transmission coefficient at on much lower cost. The limit value for the air leakage rate of a passive house must not exceed 0.6 volumes per hour and it must be verified through measurements.

With the high thermal insulation level and very efficient  $U$ -values for the other envelope element, the built passive house is air tighten. Therefore, a ventilation system is required. The passive house does not dispose of traditional heat generation such as radiators. In order to solve heating and cooling, the studied passive house uses a mechanical ventilation system with heat recovery. The house is equipped with an air-soil heat pump. The heat pump assures the heating of the house. The process consists in preheating the intake air for the ventilation system through

underground heat exchangers. The necessary equipment (with heat pump, heat recovery ventilation unit, air heating unit, 3-way valves, heat buffer tank, solar pump and domestic hot water tank) of the passive house are functioning in a mechanical room. The passive house also disposes of a solar panel used for heating.

The interior finishing of the passive house is quite simpler, with nothing in particular: laminated parquet in rooms, ceramic tiles and faience in bathrooms, kitchen and access hole, water solvent wall-plaster-paint and interior doors of wood panel. For the traditional house the same interiors were considered. The interior compartment walls are in both cases gypsum plaster boards of 150 mm thickness on metal structure. As it is presented, the two studied house are not different from structural and architectural point of view. The differences appear when it comes about airtightness, heat transmission coefficient of the envelope elements, heating and cooling methods. The passive house uses high quality materials for the envelope, in order to ensure airtightness and eliminate heat losses. Another extra cost that a passive house implies compared with the traditional house is the heat pump, the ventilation system with heat recovery, the solar panel. The evaluation of construction costs for the two buildings is made considering that the traditional house uses the same technologies and materials when possible. It is proved that standard materials and techniques can turn a traditional house into an energy efficient house if they are used properly.

The initial investment for the studied houses represents the cost for the field, project, field studies, technical assistance, execution of building with all the materials and equipment. After the evaluation and comparison of the initial investments, it is relevant that a future costs with the energy consumption evaluation to be made.

The passive house from Timisoara is under monitoring over a year ago. The purpose is to determine the building's energy consumption and control comfort parameters.

### **3.2.4 Monitoring activities**

The building that was monitored within the PASSHOUSE project, and which was designed and built according to "Passive House" standard, was erected near Timisoara (Dumbravita) Timis County. During the design stage of the building (stage that lies outside the purpose of the present project, being completed when the project had commenced) a series of theoretical calculations were performed in order to evaluate the energy consumption of the building. All evaluations were based on Romanian methodology and also on the procedures specified by the Passive House Institute in Darmstadt, a world distinguished entity for outstanding energy efficiency in buildings.

The monitoring system was conceived in such a way that it would measure 6 hygro-thermal parameters, but finally four other types of sensors were installed, reaching a value of 10 monitored parameters: 1 - Sensors for measuring exterior temperature (30 pcs); 2 - Sensors for measuring flow of heating fluid (2 pcs); 3 - Sensors for measuring airflow (2 pcs); 4 - Sensors for measuring interior temperature (135 pcs); 5 - Sensors for measuring barometric pressure (2 pcs); 6 - Sensors for measuring wind speed (3 pcs); 7 - Sensors for measuring humidity (10 pcs); 8 - Sensors for on/off power state (10 pcs); 9 - Sensors for measuring wind direction (3 pcs); 10 - Sensors for measuring insolation (3 pcs).

Constant monitored data was (and continues to be) uploaded on the website of the program (<http://www.passhouse.archenerg.eu>). Examples of the monitored and recorded data are provided inside Figure 82 and Figure 83.

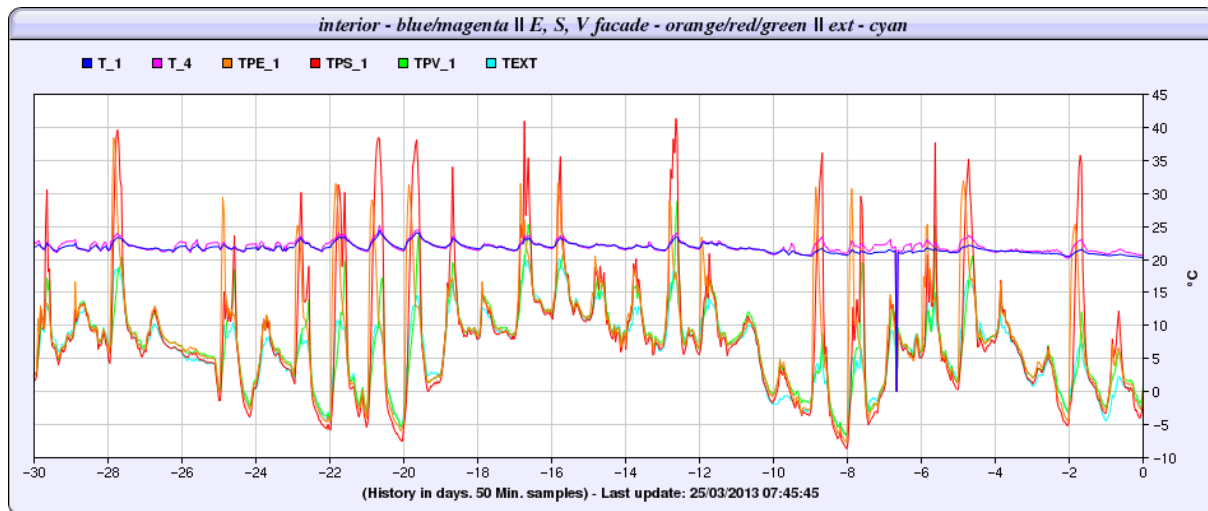


Figure 82. Air temperature inside the building, facade outer surface temperatures - 30 day history

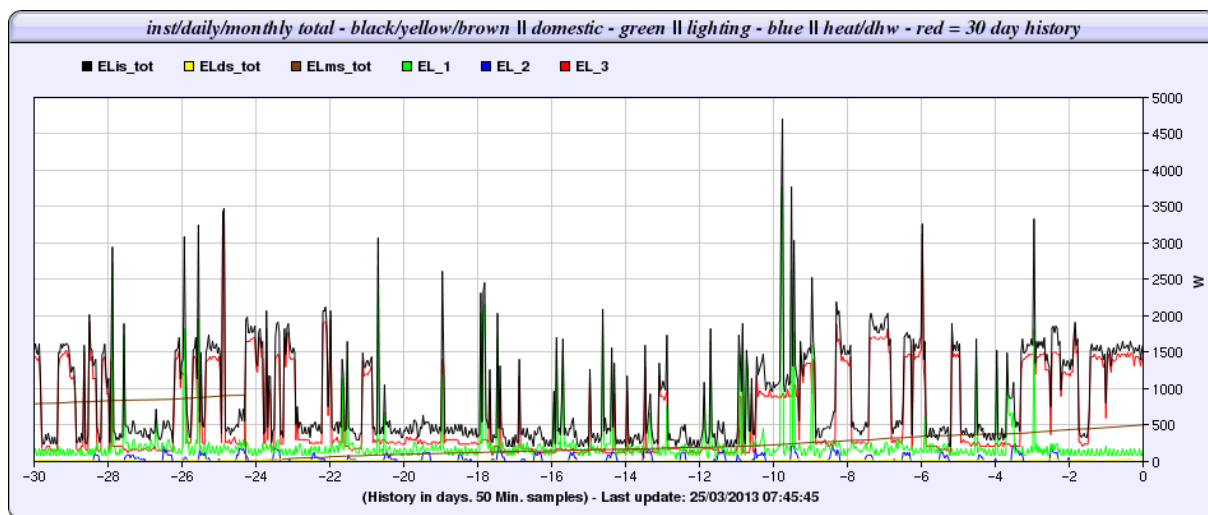


Figure 83. Electrical energy consumption - 30 day history

During the design and use of an energy efficient building the need arose to implement a monitoring system with a good quality/price balance, necessary in order to validate the theoretical design. After evaluating several turn-key solutions the decision was taken to build a system based on units that were separately available, as well as units that had to be assembled from scratch with the plan of attaining lower cost in comparison to a commercially available ready-made system and the downside of higher labour input and a longer implementation period.

The monitoring system was designed based on the above mentioned requirements, by considering also the need to make data available online and the physical measurements that had to be taken. The resulted composition of the system is presented in the following.

The central unit is commercially available under the Web Energy Logger (WEL) name the data collection unit consists of a low power embedded computer featuring a TCP/IP stack and an interface board that manages actual data collection via following channels: a 1WIRE bus (provides low-speed data, signaling, and power over a single signal), 6 counter inputs, 8 state

inputs, 2 analog inputs and the possibility to interface with IP power meters. The WEL collects the measurements from the sensors every minute and posts the data to a webserver provided by the manufacturer of the unit. The service offers the possibility to display trend graphs for collected data and to download all data in spreadsheet software friendly form.

The need to provide a low cost option for an internet connection lead to the use of a commercially available router featuring a USB port that was in turn connected to a 3G WWAN (Wireless Wide Area Network) access modem offering a flat rate internet access. The router in turn provides an ethernet connection to the WEL. Because of the unreliability of the low cost 3G WWAN access an internet connection monitoring module was set-up as the WEL has several status outputs providing information regarding the connection to the data upload server. The module is configured to reset the power to the router anytime a connection time-out is detected and also provides local data display, very useful during the setup of the system.

To monitor the temperature, low cost sensors were used, readily available at electronic component suppliers, providing a digital serial bus compatible signal.

The humidity sensors that were chosen provide a DC linear voltage output. Thus an interface circuit had to be used in order to provide the digital data necessary on the serial bus. The circuit consists of an A/D converter that is compatible with the digital serial bus and respective support circuitry.

Atmospheric pressure sensors used provided an output signal similar to the humidity sensors and a similar signal converting device was used.

The airflow sensors are actually differential pressure sensors that feature a DC square root extracted voltage output characteristic. They are connected to pitot-static tubes in the ventilation ducts. The square root characteristic is useful as it enables less processing of the data in order to derive the airflow rate. Further on an A/D converter that is compatible with the digital serial bus and respective support circuitry was used to connect the sensor.

Solar radiation was measured using silicon pyranometers with amplified output are used to collect solar radiation data. The output provided is a DC linear voltage that had to be interfaced with the serial bus in a similar manner.

For heating agent flow volume meters were used and interfaced directly with the impulse counting inputs of the WEL.

For wind speed and direction an anemometer was used, which provides an impulse output that can easily be directly connected to the WEL. The wind direction vane has DC linear output that was interfaced with the serial bus through an A/D converter.

Electricity energy meters with impulse output were directly interfaced to the impulse counting inputs of the WEL.

The state sensors consist of an optocoupler input connected in parallel with the device to be monitored for function, through a rectifier/current limiting circuit. The optocoupler output is connected to the state inputs on the WEL. A galvanic separated solution was chosen in order to avoid problems that could stem from different circuits connected to a common ground.

As availability of MEMS (Micro-Electro-Mechanical Systems) accelerometers is becoming better and their cost decreasing due to rising use of such devices in hand-held equipment the

option of including them in the monitoring system arose. The problem lay in the different use of the information they offer. As such an intelligent type of interface module was built in order to gather data via the accelerometers and make it available on the 1WIRE bus. The module continuously takes acceleration measurements, stores minimum/maximum values and calculates an average of the values. Every minute as the bus is polled data is read anew and new values are stored and calculated. The MEMS device selected is a LIS302DLH accelerometer commonly used in mobile phones and computers in order to detect movement or free fall of the device. The datasheet states a typical sensitivity selectable between 1, 2 and 3.9 mg/digit, values usually well below the noise and an output data rate selectable between 50, 100, 400 and 1000 Hz. For our application a working mode with a sensitivity of 1mg/digit and an output data rate of 50 Hz were selected as offering best resolution and sufficient sample density in order to explore even higher frequencies of oscillation.

As the accelerometers provide an I2C or SPI compatible output, it was necessary to convert the signal to make it compatible with the serial bus. Also as the bus is polled once per minute in the case of significant events the information density reported would be rather lacking for a further analysis to be pursued. As such a type of intelligent interface was designed. Comprised of a low power RISC microcontroller it reads data at a rate of 50 Hz from the accelerometer and stores the information in a ferromagnetic RAM (FRAM) for later retrieval. At 50 Hz storage rate 1Mbit of memory offers ca. 1 hour of data storage. Combined with a  $10^{14}$  read/write life cycle the arrangement offers many years of continuous operation before failure could occur.

In addition to storing the information the interface unit stores minimum, maximum and average values that are reported every minute as the bus is polled. The unit is also programmed with a threshold value that enables certain ranges of data to be protected from being overwritten until access to the unit is possible and the locally stored data can be downloaded and further analyzed.

### **3.2.5 Objective and output indicators**

The specific objectives of the project were: to bring closer the possibilities of sustainable and affordable energy to people of the cross border region; examination of Hungarian and Romanian possibilities for energy saving and contribution to sustainable development in a lower level of society; dissemination of project results. The work was divided into four project activities: Preparation activities, Project management, Communication activities, Monitoring of energy efficient houses.

Monitoring is essential for validating the energy performance of low-energy buildings; especially in countries where national codes don't have special recommendation for such type of buildings. Low-energy buildings are more and more used; monitoring these buildings can lead to further improvement in energy efficiency. One of the most important characteristic that needs to be measured is the energy consumption. It is fundamental to monitor each main consumer/equipment individually, or if not possible, the total energy consumption must be divided into at least 4 relevant categories.

### **Acknowledgement**

This research has been granted to some extent by the Hungary-Romania Cross-Border Cooperation Programme 2007-2013, through the project PASSHOUSE (HURO 1001/221/2.2.3).

### 3.3 Concept, specific details and monitoring strategy for energy efficient building

#### 3.3.1 Introduction

In Romania there are just a few energy efficient buildings, the number of such constructions that are being designed currently is much lower than is the Western European average. Moreover, even less constructions exist in which the comfort and the energy consumption are both measured. Obviously, such types of residential houses and low-energy buildings exist in Romania, but they are not documented or certified and their parameters cannot be followed.

Energy efficient school buildings, according to the authors best knowledge, have been built only in developed countries, like Germany, Austria, Great Britain, France and the USA, and their number is about 80. In 2014, the possibility to build a school in Romania using the energy efficient concept arose. From the eight-person design team, four have had experience in the design of passive houses. In the first step of the analysis, the construction and maintenance costs of the proposed building was considered, comparing a conventional and an energy efficient built version. As expected, the preliminary results showed that, with higher initial investment, the maintenance costs can be reduced significantly (Figure 84), which for the case of a long-term investment, such as a school, represents a very important issue. The payback period is roughly equal to the expected value of energy rehabilitation in Romania (INSPIRE). The initial investment of the school built in traditional solution is approximately 511 EUR + VAT/m<sup>2</sup>, while the energy-efficient version is about 565 EUR + VAT/m<sup>2</sup>. This 10% difference, based on the calculus, could be recovered in 6 years by the reduction of the maintenance costs. This was the deciding factor that convinced the investor to choose an energy-efficient solution. The school is currently under construction. Hopefully, in the spring of 2016 the entire building will be completed, regularly and rigorously supervised by the design team.

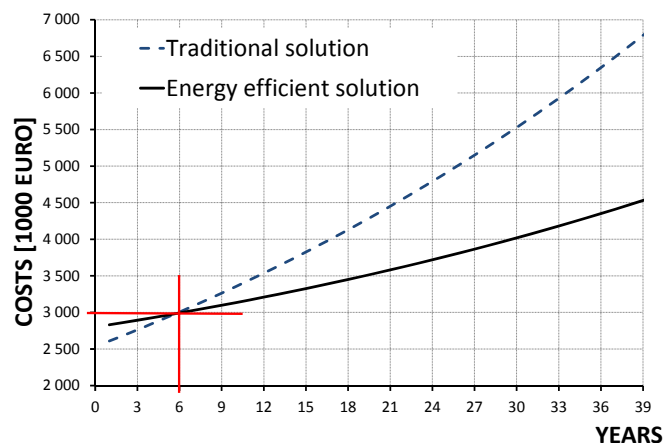


Figure 84. Lifespan - global cost comparison of the project for the two solutions

#### 3.3.2 Functionalities and the adopted solutions

The facility was very limited from architectural point of view (Figure 85), as it had to adapt to local site conditions. This multi-purpose building has a simple and compact architecture, with a total area of 4000 m<sup>2</sup> (four 1000 m<sup>2</sup> storey). On the ground floor is the main entrance, a library, storage rooms, a dining hall for 200 students and a kitchen with a capacity of 500 meals/day. The first and second floors will have classrooms, laboratories and administration

offices. The third floor has a hostel for 60 students, a recreation place and a room for the medical staff. Thus, the capacity of the school will be of 450 students, 65 teachers and auxiliary staff (Figure 86).



Figure 85. The facades of the school and a cross section

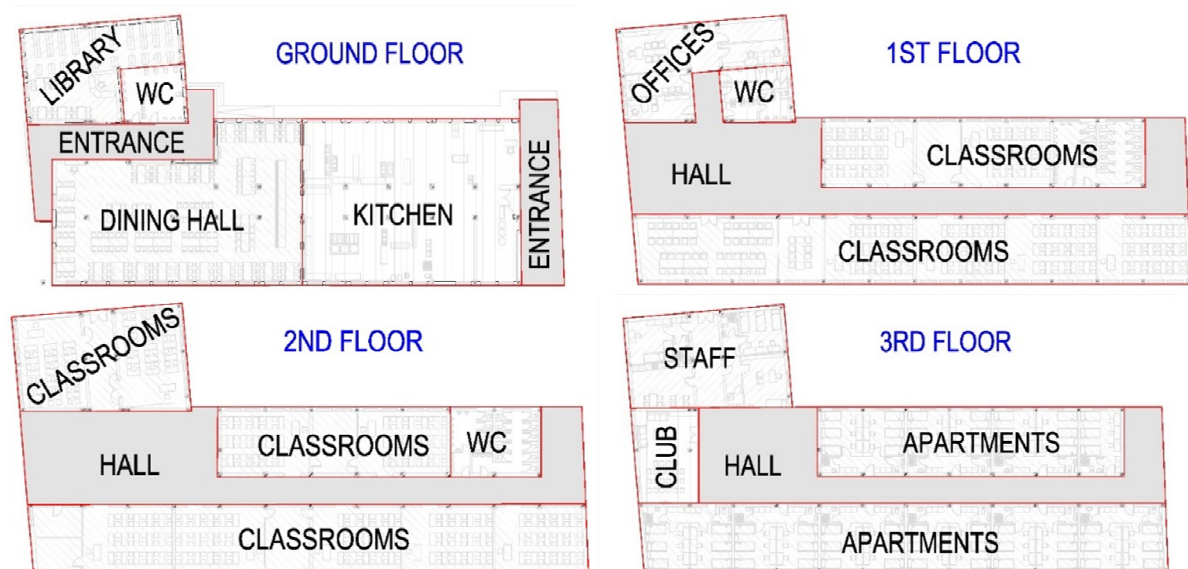


Figure 86. Floor plans and functionalities

In the structural design phase, in addition to energy efficiency requirements, the Romanian earthquake resistance requirements have also been taken into account. Since the building has 4 storeys, reinforced concrete frame structure was prescribed.

Regarding the calculation of the foundations, in addition to the economy and the construction period, the thermal insulating possibilities were also considered. Thus, reinforced concrete shallow foundation, beam-grid base foundation and base plate type foundation were analysed, the second of which proved to be the most appropriate.

The structure is covered by a pitched roof, with two firewalls. External masonry walls of 25 cm thickness are constructed of autoclaved concrete blocks, covered with 15 cm mineral wool insulation. The concrete slab of the ground floor has been insulated with 23 cm of extruded polystyrene (Figure 87), while the attic slab with 20 cm thick mineral wool (Figure 88).

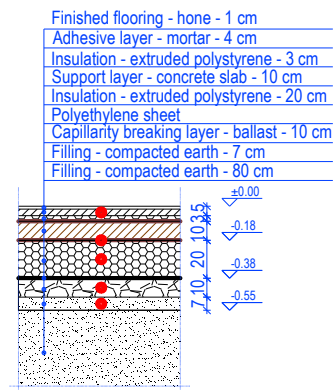


Figure 87. Specific detail for the ground floor slab and the provided thermal insulation

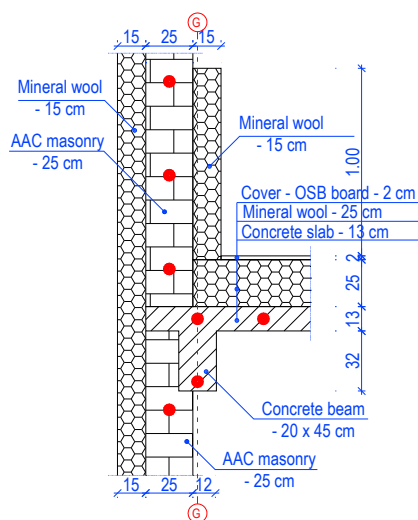


Figure 88. Detail for attic slab blind wall and the slab thermal insulation near to roof-column base

While designing of the insulation of structural element, one of the main goal was to eliminate all the possible thermal bridges. The foundation beams were insulated up to 80 cm deep and 12 cm thick thermal insulation at the vertical outer perimeter (Figure 89). These insulations are placed continuous on the exterior side of the ground floor wall's supporting beams, connected to the walls and floor insulation, without interruption (Figure 90). This solution seriously decreases the temperature variations below the building and thus the heat loss to the ground will be minimal.

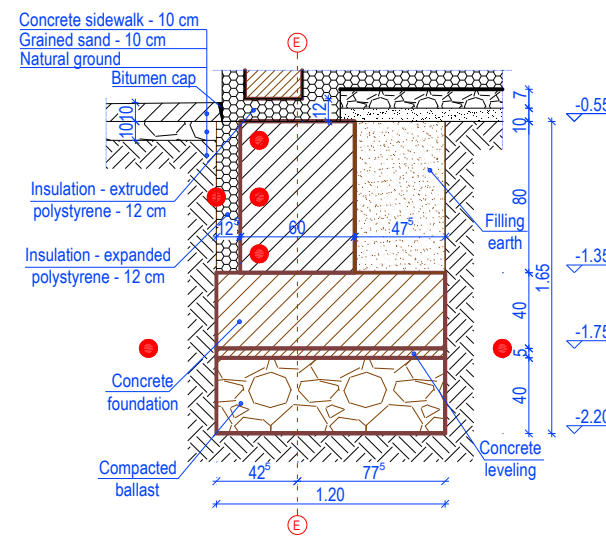


Figure 89. Detail for exterior foundation

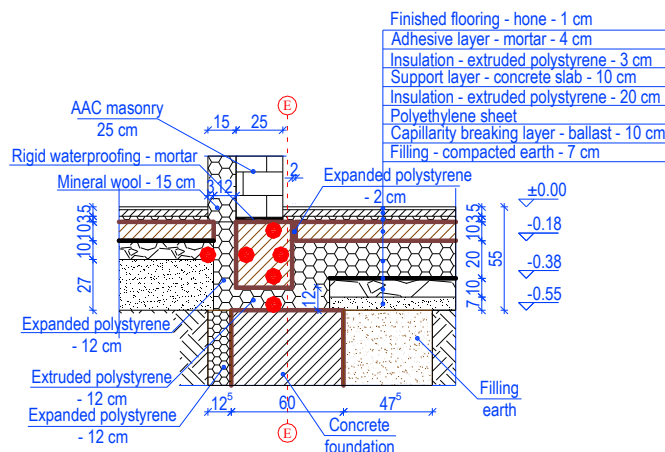


Figure 90. Detail for exterior footing beam with continues insulation

On the ground floor there is a car shed which is unheated and has been considered as an exterior environment. The insulation between the heated area and the car shed presents problem areas that can only be limited but not eliminated in terms of thermal bridges. In order to limit the heat flux through the joints, extra insulation has been applied (Figure 91 and 92).

The concrete columns, that delimit the two areas, intersect with the closing walls of the car shed which are insulated on the exterior side only to provide continuity to the façade, therefore an extra layer of insulation of 15 cm thickness has been put on the interior side of the closing wall. The exterior concrete columns that are in direct contact with the lower part of the slab thermal envelope have been insulated on their perimeter with a 5 cm thick thermal insulation to reduce the heat losses in the joint (Figure 93 and 94).

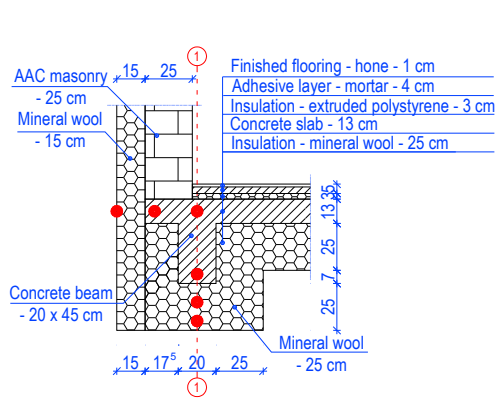


Figure 91. Detail for first floor exterior beam at the car shed

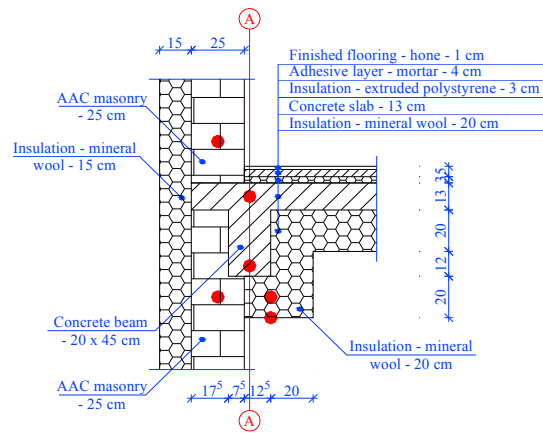


Figure 92. Detail for first floor exterior beam (current detail)

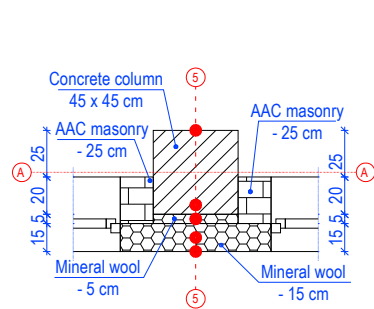


Figure 93. Detail for an intermediate column and view of the first and second layer of thermal insulation

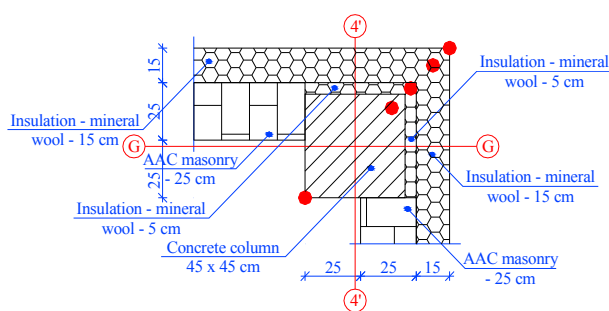


Figure 94. Specific detail for a column placed in a corner and view of the first and second layer of thermal insulation



Windows used in the building have triple glazing, PVC frame and the installation is designed with sealing belts to assure suitable air tightness (Figure 95). The external doors and windows are positioned in the thickness of the walls, so that the mineral wool insulation covers half of the width of the frame, thus reducing the formation of thermal bridges (Figure 96). The

adequate supply of natural light fundamental requirement for a school, the glass surface ratio is relative high, so this critical part of the building must seriously be considered.



Figure 95. Windows with sealing belts (interior and exterior detail)

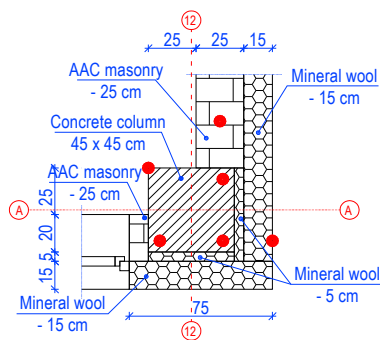


Figure 96. Detail of the ground floor column with the mounted sensors

The Heat Ventilation and Air-Conditioning (HVAC) system is composed of heat pump convactor fans for heating and cooling; also the domestic hot water demand will be solved with heat pumps. In addition, a heat recovery ventilation system is used and the ventilation rate is regulated by several CO<sub>2</sub> sensors. The power supply of the kitchen equipment is represented by a natural gas-based system, which will also be the building heating reserve system as well.

The thickness of the thermal insulation was designed according to a detailed thermal calculation with accurate local climate data (meteonorm) in order to achieve a low energy consumption for heating, using the Passive House Planning Package (PHPP), so that the heating energy is kept below 15 kWh/m<sup>2</sup>/year. The resulted thicknesses of the insulation are significantly larger than the minimum required by the local legislation. However, it is known that these dimensions depend on other essential parameters as well, as orientation, air tightness, local climatic conditions, the occupancy rate, the amount of thermal bridges, solar gain, the type and/or performance and/or efficiency of used heat pumps and exchangers, the type of control system and last but not least, the users behaviour.

### 3.3.3 Monitoring system

Due to the fact that the functionality of the structure is quite complex and that by being a school it is discontinuously utilized, it cannot be classified in a typical building category, hence the calculated energy consumption may differ from the real values. In order for these differences to be measurable, a complex monitoring system has been developed. The objective of the measurements are multiple and the obtained parameters can be used at various evaluation levels. There are 3 involved parties, who are going to use, in different way, the available monitoring system.

The Designers can use the received data as follows: 1) to justify the preliminary calculations; 2) for calibration of the models in further design processes and to improve the calculation methods; 3) to increase energy efficiency of the specific building (cost optimization); and 4) to improve the comfort-feeling of the users. In such way the monitoring system will be/could be the link between the designer and the building.

The Investor (who in this case is the operator) may use the measured data as a very helpful tool that enables him to improve the real-time energy consumption, for better regulation and a proper response to the needs/demands of users.

The Users are key players in this equation, as their needs and expectations have to be fulfilled depending on their feedback, even though no access to the measured data has to be provided.

Using the monitoring system, several parameters will be measured. These could be sorted in 4 categories.

In the first, the comfort and energy-efficiency parameters are included, which would contain: various temperatures (structural components, insulations, air, soil, cooling/heating water, heat pump water), humidity (indoor and outdoor), motion, window opening, solar radiation intensity and duration, occupancy (number of people), sound and light intensity and air tightness.

The second category would be the measurement of the equipment's parameters, as further temperatures (heat exchangers, borehole, domestic hot water, the introduction and exhaust air), water consumption, air speed, power consumption (for various customers) and natural gas consumption.

The third category would be parameter measurements dictated by medical considerations such as radon radiation, carbon dioxide (CO<sub>2</sub>), formaldehyde (CH<sub>2</sub>O) vapour, nitrous oxide (N<sub>2</sub>O), nitrogen dioxide (NO<sub>2</sub>) and volatile organic compounds.

The fourth category would be psychological measurements through questionnaire that follows the user's behaviour and behavioural changes, completed by both the students and their teachers also, thus evaluating the comfort feeling (air speed, humidity, temperature, overall comfort, etc.) and fulfilling of other requirements.

The location of the temperature sensors (represented by red dots on Figure 87 to 96) has been conceived in order to provide real-time information on theoretically studied building details, in the same time measuring in many points throughout the structure, the outdoor and indoor climate. Since the distribution of the heat flux and temperatures in the joints depend on the geometric shape of the materials and their thermal properties, the sensors have been installed in the concrete, brick and insulation layers on all relevant sides. The connection between cables

and sensors were protected with shrink tube, to ensure the proper operation even after concreting, brickwork or finishing/plastering phases.

All monitoring cables that have been installed in casted concrete, have been additionally provided with polyethylene pipes to protect the data flow from the sensors to the data logger. A number of 300 temperature sensors have been already installed (in October 2015) in every relevant section, of which 180 have been placed in ground, in foundations and in slab of the ground, in the floor, in the beams, columns and their thermal insulation. The rest are located in the masonry walls and in the roof structure. The measurements are recorded through several data acquisition unit (loggers). The processing of huge amounts of data will be implemented via an online platform. Development of this is already in progress. In the current schedule, the monitoring system will be operational in May 2016.

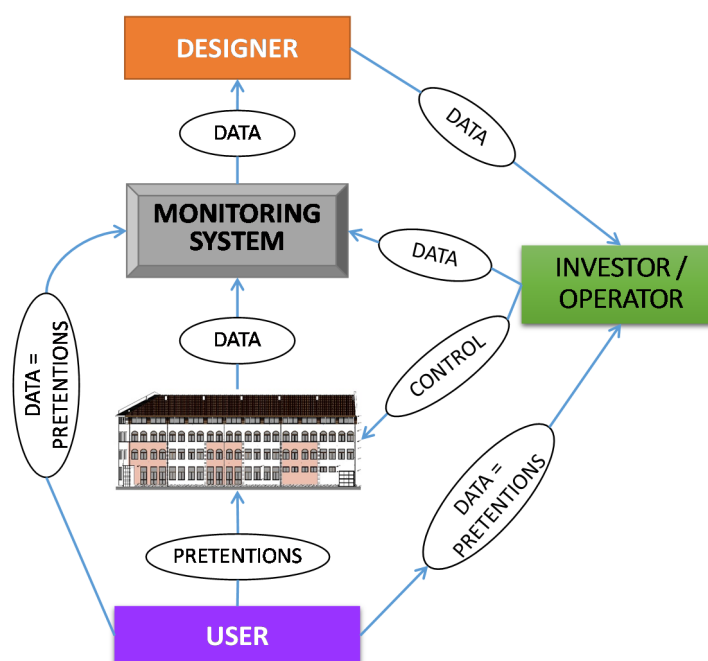


Figure 97. Monitoring system as a links between the interested parties

### 3.3.4 Experience of the planning and implementation process

In the present school building, the investor, in the same time, is the owner of the building, thus short- and long-term interests being easily compatible and convergent, since both the investment and the operating costs will be financed from the same source.

Therefore, the main interest of all interested parties (owner/investor) becomes the long-term cost minimization, a goal which forces the designers to identify the optimum solutions. If this interest agreement is missing, it's much harder to convince an investor of the short-term return of the initial additional costs.

It would be preferable that in the future, at least in the public sector for large investments, the submitted cost calculation to be done covering the entire life of the structure (life cycle cost assessment together with energy efficiency calculation).

An interesting aspect regarding this building, is represented by the fact that the design and construction cost of a traditional school and one with renewable concepts and energy-efficient solutions are almost identical. The substantial differences in the design phase is the added knowledge and in the execution phase the careful workmanship. Here must be emphasize the role of construction experts in spreading and promotion of similar or other energy-efficient solutions (Nagy Zs. et al, 2013).

Perhaps the most important role have the technical advisors who had the contact with the potential investor from the initial phase. Decisions made in the initial design phase strongly conditions the sustainability parameters of technical solutions, even if is discussed about renovations or new buildings. In recognition of this, it is essential to pay much more attention to the decisions taken in the pre-planning stage (Koukkari et al., 2014).

### **3.3.5 Preliminary results**

In recent years, the energy-efficient buildings have gained more and more attention because of the economic and internal comfort benefits that they provide. Given the previously mentioned benefits, it is extremely important to mention that a school needs to create an environment which should be functioning in certain health parameters that would increase students' achievements and ability to maintain a high attention level. At the same time, the lower maintenance costs will allow improving the quality of education by redirecting/reallocating a part of the available budget.

This school has important research potential, because it is a multi-purpose building with non-continuous utilization, designed and executed using energy efficient concepts, details and construction methods, applying renewable energy systems. The use of a complex monitoring system finally will help the operator to make the best building parameters settings, taking into account the energy and health aspects, as well as the needs of the users.

Important information is going to be obtained from the measured parameters and data, which could be used in the design and execution phases of new school buildings, in the renovation of existing buildings, thus promoting environmental awareness in education, in schools as well as in other parts of society.

### **Acknowledgement**

This study was partially supported by the research grant of the Romanian National Authority for Scientific Research, CNDI–UEFISCDI; project number PN-II-PT-PCCA-2011-3.2-1214-Contract 74/2012, coordinated by Prof. Dan Daniel, Politehnica University of Timisoara, and by the Sectoral Operational Programme Human Resources Development POSDRU/159/1.5/S/137516 financed from the European Social Fund and by the Romanian Government, respectively.

My special appreciation and thanks to Boros Iosif, Prof. Dan Daniel, Stoian Dan and Sabău Gabriel.

## **C. SCIENTIFIC, PROFESSIONAL AND ACADEMIC FUTURE DEVELOPMENT PLANS**

The candidate's opinion and view regarding the further development plans on scientific, professional and academic future, is that the main subject of interest will be in the already studied field of FRP composites in constructions, structural retrofitting and energy efficiency, without ignoring new and important research direction, especially in the field of structural use of recycled construction materials and high performance materials. The outline and some details are presented in the following.

### **C1. SCIENTIFIC DEVELOPMENT PLANS**

At the moment, the candidate activates in the Department of Civil Engineering and Building Services (CCI), as well as in the Research Centre for Rehabilitation of Constructions (RECO), which is subordinated to the Department, belonging to Politehnica University Timișoara. The existing research facilities are relatively fair, having the possibility to perform experimental tests on linear structural elements or structural components at full scale, subjected to quasi-static monotonic or cyclic alternant loads. Of course, there are some domains and directions with deficiencies or limitations, such as the data acquisition system and data processing facilities, or various software for advanced numerical studies. The improvement of technical conditions and resources for research are two important areas where the candidate will try to submit more effort.

In the following there are presented some relevant aspects related to the plans and research directions and proposals with the main expected results.

#### ***Anchorage systems for FRP composites used for structural strengthening***

The fiber reinforced polymer composite materials are widely used for structural strengthening or retrofitting of reinforced concrete, masonry or timber elements. Design methods for bending, shear and even for torsion strengthening application are well documented. However, the dominant failure mode of all these cases are represented by debonding, due to insufficient anchorage length or inadequate bond strength.

The debonding process and its diverse manifestations, e.g. plate-end debonding, intermediate crack debonding, peeling-off and ripping-off, is a complex phenomenon, which was described by numerous models with considerable discrepancies yielding to different debonding loads or strains.

Many aspects regarding the influence of some special anchorage and their influences upon the overall behaviour of the strengthened elements are far from being solved. The available anchoring techniques and devices are just a few, their efficiency is not studied or not discussed in codes. The type of FRPs which must be anchored can be fabrics, lamelas or rebars used in NSM systems. The anchorage devices used nowadays consist in fiber wraps, spikes from different fibers, as well as different plates, disks and tubes fixed by chemically or mechanically applied bolts. The research team from RECO lab has developed an innovative anchorage system, which should be investigated additionally, to be applicable in real situations.

All of the above mentioned anchoring techniques can significantly increase the ultimate load bearing capacity of the elements and improve the overall behaviour of the strengthened

elements, by avoiding premature debonding and by delaying the yielding initiation into the steel reinforcement.

Based on experimental and theoretical studies performed up to now it can be drawn the conclusion that the failure load of the FRP strengthened elements may be determined by monitoring the debonding strain, thus determining the anchorage length or the anchorage force.

In order to develop design procedures and to calibrate the existing calculation methods, extensive experimental study and numerical simulations are required, with further investigation of one of the most promising anchorage systems, developed by the RECO team.

### ***Experimental investigation of FRP strengthened disturbed regions***

Regions in an element with a complex flow of internal stresses, typically highly concentrated at the corners, are called disturbed regions (D-regions). In the precast concrete industry this kind of discontinuity often occurs at the beams' support zone, through reduction of the cross-section at their ends, called dapped-ends.

The load bearing capacity of the elements with D-regions may be affected by design errors of structural damage. To restore or to increase their capacity, externally bonded (EBR) or near surface mounted (NSM) fiber reinforced polymers (FRP) composites can be used with high efficiency. However, there is a lack of experimental and theoretical investigations regarding the strengthening of D-regions with FRPs, due to the variations in geometry, materials and loading conditions.

In the past years an extended study was initiated by the candidate to study the dapped-end zones. In the first stage full scale beams were built and tested in laboratory. Based on the obtained result calibration of the numerical models were done. In the second stage a parametric investigation was performed, in which a number of 24 EBR and NSM configurations were analysed, to identify the most effective configuration of the FRP strengthening systems. The investigated parameters were the mechanical properties of the FRP's, the strengthening procedure and the inclination of the fibers with respect to the longitudinal axis.

In order to demonstrate the reliability of the analytical study, the candidate is proposing an experimental investigation on the dapped-ends, focusing on numerically determined most efficient FRP strengthening systems. The expected results would highlight the most efficient strengthening techniques with important applicability of the obtained results on other fields of RC elements with D-regions.

### ***Efficient rehabilitation of the existing building stock***

The necessity of interventions and the rehabilitation requirements of the reinforced concrete condominium buildings, especially of those made of large panels system are obvious. Based on the seriously surprising data of the European and Romanian Statistical Institutions with regard to the housing conditions, the need of immediate and high performance interventions for rational and energy efficient rehabilitation of the block of flats type buildings is obvious.

In 2008 the European Union (EU) adopted the so called 20-20-20 Renewable Energy Directive; according to this document until 2020 the member states agreed on 20% cut in energy consumption through improved energy efficiency and on 20% increase in the use of renewable energy. The justification was, that buildings sector represents 40% of the EU total energy

consumption, and thus reducing energy consumption is a priority objective. However, this directive probably will be overwritten by a more important problem, i.e. 30 million people in the EU suffering both lack of space and poor housing conditions (see Directive 2002/91/EC).

According to data reported by the National Institute of Statistics (NIS 2009), in Romania there are 8.3 million dwellings with 21.6 million rooms. In average an apartment has 2.6 rooms and 2.6 inhabitants. 50% of the population is represented by urban resident, who mostly live in prefabricated large panel buildings. In study published by Rybkowska & Schneider (2011) can be affirmed that more than 55% of the Romanian population lives in overcrowded dwellings, which is considerably above of the European average of 18%. These problems are generally associated with more deficiencies, such as leaking roof, lack of a bath or a shower or a flushing toilet and the insufficient natural light in the rooms. By far the most unfavourable situation can be found in Romania, where over 43% of the population has at least two housing deprivation.

That problems are far more serious than somebody could see or lets to be seen. After the great construction boom between 1950 - 1990, an important aftermath is expected posterior to 2020 period because of the aging buildings. Solutions for these could be found only through deliberated coordination. A rehabilitation concept which meets both economic and psychological demands, as well as structural and feasibility criteria is required.

At a complete renovation of a building the necessity of structural interventions is obvious. These may refer to conversion or strengthening of the existing elements, or may be additional structures. In several situations the strengthening may be necessary if the existing wall and slab panels are weakened by cut-out openings due to unification of dwellings, in this way increasing the usable surface. In such cases, a straightforward, efficient and quick solution is to use the fiber reinforced polymeric (FRP) composites.

The technology for interventions is available, the engineering and architectural solutions can be very diverse, however just their comparative life-cycle cost analysis could be the right choice for categories of arguments. The action plans for the organizational background should be provided by the leading authorities of the local community, while the implementation and reasonable crediting falls to the business and economic operators.

In the renovation process the question of energy efficiency is indispensable, since it is known that the average energy consumption of the flats built between 1950-1990 representing about 55% for heating and 21% for hot water producing (MRDT, 2009). Thus would be necessary to assess and study the energy-impact of the interventions, estimating the life-cycle performances.

To evaluate and control the energy parameters for several buildings with different functionalities a monitoring strategy is under development, with the aim to identify and measure the most relevant and important parameters. The results of the study should be in forms of guidelines for investors, designers and builders, as well as could be delivered as specialised trainings for construction workers and through publication of examples for good practice.

## **C2. PROFESSIONAL DEVELOPMENT PLANS**

Design and expertise of structures are constant concerns regarding to professional activity. Over time, the candidate participated in over 150 important projects. These activities and the accumulated experience are considered extremely important for a Civil Engineer, which can be used both in everyday teaching and research. The projects provides realism in work, offers and demands contact with new technologies, could be a source of inspiration or even can help understand a phenomena or choose the right solutions. At the same time, the knowledge and experience resulted from research and teaching activities can be used very well in the design and expertise activities.

The experience gathered through projects, through interaction with entrepreneurs, with economic environment (non-academic), even with simple workers, helped the candidate to develop both as a teacher and as a researcher. In the following, the candidate intends to continue the design activities, to ensure a parallel development with the research and academic fields.

The most important results of the professional activities the candidate will disseminate for the engineering community in public presentations, in conference and journal papers, as well as in technical books for practical engineers.

## **C3. ACADEMIC DEVELOPMENT PLANS**

Academic development is closely linked to the scientific, professional and managerial aspects. Application of theoretical knowledge, the use of experience from research, correlated with organizational principles and practices acquired can ensure competitive and healthy professional growth. There are many conditions that affect, positively or negatively, the progress. However, the candidate believes that by providing a pleasant working atmosphere, based on many discussions and confrontations of ideas and opinions, through a healthy and constructive competition, by promoting, respecting and supporting values, an advantageous development from didactic, scientific, managerial and professional point of view can be reached for all members of the collective they belong.

The experience gained in several national and international research grants as coordinator, managing team member, or research assistant, the candidate considers that he has the competence to manage the above mentioned research ideas. Based on the grants proposed and conducted so far in the field of FRP strengthening/retrofitting, four candidates already obtained the PhD title, and other three PhD students continue those research. The further intention of the candidate is to continue the didactic actions, to follow the creative and well-prepared students, to select them for PhD studies and finally to offer them a proper climate to continue their work/research in the research collective of Faculty of Civil Engineering, in Politehnica University Timișoara.

**REFERENCES**

- Abrams D.P., Laboratory definitions of behavior for structural components and building systems. ACI SP-127 Earthquake-resistant Concrete Structures. Inelastic Response and Design, 1991, 99-152.
- ACI 440.2R-08. Guide for the design and construction of externally bonded FRP systems for strengthening concrete structures. Farmington Hills: American Concrete Institute, 2008.
- ACI 318-08. Building code requirements for structural concrete and commentary: American Concrete Institute, 2008.
- AIJ Standard for Structural Calculation of Reinforced Concrete Structures Based on Allowable Stress Concept, Architectural Institute of Japan, 1999.
- Alkhrdaji T., Thomas J., Design, application techniques key to successful structural repair, strengthening of aging concrete facilities, Concrete Monthly, 2004.
- Antoniades K.K., Salonikios TN. and Kappos A.J., Cyclic tests on seismically damaged reinforced concrete walls strengthened using fiber-reinforced polymer reinforcement, ACI Structural Journal, 100(4), 2003, pp. 510-518.
- Antoniades K.K., Salonikios TN. and Kappos A.J., Tests on seismically damaged reinforced concrete walls repaired and strengthened using fiber-reinforced polymers, Journal of Composite for Construction, 9(3), 2005, pp. 236-246.
- Biskinis, D.E., Roupakias, G.K. and Fardis, M.N., Degradation of shear strength of reinforced concrete members with inelastic cyclic displacements, ACI Struct. J., 101(6), 773-783, 2004.
- C107-2005 - Normative act concerning the thermo-technical calculation of the construction elements of buildings. Bucharest: Ministry of Regional Development and Tourism.
- Cervenka V, Jendele L, Cervenka J. ATENA program documentation. Part 1: Theory. Cervenka Consulting Ltd; 2012.
- Chen BS, Hagenberger MJ, Breen JE. Evaluation of strut-and-tie modeling applied to dapped beam with opening. ACI Struct J 2002; 99:445-50.
- CNR DT200. Guide for the design and construction of externally bonded FRP systems for strengthening existing structures. Rome: Italian National Research Council; 2004.
- Cyclic Loading Test Data of Reinforced Concrete Bridge Piers, Tokyo Institute of Technology, Kawashima Lab, <<http://seismic.cv.titech.ac.jp/en/titdata/titdata.html>>, [accessed September 14, 2011].
- DABASUM - Database for FRP-Based Shear Strengthening of Reinforced Concrete Beams, University of Minho, <<http://dabasum.civil.uminho.pt/index.php>>, [accessed May 5, 2011].

- Dăescu AC., Rehabilitation of structural elements using composite materials, PhD Thesis, 2011, UPT, Politehnica, ISBN 978-606-554-330-0.
- Dăescu AC, Nagy-György T, Sas BG, Barros J.A.O., Popescu C. Assessment of the strengthening effectiveness of EBR and NSM techniques for beams' dappedend by FEM analysis, FRPRCS-11, Guimarães, Portugal; 2013. p. 1–9.
- Dan D., Nagy-György T., Stoian V., Fabian A., Demeter I., FRP Composites for Seismic Retrofitting of Steel-Concrete Shear Walls with Steel Encased Profiles, STESSA 2012, Santiago, Chile, 2012, ISBN 978-0-415-62105-2, pp1071-1076.
- De Lorenzis L, Teng JG. Near-surface mounted FRP reinforcement: an emerging technique for strengthening structures. *Composites Part B* 2007; 38(2):119–43.
- Demeter I., Seismic retrofit of precast RC walls by externally bonded CFRP composites, PhD Thesis, UPT, Politehnica, 2011, ISBN 978-606-554-338-6.
- Demeter I., Nagy-György T., Stoian V., Dan D., Quasi-static Loading Strategy for Earthquake Simulation on Precast RC Shear Walls, 12th WSEAS International Conference on SYSTEMS, Greece, 2008, ISBN 978-960-6777-83-1, pp 813-829.
- Demeter I., Nagy-György T., Stoian V., Dăescu C., Dan D., FRP Composites for Seismic Retrofitting of RC Wall Panels with Cut-Out Openings, ICSEA2010, Guimaraes, Portugal, 2010, ISBN 978-0-415-49249-2, pp 1902-1908.
- Demeter I., Nagy-György T., Stoian V., Dăescu C., Dan D., Seismic Performance of Precast RC Wall Panels with Cut-Out Openings, 14ECEE, Ohrid, Macedonia, 2010, Paper No. 1004.
- Diaconu D., Strengthening RC Structural elements with FRP composites using different anchorage systems, PhD Thesis, UPT, Politehnica, 2011, ISBN 978-606-554-339-3.
- Diaconu, D., Dăescu, C., Stoian, V., Nagy-György, T., Strengthening reinforced concrete beams for bending and shear Using FRP Composite Materials –Economical Study, Student Scientific Communication Conference, Cluj-Napoca, Romania, 2005, 12 pp
- Diaconu D., Nagy-György T., Stoian V., Dan D., Floruț S. C., Dăescu C. A., Demeter I., Economic Assessment of Different Shear Strengthening Methods for Clay Brick Masonry Walls, PROHITECH, Rome, 2009, ISBN 978-0-415-55804-4, pp 1275-1280.
- Directive 2002/91/EC of the European Parliament and of the Council on the Energy Performance of Buildings. EU
- Dogariu, A., Stratan, A., Dubina, D., Nagy-György, T., Dăescu, C. & Stoian V., Strengthening of masonry walls by innovative metal based techniques. COST Action C26 Proceedings – Urban Habitat Constructions under Catastrophic Events, Prague, Czech, 2007, pp 201-211.
- Dubina, D., Dogariu, A., Stratan, A., Stoian, V., Nagy-György, T., Dan, D. & Dăescu, C., Masonry walls strengthening with innovative metal based techniques, ICSCS07, Manchester, 2007, ISBN 978-0-415-45141-3, pp 1071-1078.

- Dubina, D., Stoian, V., Dogariu, A., Nagy-György, T., Stratan, A., Dăescu, C. & Diaconu, D., Strengthening of masonry walls by innovative metal based technique, 2008, PROHITECH WP7 report.
- EN 1992-1-1:2004. Eurocode 2: Design of concrete structures – Part 1-1: General rules and rules for buildings, 2004.
- EN 15459:2006, Energy Efficiency for Buildings – Standard economic evaluation procedure for energy systems in buildings, 2006.
- Enochsson O., CFRP strengthening of concrete slabs, with and without openings. Experiment, analysis, design and field application. Licentiate thesis, Luleå University of Technology (2005).
- European Energy Security Strategy ([http://ec.europa.eu/energy/efficiency/index\\_en.htm](http://ec.europa.eu/energy/efficiency/index_en.htm), last accessed in October 2015).
- European Parliament, Directive 2010/31/EU of the European Parliament and of the Council of 19 May 2010 on the energy performance of buildings (recast), Bruxelles.
- Farrar, C.R., Reed, J.W. and Salmon, M.W., Failure modes of low-rise shear walls, *J Energy Eng., ASCE*, 119(2), 119-138, 1993.
- Farvashany, F.M., Foster, S.J. and Rangan, B.V., Strength and deformation of high-strength concrete shearwalls, *ACI Struct. J.*, 105(1), 21-29, 2008.
- fib Bulletin 14. Externally bonded FRP reinforcement for RC structures. Lausanne: International Federation for Structural Concrete, 2001.
- Fintel, M. (1990). Performance of buildings with shear walls in earthquakes of the last thirty years. *PCI Journal*. 40:3, May-June, 62-80.
- Floruț S. C., Performance study of the elements subjected to bending strengthened with FRP composites, PhD Thesis, UPT, Politehnica, 2011, ISBN 978-606-554-334-8.
- Floruț S. C., Stoian V., Nagy-György T., Dan D., Diaconu D, Performance assessment of mixed CFRP retrofitting solution for RC slabs, *ICSA2013*, 2013, Guimaraes, Portugal, ISBN 978-041566195-9, pp. 727-732.
- Floruț S. C., Stoian V., Nagy-György T., Dan D., Diaconu D, Experimental Results of Research Program on RC Slabs Retrofitted by Mixed CFRP System, *Structural Faults & Repair-2012*, Edinburgh, UK, 2012, ISBN 0-947644-70-9, pp 70.
- Gold WJ, Blaszk GJ, Mettemeyer M, Nanni A, Wuerthele MD. Strengthening dapped ends of precast double tees with externally bonded FRP reinforcement. In: Elgaaly M, editor. *ASCE structures congress*. Philadelphia; 2000. p. 9 [CD version #40492-045-003].
- Gulec, C.K., Ultimate shear strength of squat rectangular reinforced concrete walls, MSc Thesis, State Univ. New York, Buffalo, NY, 2005.
- Gulec, C.K. and Whittaker, A.S., Performance-based assessment and design of squat reinforced concrete shear walls, Technical Report MCEER-09-0010, 2009.

- Hidalgo, P.A., Ledezma, C.A. and Jordan, R.M. (2002). Seismic behavior of squat reinforced concrete shear walls. *Earthquake Spectra*. 18:2, 287-308.
- Hirosawa, M., Past experimental results on reinforced concrete shear walls and their analysis, (in Japanese, ref. in Orakcal et al., 2009), 1975.
- Huang PC, Nanni A. Dapped-end strengthening of full-scale prestressed double tee beams with FRP composites. *Adv Struct Eng* 2006; 9:293–308.
- In-depth study of European Energy Security – SWD (2014) 330 final/3 - Brussels, 2.7.2014.
- Integrated Strategies and Policy Instruments for Retrofitting Buildings to Reduce Primary Energy Use and GHG Emissions (INSPIRE), Final Draft – Dec. 2014, ERACOBUILD.
- International Energy Agency - Redrawing the energy-climate map - World Energy Outlook Special Report, 2013.
- Iso M., Matsuzaki Y., Sonobe Y., Nakamura H., Watanabe M. Experimental study on reinforced concrete columns having wing walls retrofitted with continuous fiber sheets. WCEE12, New Zealand, Paper No. 1865, 2000.
- Kakaletsis, D.J. and Karayannis, C.G. (2009). Experimental investigation of infilled concrete frames with openings. *ACI Structural Journal*. 106:2, 132-141.
- Kashreen, M.M., Banfill P.F.G., Menzies G.F. 2009. Life-Cycle Assessment and the Environmental Impact of Buildings: A Review. *Journal Sustainability* 1: 674-701.
- Kitano A., Joh O., Goto Y. Experimental study on the strengthening and repair of R/C wall-frame structures with an opening by CF-sheets or CF-grids, CICE 2004, Australia, 2004.
- Kobayashi K., Innovative application of FRPs for seismic strengthening of RC shear wall, FRPRCS 7, (CD-ROM), ACI, Farmington Hills, MI, Paper No. 72, 2005.
- Koukkari H. et al., Sustainable Building Project in Steel (SB-Steel), Final Report RFSR-CT-2010-00027, 2014. (<http://www.onesource.pt/sbsteel/site/>).
- Limam O., Foret G., Ehrlicher A., RC two-way slabs strengthened with CFRP strips: experimental study and a limit analysis approach, *Composite Structures* 60 (2003).
- Lombard J., Lau D. T., Humar J. L., Foo S., Cheung M. S. Seismic strengthening and repair of reinforced concrete shear walls, WCEE12, New Zealand, Paper No. 2032, 2000.
- Lu WY, Lin IJ, Hwang SJ, Lin YH. Shear strength of high-strength concrete dapped-end beams. *J Chin Inst Eng* 2003; 26:671–80.
- Mattock AH. Design and behavior of dapped-end beams. *J Prestr Concr I*, 1979; 24:28–45.
- Mattock AH, Theryo TS. Strength of precast prestressed concrete members with dapped ends. *J Prestr Concr I* 1986; 31:58–75.
- Meteonorm, <http://www.meteonorm.com/> (data from 2014).

- Ministry of Regional Development and Tourism (MRDT). 2009. Presentation of the Thermal Rehabilitation Pro-gramme for Blocks of Flats. <http://www.mdrdt.ro/lucrari-publice/programul-de-reabilitare-termica>. Romania: MRDT.
- Mohamed Ali MS, Oehlers DJ, Griffith MC, Seracino R. Interfacial stress transfer of near surface-mounted FRP-to-concrete joints. *Eng Struct* 2008; 30(7):1861–8.
- Monitoring system data (<http://www.sdac.ro/site/archives/category/monitoring> last accessed in October 2015).
- Mosallam, A. S., Mosalam, K. M., Strengthening of two-way concrete slabs with FRP composite laminates, *Construction and Building Materials* 17 (2003), pp. 43-54.
- Mosallam, A. S., Haroun, M., Elsanadedy, H. and K. Gillette, Experimental and Numerical Analysis of Two-Way Concrete Slabs Repaired with Polymer Composites, *Proceedings of the Composites in the Transportation Industry*, Sydney, Australia, 2000, pp. 185-190.
- Muto, K., Ohmori, N. and Takahashi, T. (1974). A study on reinforced concrete shear walls for high-rise buildings. *The 5th World Conf. on Earthquake Engineering*, Vol. 1: 1135-1138.
- Nagy-György, T. (2004), *Using the FRP Composite Materials for Strengthening of Brick Masonry and Reinforced Concrete Elements*, Ph.D. Thesis, Politehnica University of Timișoara, Romania.
- Nagy-György Tamás, *Materiale compozite polimerice pentru consolidarea elementelor din zidărie și beton*, Ed. Politehnica, 2007, pp 295, ISBN 978-973-625-445-1.
- Nagy-György T., Stoian V., Gergely J., Dan D., „Masonry walls retrofitted with composites”, COST C12 – Improvement of Buildings Structural Quality by New Technologies (WG2), Final Scientific Report, Datasheet II. 3.2.6.1, A. A. Balkema Publishers, 2004.
- Nagy-György T., Moșoarcă M., Stoian V., Gergely J., Dan D., Retrofit of reinforced concrete shear walls with CFRP composites, *fib Symposium - Keep Concrete Attractive*, Budapest, Hungary, 2005, ISBN 963 420 838 X, pp. 897-902.
- Nagy-György T., Stoian V., Gergely J., Dan D., High Performance Materials Used in Retrofitting Structural Masonry Walls, *IABSE Symposium on Responding to Tomorrow's Challenges in Structural Engineering*, Budapest, Hungary, 2006, ISBN 963 420 838 X.
- Nagy-György T., Stoian V., Dan D., Dăescu C., Demeter I., Diaconu D., Dogariu A., Experimental assessment on shear strengthening of clay brick masonry walls using different techniques, *PROHITECH*, Rome, 2009, ISBN 978-0-415-55804-4, pp 1653-1658
- Nagy-György T., Sas G., Dăescu C., Barros J.A.O., Stoian V., Experimental and numerical assessment of the effectiveness of FRP-based strengthening configurations for dapped-end RC beams, *Engineering Structures* 44 (2012) 291–303, ISSN: 0141-0296.
- Nagy-György T., Demeter I., Floruț C., Dan D., Causes and required interventions on the rehabilitation process of large panel buildings in Romania, *CEBM 2012*, Hong-Kong, 2012.

- Nagy Zs., Fülöp L. and Talja A., Reconversion of Flat Buildings Administration: New Romanian Business Opportunities, *Advanced Engineering Forum*, vol. 8–9, 2013.
- National Institute of Statistics (2002). Census of population and dwellings 2002, Vol. 5, B-D-H, [online], from: <<http://www.insse.ro/cms/files/RPL2002INS/vol5/tablesdwelling.htm>>, [accessed October, 2011].
- Ochs F., Feist W., Janetti M.B., Peper S., Pfluger R., Schnieders J., Monitoring and Simulation of a Passive House with Innovative Solar Heat Pump System, *ISES Solar World Congress 2011*, Kassel, Germany, 2011.
- Palermo D., Vecchio F. J. Behavior of three-dimensional reinforced concrete shear walls. *ACI Struct. J.*, Vol. 99, No. 1, 2002, pp. 81-89.
- Passive House Database, <http://www.passivhausprojekte.de/> (Accessed in July 2015).
- Passive House Planning Package (PHPP), [http://passiv.de/en/04\\_phpp/04\\_phpp.htm](http://passiv.de/en/04_phpp/04_phpp.htm) .
- Paterson J., Mitchell D. Seismic retrofit of shear walls with headed bars and carbon fiber wrap. *J. Struct. Eng.*, Vol. 129, No. 5, 2003, pp. 606- 614.
- PCI design handbook: precast and prestressed concrete. Illinois: Ed. (MNL 120-04); 2004.
- PEER, Structural performance database, Available from: <<http://nisee.berkeley.edu/spd/>>, [accessed December 3, 2010].
- Pilakoutas K., Elnashai A. Cyclic behavior of reinforced concrete cantilever walls, Part I: Experimental results. *ACI Struct. J.*, Vol. 92, No. 3, 1995, pp. 271-281.
- Ramirez JA, French CW, Adebar PE, Bonacci JF, Collins MP. Recent approaches to shear design of structural concrete. *J Struct Eng* 1998; 124:1375–417.
- Reynolds GC. The strength of half-joints in reinforced concrete beams. London: Cement and Concrete Association; 1969.
- Rybkowska, A. & Schneider, M. 2011. Population and social conditions, Eurostat 4/2011, Statistics in focus. EU.
- RILEM, TC 223-MSC Data warehouse, MSC: masonry strengthening with composite materials, Available from: <<https://rilem223dwh.isqweb.it/>>, [accessed May 5, 2011].
- Riva P., Meda A., Giuriani E. Cyclic behaviour of a full scale RC structural wall. *Engineering Structures*, Vol. 25, 2003, pp. 835-845.
- Rizzo A, De Lorenzis L. Behavior and capacity of RC beams strengthened in shear with NSM FRP reinforcement. *Constr Build Mater* 2009; 23(4):1555–67.
- Sabău C., Stoian D., Dan D., Nagy-György T., Floruț C., Stoian V., Partial results of monitoring in a passive house, *JAES*, V1(16), Issue 1, 2013, ISSN 2247-3769, pp 107-111

- Salonikios T. N., Kappos A. J., Tegos I. A., Penelis G. G. Cyclic load behavior of low-slenderness reinforced concrete walls: Design basis and test results. *ACI Struct. J.*, Vol. 96, No. 4, 1999, pp. 649-660.
- Sas G, Carolin A, Täljsten B. A model for predicting the shear bearing capacity of FRP-strengthened beams. *Mech Compos Mater* 2008; 44(3):245–56.
- Sas G., Dăescu C., Popescu C., Nagy-György T., Numerical optimization of strengthening disturbed regions of dapped-end beams using NSM and EBR CFRP, *Composites Part B: Engineering* 67 (2014), 381-390, ISSN: 1359-8368.
- Schlaich J, Schafer K, Jennewein M. Toward a consistent design of structural concrete. *J Prestr Concr I* 1987;32:74–150.
- Shear wall database, University of Ottawa, Available from: <http://by.genie.uottawa.ca/~palermo/Wall.htm>, [accessed May 5, 2011].
- Smith S.T., Kim S.J., Strengthening of one-way spanning RC slabs with cutouts using FRP composites, *Construction and Building Materials*, Volume 23, Issue 4, 2009, pp 1578-1590.
- Stanic, A., Sigmund, V. and Guljas, I., Behavior of the walls under in-plane horizontal loadings, *Proc., fib-Symposium, Athens, Greece, 2003.*
- Stoian V., Nagy-György T., Dăescu C., Diaconu, D., Theoretical and experimental study of prestressed concrete beam support zone strengthened with composite materials, *Proceedings of the Second fib Congress, Naples, Italy, 2006.*
- Stoian V., Nagy-György T., Dan D., Gergely J., Dăescu C., *Materiale compozite pentru construcții – II revised edition*, Ed. Politehnica, 2009, pp 316, ISBN 973-625-948-7.
- Sugiyama T., Uemura M., Fukuyama H., Nakano K., Matsuzaki Y. Experimental study on the performance of the RC frame infilled cast-in-place non-structural RC walls retrofitted by using carbon fiber sheets, *WCEE12, New Zealand, Paper No. 2153, 2000.*
- Taleb, R. and Kono, S. (2010), Shear behavior of multi-story reinforced concrete walls with openings. *Bulletin of IISEE.* 45, 55-60.
- Tan KH., Shear strengthening of dapped beams using FRP systems. In: Burgoyne C, editor. *FRPRCS-5*. Cambridge: Thomas Telford Ltd.; 2001. p. 249–58.
- Tan K. H., Zhao H., Strengthening of openings in one-way reinforced-concrete slabs using carbon fiber-reinforced polymer systems, *J. Compos. for Constr.*, Volume 8, Issue 5, pp. 393-402 (September/October 2004).
- Taher S., Strengthening of reentrant corner zone in recessed RC beams. *11<sup>th</sup> International colloquium on structural and geotechnical engineering*, Egypt, Cairo, 2005.
- Todoș C., Seismic strengthening of precast RC wall panels using FRP composites, PhD Thesis, UPT, Politehnica, 2015, ISBN 978-606-554-919-7.

- Todoş C., Stoian V., Demeter I., Nagy-György T., Dan D., Ungureanu V., Seismic Strengthening of a Precast Reinforced Concrete Wall Panel Using Combined NSM and CFRP-EBR Method, FRPRCS-11, Guimaraes, Portugal, ISBN 978-972-8692-84-1.
- UN Climate Change Newsroom (<http://newsroom.unfccc.int/>, last accessed in October 2015).
- Yanez F.V., Park R. and Paulay T. (1992). Seismic behaviour of walls with irregular openings. The 10th World Conf. on Earthquake Engineering, Vol. 6: 3303-3308.
- Yang KH, Ashour AF, Lee JK, Shear strength of reinforced concrete dapped-end beams using mechanism analysis. Mag Concr Res 2011; 63(2):81–97.
- Vasquez A., Karbhari V. M., Fiber-reinforced polymer composite strengthening of concrete slabs with cutouts, ACI Structural Journal, V. 100, No. 5, 2003, pp. 665-67.
- Warashina M., Kono, S., Sakashita, M. and Tanaka, H. (2008). Shear behavior of multi-story RC structural walls with eccentric openings. WCEE14, S15-029.
- Wood S.L., Minimum tensile reinforcement requirements in walls, ACI Struct. J., 86(4), 582-591, 1989.
- Wood S.L., Shear strength of low-rise reinforced concrete walls, ACI Struct. J., 87(1), 99-107, 1990.